A Decade of Primary Productivity in Wadden Sea from MERIS: The Effects of Ancillary Climate Variables

MARYAM GOLMOHAMMADI
MARCH, 2013

SUPERVISORS:
Dr. Ir. Mhd. Suhyb Salama
Dr. Ir. Rogier Van Der Velde

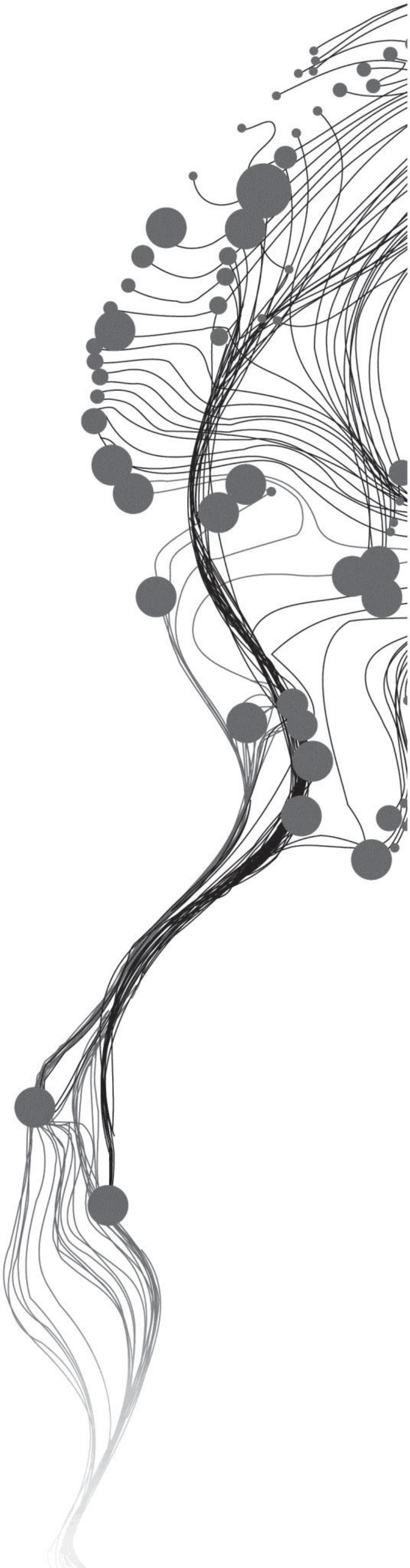

A Decade of Primary Productivity in Wadden Sea from MERIS: The Effects of Ancillary Climate Variables

MARYAM GOLMOHAMMADI
ENSCHEDE, THE NETHERLANDS, MARCH, 2013

Thesis submitted to the Faculty of Geo-Information Science and Earth Observation of the University of Twente in partial fulfilment of the requirements for the degree of Master of Science in Geo-information Science and Earth Observation.
Specialization: Water Resources and Environmental Management

SUPERVISORS:
Dr. Ir. Mhd. Suhyb Salama
Dr. Ir. Rogier Van Der Velde

THESIS ASSESSMENT BOARD:
Prof. Dr. Ing. Wouter Verhoef
Dr.ir. D.C.M.Augustijn (External Examiner, WEM department, Twente University)

ABSTRACT

Marine primary productivity is a process by which inorganic matters convert to organic materials with the help of CO_2 and light through photosynthesis. In current research, we tried to lead two main objectives. The preliminary step is to provide a satellite-based quantification of long-term Primary Production (PP) which has been done as the first attempt for the entire coastal area of Wadden Sea (WS) as well as 4 West Frisian Islands (WFIs). Vertically Generalized Production Model (VGPM) was utilized to determine the spatially and temporally oscillation of Depth Integrated PP from Jan-2003 till Mar-2012 with the help of MERIS and MODIS ocean products. Short-term investigation demonstrates that WS daily PP varies between 0.12 to 13.4gC.m^{-2}d^{-1} which occurred in Oct-2003 and May-2008 respectively. Between 2003 and 2012, monthly PP was estimated in the range of 9.81 and 0.28gC m^{-2}d^{-1} which in sequence recorded in Jun-2004 and Nov-2008 for the Wadden Sea region. Long-term oscillation of primary production presents a year to year cyclic seasonally pattern in such a way that the peaks and falls in biomass growth rate respectively occurred in summer (for 2011 it appears in spring) and winter (it happened in autumn for the year 2008). Two strong blooms of spring and summer were detected for Texel and Ameland which happened late in June and in August respectively while similar to WS, Vlieland and Terschelling experienced only one summer bloom between July and August. Decadal weighted average was computed about 122.8gC m^{-2}y^{-1} for the Wadden Sea whereas for WFIs it is appeared more or less than 70gC m^{-2}y^{-1}. This difference illustrates the cumulative effect of Greman and Danish productivity on total pp. No harmonic trend was detected between productivity variations starting from 2003 to 2012. The year 2008 was highlighted as the highest value of total PP less than 190gC m^{-2}y^{-1}. 10 years tracing of primary production shows lowest amount of productivity in cold seasons as a result of more rainfall, runoff and more sediment loads which flows into the sea through neighbor rivers and streams. These suspended materials then limit the penetrated light and reduce the euphotic zone. According to spatial distribution of PP, WS showed higher amount of productivity than WFIs, since it consists of German and Danish coasts rather than Dutch region. German coasts represented relatively high variability during a decadal observation. Along with this, Texel labelled as the most temporally variable area with the daily coefficient of variation about 68% since it is affected by nutrient loads of Marsdiep inlet and Lake Ijsselmeer. However the direct and indirect effect of North Sea on physical and biological variability of Wadden Sea coastal area should be taken into account.

As the second goal of this research, we identified the plausible consequences of two ancillary climate variables (SST & PAR) on marine chlorophyll concentration. Statistical analysis shows an inverse (negative slope) but strong ($0.56 \leq R^2 \leq 0.74$) relationship between physical parameters and biomass activities in the coasts of WS. As such, whenever Chl_a concentration rises as a reason of tidal mixed-layer growing caused by North Sea severe flows toward the inner parts of WS, SST and PAR decreases by less temperature and light in early winter. Finally, it is concluded that the determined ancillary climatic variables are not perfectly able to reflect the marine biological responses since they might be strongly controlled by other dominant factors which should be investigated by further studies.

ACKNOWLEDGEMENTS

First and foremost, my humble thanks goes to God for his grace and love that has taken me this far.

My profound and hearty gratitude goes to my first supervisor Dr. Suhyb Salama for his insightful comments, advice, suggestions that contributed in completing this thesis and for his guidance to carry out the research in scientific framework.

My earnest thanks to Dr. Van Der Velde, my second supervisor, for his help and encouragement during the Msc. Period.

I would like to thank the European Union for granting me with a scholarship through the Erasmus Mundus-Lot8 (EM) that enabled me to realize my dream.

I also would like to express my heartfelt thanks to the European Space Agency (ESA) for providing full resolution MERIS images and NASA for providing MODIS products over the Wadden Sea.

I would like to express my thanks to the IN PLACE team for providing field Chl-a data and the IDL codes to process MERIS and MODIS images to primary production maps.

To my family words are not enough to express my sincerely appreciation for your love and motivation which contribute to my overall well-being.

Thanks also to all my WREM colleagues who have been with me since the beginning of ITC study till completion of the course.

TABLE OF CONTENTS

1. Introduction ... 1
   1.1. Background ... 1
   1.2. Problem definition ... 2
   1.3. Research objective ... 2
   1.4. Research question ... 2
2. Literature review ... 3
   2.1. Remotely sensed primary production ... 3
   2.2. Primary production models ... 3
   2.3. Primary production and climate variability ... 5
3. Materials ... 7
   3.1. Study area ... 7
   3.2. Primary production in Wadden Sea ... 8
   3.3. Data sets ... 8
   3.4. Photoperiod (Dirr) ... 10
4. Methdology ... 11
   4.1. Improved Contrast Over Ocean and Land (ICOL) ... 11
   4.2. Coastal Case-2 Regional Processor (C2RP) ... 11
   4.3. Spatial and temporal match-up ... 12
   4.4. Data validation and verification ... 13
   4.5. Vertically Generalized Production Model (VGPM) ... 14
   4.6. Nominal Range Sensitivity Analysis (NRSA) ... 14
5. Results ... 16
   5.1. Atmospheric correction ... 16
   5.2. Validation and verification ... 17
   5.3. Spatial and temporal time series of VGPM inputs ... 20
   5.4. Sensitivity analysis ... 31
   5.5. Ancillary climate variables and Chl_a ... 31
6. Discussion ... 36
   6.1. VGPM input variables interaction with IPP ... 36
   6.2. Short-term variation of primary production ... 38
   6.3. Seasonally and long-term variation of primary production ... 38
   6.4. Wadden Sea and West Frisian Islands temporal trend of primary productivity ... 39
   6.5. VGPM assessment ... 41
   6.6. Chlorophyll_a interconnection with PAR and SST ... 41
7. Conclusion and recommendation ... 43
   7.1. Summary and conclusion ... 43
   7.2. Limitations ... 43
   7.3. Recommendation ... 44

List of References ... 45
Appendix A ... 52

LIST OF FIGURES

Figure 2-1- MODIS and MERIS instruments main characteristics. 4
Figure 3-1- The schematic view of the study area and its boundary (The Wadden Sea) (CWSS, 2008) 7
Figure 3-2- Map of West Frisian Islands (Worldatlas, 2012). 8
Figure 3-3- Location of picked in-situ ground stations (marked by star) 9
Figure 4-1- Flowchart of research procedure 12
Figure 4-2- Frequency of MERIS L-1 images before (a) and after (b) temporal match-up (2003-2012). 13
Figure 5-1- MERIS Full L1 Radiance image before (left) and after (right) adjacency and atmospheric effect correction (06-Feb-2008).The weakness of C2R model to remove cloud effect. 16
Figure 5-2- Typical MERIS 300m chlorophyll_a image retrieved by applying atmospheric effect correction on a clear sky image (09-Apr-2008). 16
Figure 5-3- Linear regression trend result between Chl-a modelled by C2R and field measurement Chl_a concentration. The comparison was only done for the year 2009. 17
Figure 5-4- Comparison between daily MODIS sea surface temperature and the observed air temperature (R2=0.87). SST verification for Texel island. 18
Figure 5-5- Average monthly SST versus monthly air temperature using linear trend in year 2007 for 4 West Frisian Islands: R1(Texel), R2(Vlieland), R3(Terschelling), R4(Ameland) 18
Figure 5-6- Daily variation of Texel MODIS PAR and De Kooy in-situ global radiation for the year 2007 19
Figure 5-7- Photosynthetically Active Radiation and Global radiation ration (PAR/Rn) presented as percentage 19
Figure 5-8- Average monthly PAR versus monthly global radiation using linear trend in year 2007 for 4 West Frisian Islands: R1(Texel), R2(Vlieland), R3(Terschelling), R4(Ameland) 20
Figure 5-9- Schematic map of region of interests separated for the time series analysis. Wadden Sea coastal area (left) and West Frisian Islands (right) (Worldatlas, 2012) 20
Figure 5-10- Seasonally mean variation of Chl_a concentration calculated for all regions of interests (2003 to 2012). 21
Figure 5-11- Regional mean Chl_a deviation of Chl_a (WS) for the period of 2003 to 2012. 22
Figure 5-12- Spatial distribution of Chlorophyll_a concentration in seasonal nominated dates of the year 2008 including: 09-Feb, 11-May, 30-Aug and 09-Nov. The values are evaluated in $mg.m^{-3}$ and it also included North Sea area. 22
Figure 5-13- Monthly Euphotic depth and PAR relationship after temporal match-up 23
Figure 5-14- Daily time series of Euphotic Depth (Z_{eu}) over WS and WFIs during 2003 till 2012. 23
Figure 5-15- Seasonal variation of Euphotic Depth (Zeu) in WS and 4 WFIs. 24
Figure 5-16- Spatial distribution of Euphotic Depth(Zeu) In nominated dates of spring and summer 2008 (11-May and 30-Aug). Values are presented in meter and it also included North Sea area. 24
Figure 5-17- Monthly mean PAR variation over the ROIs. Missed values are as a result of temporal match-up. 25
Figure 5-18- Mean PAR variation in seasonal nominated dates of the year 2008. (9-Feb, 11-May, 30-Aug and 9-Nov). All values are computed in $E.m^{-2}d^{-1}$ and it also included North Sea area. 25
Figure 5-19- Regional mean PAR anomalies of WS mean PAR depicted in annual scale 26
Figure 5-20- Seasonal changes in P_b^{opt} plotted over 10 years (2003-2012). 26
Figure 5-21- Spatial variation of optimum carbon fixation rate (Pbopt) in seasonal nominated dates of the year 2008 (09-Feb, 11-May, 30-Aug and 09-Nov). Values are in $mgC(mgChl^{-1})h^{-1}$ and it also included North Sea area. 27

Figure 5-22- Daily distribution of VGPM primary production (scatter plot). Straight line represents the diurnal mean value over 10 years. 28
Figure 5-23- Seasonal alteration of depth integrated primary production over WS and WFIs. 28
Figure 5-24- Monthly average of depth integrated primary production over 10 years (2003-2012). 29
Figure 5-25- Annual mean PP in conjunction with calculated standard deviation. 29
Figure 5-26 - Spatial variability of yearly mean PP over a decade of 2003 to 2012. Red and dark blue colors indicates maximum and minimum production respectively. The values are also included part of North Sea. area. 30
Figure 5-27- Regional scale Nominal Range Sensitivity Analysis results applied on daily parameters. 31
Figure 5-28- Daily variation of MODIS PAR, SST and MERIS Chl_a concentration. plotted for a location with coordinate of 52.99N and 4.85E in Texel island. 32
Figure 5-29- The mean monthly relationship of Chl_a with SST(a) and PAR(b) for a location with coordinate of 52.99N and 4.85E in Texel island. 32
Figure 5-30- The exact location of selected ground control points over the Wadden Sea (a & b). 33
Figure 5-31- Spatial seesaw of SST and PAR accompanying Chl_a concentration delineated for 5th Aug-2007. 25 GCPs assigned covering the entire study area. 33
Figure 5-32- 2003-2012 monthly averaged PAR, SST and Chl_a concentration. 34
Figure 5-33- Linear regression analysis results performed for each single variable against another (a) Chl_a-PAR, (b) Chl_a-SST and (c) SST-PAR 35
Figure 6-1- Decadal averaged Chl_a concentration in each month plotted for WFIs and WS. Maximum and minimumvaluesbelong to Ameland (~28.5mg.m-3) and Texel (~12.1mg.m-3) respectively. 36
Figure 6-2- The ratio between daily PP and Chl_a concentration over the range of euphotic zone in Wadden Sea. At the same time, the graph shows the inter relationship between Chl_a, Zeu and PP. 37
Figure 6-3- The organic matter feeding process of WS by North Sea and riverine nutrient inputs which then leads to productivity of WS constructed by van Bueskom (2005) 39
Figure 6-4- Total amount of annual pp variation year by year from 2003 till 2012. The gray space represents the rest of WS area (German+Danish) 40

LIST OF TABLES

Table 2-1- List of 21 ocean colour PP models which evaluated by Saba et al. (2011). 5
Table 3-1- Required data characterization for processing the research steps. 8
Table 3-2- The characteristics of selected in-situ stations for SST and PAR verification 10
Table 5-1– Statistical result of linear regression of monthly SST versus air temperature 18
Table 5-2- Statistical analysis results calculated using monthly Chl_a data for defined ROIs from 2003 till 2012. 21
Table 5-3- Monthly average of primary productivity domain values (max &min) 28
Table 5-4- The statistical analysis of total VGPM depth-integrated primary production obtained for different coastal areas. 29
Table 5-5- Initial statistic results containing minimum, maximum, weighted average and coefficient of variation...... 34
Table 5-6- Regression analysis results for a decade of 2003 to 2012 between Chl_a, SST and PAR. 34
Table 6-1- Mean monthly values of VGPM inputs and output estimated as daily variation of.......... 38

1. INTRODUCTION

1.1. Background

Primary production (PP) is the process in which single-celled organisms, inhabiting the water column, use sunlight and nutrients to produce oxygen and organic carbon through photosynthesis (Ebbesmeyer & Helseth, 1977). Phytoplankton is the main organism that contributes to the primary production in the ocean and is generally used to characterize the trophic status of water bodies. One of the commonly used proxies of phytoplankton biomass is its green pigment, chlorophyll-a (chl-a) which initiates the photosynthetic activities. Photosynthesis procedure fundamentally depends on the captured energy from sunlight which is spent by micro and macro organisms to produce inorganic substances.

Meanwhile, aquatic PP changes in photosynthetic rate per chlorophyll are strongly related to the availability of nutrients and the intensity of visible light. Nutrient and light, are limiting factors of phytoplankton growth. Besides, Primary production varies with respect to climate indicators (e.g., temperature, aerosol, sea roughness, tide, cloud cover, time of the day (Aas, 2010)) and bio-physical activities, e.g., runoff and attenuation in the water due to suspended and dissolved matter other than Chl-a (Anthony et al., 2004). In the Wadden Sea, variation in water quality (e.g. biomass and nutrient loading), solar insolation and sea temperature are among the most main factors contributing to the variability of primary productivity and hence the carrying capacity (biomass per trophic level) of its marine ecosystem. Among these issues, changes of solar radiation and sea surface temperature on PP in the water column are less taken into account in this specific area.

Nowadays scientists attempt to develop methods and tools for measuring the amount of organic matters based on general knowledge of primary productivity. In this way, remote sensing (RS) and field measurements are defined as the two preliminary data collection procedures. In situ data are noticeably restricted by space, synoptic spatial coverage, whereas RS data are virtually able to fill the absence of field measurements. Remote sensing approaches provide high spatial and temporal resolution information on key components controlling primary production such as Chlorophyll-a concentration (Chl_a), Sea Surface Temperature (SST) and Photosynthetically Available Radiation (PAR)(Yamada et al., 2005). Although the satellite observed data are commonly endangered with inherent errors, in situ data are considered as a reliable validation tool to reduce these uncertainties.

Owing to the complex bio-optical characteristics of coastal waters (Vantrepotte et al., 2006) that classified as Case-2 waters, less studies have been tackled on these type of regions rather than open ocean and clear-water lakes [e.g. (Siegel et al., 2001; Smith et al., 1998)]. The Wadden Sea (located in southeastern part of the North Sea) is categorized as a shallow coastal sea with high benthic-pelagic primary production rates (Loebl et al., 2007). It is also considered as an optically complex area because of its high turbidity and quick changes in optically active substances concentration (Hommersom et al., 2009). In year 2009, a large part of the Wadden Sea was recently considered as a UNESCO World Heritage Site because of its international important role as one of the main breeding, staging and wintering regions for millions of migratory water birds (Heritage WS, 2012). It considers as one of the rich sources of food either for birds to temporarily rest and revitalize (Tentij et al., 2009) or several kinds of fishes. Besides, the interference of climatic alteration is damaging the fragile ecosystem of the sea. This climatic issue makes the investigation of WS phytoplankton as a preliminary element of sea food chain, either for up of water ecosystem (e.g. birds) or underwater (e.g. algae & fishes), more outstanding. This subject is important especially for stakeholders to realize how to face up to the consequences of climate change, and to become aware of essential adaptations to maintain this rich and attractive area for birds (Tentij et al., 2009).

This research deals with: 1- Spatial and temporal variability of primary production in Wadden Sea as derived from Earth observation (MERIS and MODIS) data in the last decade (from Jan-2003 till Mar-2012); 2- The possible contribution of PAR and sea surface temperature (SST) to the alteration of phytoplankton biomass, focusing on Chl_a, will be revealed comparing related images and time series.

1.2. Problem definition

The Wadden Sea has significant socio-economic and ecologic services which make it a strategic and rich nutritive territory for flora and fauna like birds and fishes. It is essential to evaluate the ecological services of this region with respect to climatic modulation. Important aspects here can be addressed as:

- Any plausible oscillation in climate variables will modify the supply of nutrients which in turn affects PP in water column. SST and PAR are two ancillary factors which are less considered for the area.
- The imbalance between phytoplankton growing and the sea carrying capacity is an important matter which will cause oxygen deficit in the deep water layer, the marine habitat alteration, migration of domestic species, and marine mortality as a result of changing the food-web cycle.
- Since 2002, no scientific published research was found to assess the long term variation of primary production neither for the entire Wadden Sea coastal area nor for the separated Islands owned to German, Danish or Dutch coasts.

1.3. Research objective

The main objective is to

- Understand a decade of temporal and spatial variation of primary production and phytoplankton biomass, in the Wadden Sea in relation to climatic variability of SST and daily PAR.

To achieve the main objective of the research the following tasks are identified:

- Apply the Vertically Generalized Production Model (VGPM) on the study area;
- Calculate long term spatio-temporal primary production rate using MERIS and MODIS 10 years records;
- Represent and reveal the plausible interaction of Chl_a growth, the main proxy of phytoplankton biomass, with available solar radiation considering the secondary essential climate variables interference in space and time.

1.4. Research question

In order to reach the aim of the research, questions below should be responded:

- How reliable VGPM is when applied to the Wadden Sea?
- What is the long term distribution of the modelled primary production in space and time in the Wadden Sea?
- Changes in which model input parameters will make the primary productivity more variable and sensitive?
- How can we attribute climate change-driven trends and time series to chlorophyll concentration variability?
- Are there any other physical factors which might influence on biological activities of Wadden Sea?

2. LITERATURE REVIEW

2.1. Remotely sensed primary production

Before launching the satellite instruments, in situ datasets as well as model outputs were considered as the main ways to acquire the required input for research performance. In this way plenty of studies have been done using field data either as a primary production evaluator in the water column [e.g. (Odum, 1955; Bot & Colijn, 1996; Migné et al., 2004; Isada et al., 2010)] or as a reliable criteria to validate the proposed PP models and remote sensing retrieved data [e.g. (Yamada et al., 2005; Cannizzaro & Carder, 2006; Honda et al., 2009). Pelagic primary production was estimated in the Dutch Wadden Sea utilizing field measurements and time series reduced from 440 $gCm^{-2}y^{-1}$ representing maximum PP for mid-1990s to 200–250 $gCm^{-2}y^{-1}$ in 2000 (Loebl et al., 2007).

Later on, advances in instrument design and data analysis techniques become stimuli which exhibit the feasibility of remote sensing approaches for applying in water colour studies (Klemas, 2010). Consequently, ocean-colour remote sensing has become a powerful tool for identifying spatial and temporal variability of surface phytoplankton biomass in terms of chlorophyll-a concentration (Moses et al., 2009; O'Reilly et al., 1998; O'Reilly et al., 2000) and phytoplankton functional types (McClain, 2009; Nair et al., 2008). Furthermore, in order to prevail the scarcity of field PP, ocean color data have been used to assess PP in the upper mixed layer of the water (Joint & Pomroy, 1981; Ishizaka, 1998; Kameda, 2003; Kameda & Ishizaka, 2005). Despite of studies done in different regions, the gains from specific areas cannot be easily generalized to the other coastal systems. Recently two different attempts were carried out in the Dutch Wadden Sea to evaluate primary production with Medium Resolution Imaging Spectrometer (MERIS), Moderate Resolution Imaging Spectrometer (MODIS) and Landsat data (Dube, 2012; Woldegiorgis, 2012). In current research we tried to apply MERIS (e.g. Chl-a) and MODIS (e.g. SST) ocean colour data simultaneously to promote the spatial resolution up to 300m as they are known as the best candidates for turbid waters. Figure 2-1 shows the basic characteristics of MERIS and MODIS from Freitas (2009)(after permission).

2.2. Primary production models

It`s been a long time that several scientists are struggling to develop a suitable model which can help them to obtain a well-estimated primary production rate from remote sensing. In 2008, Arst and his colleges proposed a semi-empirical algorithm for calculating the phytoplankton primary production in turbid waters. This algorithm has got two model versions, integral and spectral, which were able to compute the vertical profiles of primary production. Finally they conclude that although their models are strongly comparable with each other and perform well in turbid lakes, they were limited into conditions in which Chl-a concentration drops in the ranges of 4.2 to 79 mg m^{-3} and 0.1 to 3 m for Secchi depth (The depth at which the pattern on the Secchi disk is no longer visible due to turbidity).

However, bio-physical parameters such as surface Chl-a concentration, SST and PAR can also be the fundamental parameters to calculate primary productivity in the water column [e.g. (Longhurst et al., 1995; Antoine et al., 1996; Behrenfeld & Falkowski, 1997; Carr et al., 2006)]. In this way Behrenfeld and Falkowski (1997) proposed a simple linear model named Vertically Generalized Production Model (VGPM) to assess the rate of daily primary production in the euphotic layer of Open Ocean. It should be mentioned that because this model was basically built for general estimates of primary productivity at a global scale, it could generate significant over- or under-estimates of primary productivity at local scales (Siegel et al., 2001; Behrenfeld et al., 2002; Campbell et al., 2002). Therefore, a regional specified algorithm should be established for accurate estimates (Platt & Sathyendranath, 1988). To compensate the weakness of ocean color models, nowadays scientists have attempted to improve VGPM to be applicable in shallow depths or possibly Case-2 waters that are next to coastlines (Eleveld et al., 2007; Ishizaka et al., 2007; Milutinović & Bertino, 2011; Tripathy et al., 2012).

Specifications	MERIS		MODIS (Aqua)	
Name	Medium Resolution Imaging Spectrometer		Moderate Resolution Imaging Spectroradiometer	
Agency	European Space Agency (ESA)		National Aeronautics and Space Administration (NASA)	
Satellite	Envisat		Aqua	
Launched on	March 2002		May 2002	
Software	BEAM – Visat		SeaDAS	
Altitude	800 km		705 km	
Spatial Resolution	1040m x 1200m (reduced) or 260m x 300m (full)		1000m x 1000m for ocean bands	
Swath Width	1150 km		2330 km	
Viewing angle	68.5°		+/- 55°	
Imaging method	Push-broom		Whisk-broom	
Equator crossing time	10:30 (descending node)		13:30 (ascending node)	
Revisit time	~3 days		~2 days	
Repeat cycle of reference orbit	35 days		16 days	
Known corrections to be performed	Smile effect[1a]		Bowtie effect[1b]	
Default geolocation	Ellipsoid WGS84		Sinusoidal Projection	
Solar spectral range	Reflective		Reflective and emissive	
Number of pixels in Rows/columns	1121 / 1121 (reduced res.) 2241 / 2241 (full resolution)		1354 / 2030 (ocean bands)	
Wavebands	15, in the VIS and NIR		36: 20 in the VIS and NIR, 10 in the SWIR, and 6 in the LWIR	
Ocean colour bands	*Centre*	*Width (nm)*	*Centre*	*Width (nm)*
	412.5	10	412.5	15
	442.5	10	443	10
	490	10	488	10
	510	10	531	10
	560	10	551	10
	620	10		
	665	10	667 (hi/lo)	10
	681.25	7.5	678 (hi/lo)	10
	708.75	10		
	753.75	7.5	748	10
	761.875	3.75		
	778.75	15		
	865	20	869.5	15

Figure 2-1- MODIS and MERIS instruments main characteristics.

Eventually, Saba et al. (2011) assessed the efficiency of 21 ocean colour PP models by comparing their results of depth-integrated net primary production (NPP) to 1156 in situ ^{14}C measurements containing ten marine regions. Their results can, however, be used to understand which set of ocean models might be best to use for any given application. The models were then assorted based on best fit with the type of study area. As an example the model created by Kameda & Ishizaka (2005) is more efficient in shallower water (<250m) than Model 2 (Howard & Yoder, 1997) or Model 21 (Ondrusek et al., 2001). They believe that the best choice for deeper water can be Model 16 (Antoine & Morel, 1996). They also suggest applying Model 3 (Carr, 2002) for warm open ocean areas instead of Model 5 which might be specific choice for warm shallow waters near the shore (Scardi, 2001).

Table 2-1 represents 21 ocean colour PP models which evaluated by Saba et al. (2011).

Table 2-1- List of 21 ocean colour PP models which evaluated by Saba et al. (2011).

Model	Developer (Referenced)	Input Variable Used				Description
		Chl-a	SST	PAR	MLD	
1	Eppley et al., 1985	*				It ignores any external forcing or changes in physiological state.
2	Howard & Yoder, 1997	*	*	*	*	Maximum growth rate is parameterized as a function of SST. NPP is integrated to the MLD rather than to the euphotic depth.
3	Carr, 2002	*	*	*		It`s a variant of the original Howard &Yoder model. It integrates photosynthesis to the euphotic depth rather than to the MLD.
4	Dowell, unpublished data	*	*	*	*	It is based on the formulation obtained through dimensional analysis by . The photosynthetic parameter (P^B_{max}) is assigned by combining a temperature-dependent relationship for the maximum growth rate with a variable carbon to chlorophyll ratio.
5	Scardi, 2001	*	*	*	*	This model uses an artificial neural network to perform a generalized nonlinear regression of NPP on several predictive variables, including latitude, longitude, day length, MLD, SST, P^B_{opt}.
6	Morel & Maritorina, 2001	*	*	*		This is variant version of the Vertically Generalized Production Model (VGPM) .
7	Kameda & Iahizaka, 2005	*	*	*		This VGPM variant formulates P^B_{opt} as a function of SST and Chl-*a. It assumes that* phytoplankton consists of large and small phytoplankton groups, which have specific Chl-*a* productivities and temperature functions.
8	. Behrenfeld & Falkowski, 1997	*	*	*		The original VGPM is one of the most widely known and used NPP models.
9	Behrenfeld & Falkowski, 1997	*	*	*		This model only differs from Model 8 in that P^B_{opt} is estimated as an exponential function of temperature.
10	Tang et al., 2008	*	*	*		This model uses support vector machine (SVM) as the nonlinear transfer function between ocean primary productivity and Chl-a concentration, euphotic layer depth, PAR, maximum carbon fixation rate and day length.
11	Tang et al., 2008	*	*	*		The maximum carbon fixation rate was estimated as a SVM-based nonlinear function of SST, Chl-*a* and PAR. It is similar to Model 10.
12	Armstrong, 2006	*	*	*		Total productivity is empirically estimated and integrated from surface to 1 % euphotic zone and for a day light time as a function of SST, depth-dependent PAR, Chl-*a*, latitude, and seasons.
13	Armstrong, 2006	*	*	*		Photosynthesis per unit Chl-*a* was determined using an optimality-based model of nitrogen allocation and photoacclimation. Column productivity is the integral over the photic zone of (photosynthesis/Chl-*a*) x Chl-*a*
14	Asanuma, 2007	*	*	*		This is a variant of Model 13 where the photic zone was divided into two equal depth.
15	Marra & Trees, 2003	*	*	*		Productivity is calculated for the 100 layers in the euphotic zone and summed to compute the integral daily productivity.
16	Antonie & Morel, 1996	*	*	*	*	This is a spectral light-photosynthesis model. NPP is the product of integral biomass, the daily irradiance, and ψ*(the cross-section of algae for photosynthesis per unit of areal Chl-a biomass).
17	Uitz et al., 2008	*		*	*	This is a variant of Model 16 that considers separately the micro-, nano-, and pico-phytoplankton size classes to determine NPP.
18	M'elin & Hoepffner, 2011	*		*		It uses biogeographical provinces to define the values of the parameters to describe the light-photosynthesis curve and the Chl-a depth profile.
19	Smyth et al., 2005	*	*	*		The depth distribution of Chl-a is assumed constant throughout the water column. The model uses 60-minute time and 10-m depth steps at 5-nm wavelength resolution when run using the global datasets.
20	Ondrusek, 2001	*	*	*	*	This model assumes a vertically uniform Chl-a profile. Temperature dependence was assumed to be sigmoidal, and was based on a vertical profile of temperature derived from SST and MLD.
21	Ondrusek et al., 2001	*		*	*	This model is identical to Model 20 except the temperature dependent term is removed.

2.3. Primary production and climate variability

More than 70% of the globe`s surface is covered by the oceans and hence we must endeavour to understand how a changing climate (the weather averaged over a long period of time) will influence the biota either in terrestrial systems or in marine environments (Miller, 2004). Marin phytoplankton is responsible for relatively half of the global primary productivity and plays a key role in global biochemical variability (Feng & Zhu, 2012). The weather has affected the intensity of ocean mixing which, then, influences light penetrating levels, sea surface temperatures and the magnitude of nutrient recycling from deep layers. This state will, in next level, provoke phytoplankton photosynthesis and productivity (Richardson & Schoeman, 2004). In this way, numbers of researches have investigated how plankton, as the main primary and secondary component of aquatic food-web, can generate the variation of marine

ecosystem (Hays et al., 2005). Archer et al. (2000) showed that global ocean annual primary production has reduced more than 6% since the early 1980's.
Among plenty of important climate variables, the ones which influence the underwater lives directly or indirectly can be noticed as sea surface temperature, solar radiation, humidity, wind speed, evaporation, precipitation, cloud cover and so on. The outcome of global temperature variation, in combination with altered wind patterns, is to vary the oceanic mixing layer depth and to change the stratification of the surface ocean [e.g. (Sarmiento et al., 2004)] which in turn will confine the supply of nutrients to the euphotic zone, and is probably lead to reduced PP (Henson et al., 2010).
Discovering the climate change-origin instability over the Wadden Sea will help in monitoring and assessing the growth of phytoplankton in the water for ecological and environmental sustainability of the region. We restrict this study to photosynthesis active radiation and sea surface temperature as two effective representatives of climatic change. These are assorted as the potential climatic variables to all of which less studies has been done for the Wadden Sea region.

2.3.1. Sea Surface Temperature (SST)

Based on hydrographic properties such as temperature, coastal regions differs from oceans and offshore regions particularly if they consist of several isolated areas (MacKenzie & Schiedek , 2007). As such, tracing long term changes of climatological systems will help to detect the pattern of coastal ecosystem either biologically or physiologically. There are ample of studies in which scientists used remotely sensed products of sea surface temperature in order to study its influences on other climatological factors as well as biological activities [e.g., Fox et al., 2005; Messie & Radenac, 2006; Galbraith et al., 2012; Feng & Zhu, 2012]. Several studies have been done on investigating sea skin temperature consequences [e.g. (Kaplan et al., 1998; Silva et al., 2006; MacKenzie & Schiedek, 2007)], while less considered marine ecosystem as a sensitive and risky subject to take into account especially in contemporary years.
The Wadden Sea coastal area is characterized as a shallow water system (Loebl et al., 2007), therefore it has got a relatively quick reaction to air temperature variation. So, it has a different response to the variation of SST (van Aken, 2009). Since few number of studies have been presented the variation of SST in WS coastal region which mostly focused on Dutch coasts [e.g., (van Aken, 2009)], we decided to evaluate the long-term MODIS SST variation and its effect on phytoplankton biomass growth for the whole WS.

2.3.2. Photosynthetically Active Radiation (PAR)

Gain radiation can be distributed as full at the sea surface to almost zero at complete darkness deep in the water depending on the amount of permeated light rate through the water column (Gilmore, 2006). Based on the study done by Harris and Lott (1973), photosynthesis rates almost certainly depend on level of available radiation.
Photosynthetically Available Radiation is nothing more than the portion of solar radiation received by the water body after passing through atmospheric limited factors such as aerosols, cloud covers and etc. It is commonly evaluating for water surface through euphotic depth (Z_{eu}). Evermore scientists attempt to estimate incident PAR using satellite [e.g. (Eck & Dye, 1991)]. Here MODIS Ocean Color PAR images were utilized to compute time series of daily PP.

3. MATERIALS

3.1. Study area

3.1.1. The Wadden Sea

The Wadden Sea is located between North Sea and the Danish, German and Dutch coastline. It stretches for 450 km along the coast from Den Helder (NL) at 53°N to the peninsula of Skallingen (Denmark) at 55°30' N (CWSS, 2008). With regard to ecological and biotic aspect it can be divided into three main regions including the Northern Wadden Sea, the Southern Wadden Sea and the Central Wadden Sea (CWSS, 2008), each of which in turn compartments into subareas. Since the sea covers a total area of almost 13,000 km² (Tunnell, 2002), it can be categorized as one of the largest wetland regions in the world (Figure 3-1).
The Wadden Sea is optically crucial and complex region according to its shallowness, high turbidity and non-uniform variation in concentration of optically active substances. It is prominently known due to its great biological productivity and diversity of coastal ecosystems.

3.1.2. West Frisian Islands (WFI)

The Wadden Sea has been separated from North Sea by a series of barrier islands. The Frisians are consists of several regions created a chain of islands extended from 5 to 32 km (Britannica, 2012). It is divided into North Frisian, East Frisian and West Frisian Islands (WFIs) which belong to Germany and Denmark, Germany and Netherlands respectively (Britannica, 2012).
West Frisian Islands are included 5 inhabited islands known as Texel, Vlieland, Terschelling, Ameland and Schiermonnikoog which cover most part of Southern WS. These islands look like deltas which have been produced as a result of flooding and land erosion (Worldatlas, 2012). In this way, regionally different characteristic is expected from each of the aforesaid islands, since they have been fed by various nutrient-rich sources such as streams and tidal inlets. This might generate a different pattern of marine primary producing variability in each of these islands as a result of distinctive bio-optical, bio-physical and bio-logical activities. This motivated us to compare Frisian Islands with the whole Wadden Sea with respect to primary production oscillation. Figure 3-2 indicates the location of West Frisian Islands.

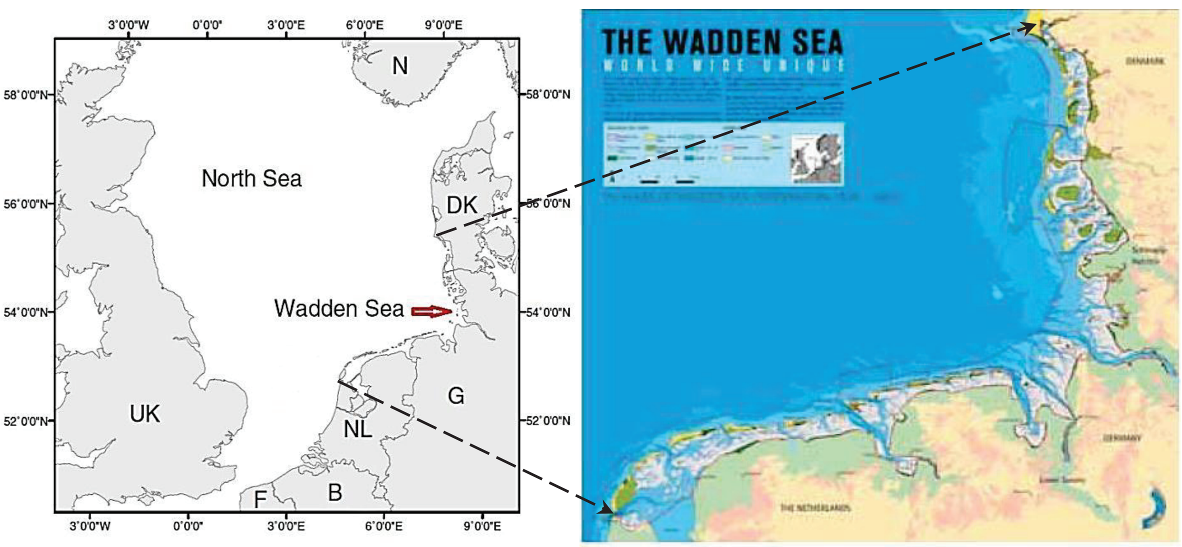

Figure 3-1- The schematic view of the study area and its boundary (The Wadden Sea) (CWSS, 2008)

Figure 3-2- Map of West Frisian Islands (Worldatlas, 2012).

3.2. Primary production in Wadden Sea

The primary production in the Wadden Sea . Over the last decades, a two- to threefold increase in phytoplankton primary production has been reported throughout the entire Wadden Sea (Cadée, 1986; Cadée & Hegeman, 1993; de Jonge et al., 1996; Asmus et al., 1998). However, the rate of productivity by phytoplankton is limited with increasing the depth as a consequence of less penetrated light in turbid waters. At present, the annual summed pelagic and benthic production is estimated at ~170gC$m^{-2}y^{-1}$ for the Marsdiep tidal inlet (Postma & Rommets, 1970), whereas for the western Wadden Sea, this has been approximated at ~55 to 80gC$m^{-2}y^{-1}$ annually before industrialization (van Beusekom, 2005).

3.3. Data sets

In this study two types of data sets comprising satellite products and field data were used. The in-situ measurements were obtained from 3 different databases whereas Earth observation products were derived from NASA data centres. In following sections, the explanation of each sort of retrieved data was presented. Detailed information on the whole dataset used in this work is represented in table 3-1.

Table 3-1- Required data characterization for processing the research steps.

No	Data	unit	Symbol	Acquisition	Source	Application
1	**Chlorophyll-a**	mg m^{-3}	Chl-a	-MERIS L1B- FR	ESA	-Validation
				-in situ	MWTL	-VGPM input
2	**Diffuse Attenuation Coefficient**	m^{-1}	K_d	MERIS L1B- FR	ESA	-To calculate Z_{eu}
3	**Euphotic Depth**	m	Z_{eu}	f(K_d)	-	-VGPM input
4	**Photosynthetically Active Radiation**	E $m^{-2}d^{-1}$	PAR	-MODIS Ocean Color-L2- MOD22	NASA-Ocean Color	-VGPM input - To detect interaction with Chl-a
5	**Sea Surface Temperature**	^{o}C	SST	-MODIS- Ocean Color-L2- MOD28	NASA-Ocean Color	-To calculate P^B_{Opt} -To detect interaction with Chl-a
6	**Optimum Carbon Fixation**	mg C(mg $Chl)^{-1}$ h^{-1}	P^B_{Opt}	computed	Computed from SST	-VGPM input
7	**Photoperiod**	hr	Dirr	f(Lat/Long,day)	-	-VGPM input
8	**Global Radiation**	J cm^{-2}	Q	in situ	KNMI	-PAR verification
9	**Air Temperature**	^{o}C	TG	in situ	KNMI	-SST verification

3.3.1. Satellite data and products

MODIS (vital instrument of Terra and Aqua satellites) provides global covered images every 1 to 2 days with different spatial resolutions, 250m at nadir, 500m and 1 km, in 36 spectral bands (http://modis.gsfc.nasa.gov/about/design.php). On the other hand, MERIS (core push-broom imaging spectrometer of ENVISAT funded by ESA) senses the global earth`s sun radiation reflectance in 15 spectral bands every 3 days with spatial resolution of 300 m (http://wdc.dlr.de/sensors/meris/).
We used two EO datasets of MERIS to derive IOPs (Inherent Optical Properties) and MODIS products of SST and PAR. Cloud free MERIS Level 1 Full Resolution (FR) images were applied to derive Chl-a concentration ($mg.m^{-3}$) and Euphotic Depth (m) from Eolisa-ESA[1]. The MODIS level 2 Ocean Colour datacentre[2] were utilized to achieve daily 11 µm SST in degree Celsius (^{o}c) and PAR in Einstein per square meter per day ($E.m^{-2}d^{-1}$).

3.3.2. In situ measurement

The in-situ data sets include point measured Chl_a concentration which was acquired using Monitoring Waterstaatkundige Toestand des Lands (MWTL)[3] plus daily mean temperature (TG) and global radiation (Q) which were drawn out of The Royal Netherlands Meteorological Institute (KNMI)[4] database. We tried to choose the closest ground measurement centres (KNMI stations) to each relevant study island. Figure 3-3 represents the exact point of each selected KNMI station.
Thereafter, the entire derived field measurements were then used to validate and verify remote sensing data for the region. Table 3-2 declares the characteristics of all handled stations for verification. Complete list of MWTL field stations was represented in Appendix1.

Figure 3-3- Location of picked in-situ ground stations (marked by star)

[1] https://earth.esa.int/web/guest/home
[2] http://oceancolor.gsfc.nasa.gov/
[3] http://www.rijksoverheid.nl/documenten-en-publicaties
[4] http://www.knmi.nl/climatology/daily_data/selection.cgi

3.4. Photoperiod (Dirr)

Photoperiod data (Dirr) which is one of the dominant parameters in calculating production rate stands for daily solar hours or duration of phytoplankton daily exposure to sun radiation. According to the latitude and longitude of the study area and also Julian day of the year, Dirr can be computed in decimal hours in order to apply in primary production model. Here, an IDL code was provided by Salama (IN PLACE project) to compute pixel by pixel Dirr for the entire study period.

Table 3-2- The characteristics of selected in-situ stations for SST and PAR verification

No	name	Coordinate		type	Data & unit	Duration	Source	Application
		Lat	Lon					
2	**De Kooy**	**52.9**	**4.7**	**Meteorological**	**Global Radiation** ($J.cm^{-2}$) **Air Temperature** (^{o}c)	10 years (daily)	KNMI	verification
3	**Vlieland**	**53.2**	**4.9**					
4	**Hoon**	**53.3**	**5.3**					
5	**Lauwersoog**	**53.4**	**6.1**					

4. METHDOLOGY

Recording undesirable signals of unwanted targets by satellite sensors might usually produce some sort of uncertainty on received data which should be removed. Improve Contrast Over Ocean and Land (ICOL) and Coastal Case-2 Regional processor (C2R) were pre-processed on MERIS L1 data in order to correct the adjacency effects and atmospheric interferences respectively. In order to speed up the procedure and since we were working on a long time series, Bulk Processing script for MERIS images would be helpful. The script was developed by Brockmann Consult (2011) team which was then improved by Salama (IN PLACE project) to apply multiple tasks at the same time. The original version of the code is accessible by http://www.brockmann-consult.de/beam-wiki/display/BEAM/Using+BEAM.
Vertically Generalized Production Model (VGPM) is the main model which was utilized in order to estimate the primary production. The explanation of each model is described in details in the following sections. In order to achieve the aim of this study the stages shown in Figure 4-1 have been applied. The parameters entailed to enforce into the VGPM include the chlorophyll-a (Chl-a), Euphotic depth (Z_{eu}) and water leaving reflectance which were retrieved using the aforesaid bulk script. 1-km spatial resolution Sea Surface Temperature and Photosynthetically Active Radiation (PAR) products were derived by MODIS L2 Ocean Colour and downscaled to spatially match with MERIS 300m images.

4.1. Improved Contrast Over Ocean and Land (ICOL)

It has always been an issue that satellite instruments can detect adjacency signals as well as the target signals. In this way neighbour land surfaces signals can effect on what satellite receives on top of the open water which in turn produce artificial traces on images. Such algorithms like the Improved Contrast Over Ocean and Land (ICOL), which was developed by (Santer et al., 2007) and (Santer & Zagolski, 2009), can help to correct images for adjacency influences before applying atmospheric correction. It is a processor tool of BEAM VISAT software package which is able to correct for an area up to 30 km perpendicular to the coast (Kratzer & Vinterhav, 2010). This algorithm was recently examined by Chawira (2012) and Andebrhan (2012) for the Dutch Wadden Sea in which they agreeably concluded a better retrieval of Chl_a after adjacency effect correction.

4.2. Coastal Case-2 Regional Processor (C2RP)

The Coastal Case-2 is a model constructed by Doerffer et al. (2006) and implemented in Beam Visat software. This algorithm corrects the image for atmospheric influence and derives optical properties and concentrations of water constituents. We used C2R processor to analyse and retrieve the required IOPs out of MERIS Level 1 top of atmosphere radiances (TOA). It is neural network (NN) based method which is developed for coastal and turbid waters (Moses et al., 2009). The processed product concludes water leaving reflectance of Inherent Optical Properties (IOP) such as Chl-a concentration, diffuse attenuation coefficient (K_d) and other water constituents.

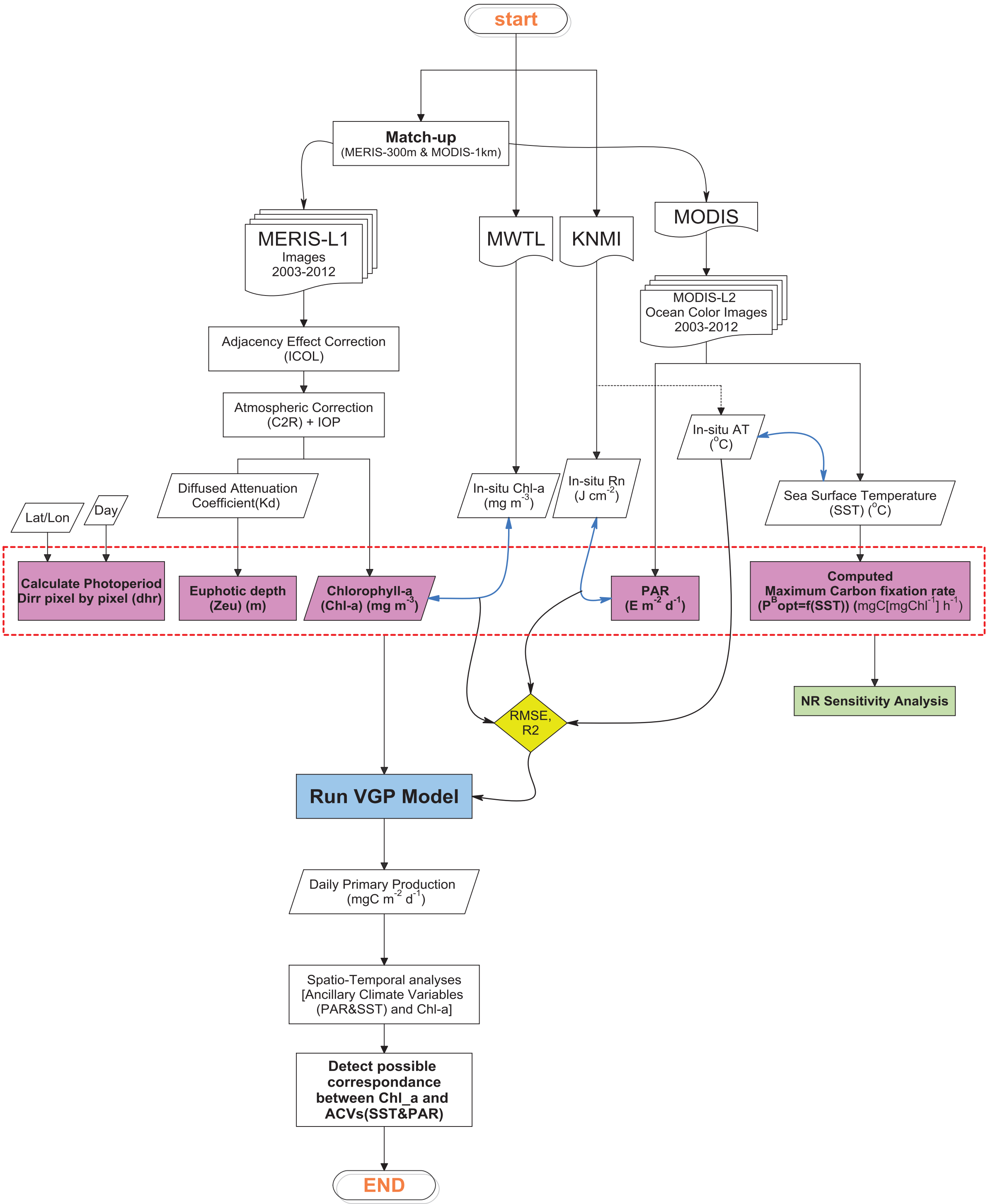

Figure 4-1- Flowchart of research procedure

4.3. Spatial and temporal match-up

Since current study was being done in daily time scale and in order to obtain primary productivity in fine resolution (300m), MERIS and MODIS acquired images were matched up either spatially and temporally., Before doing match-up and as the main part of the analysis was going to be done for the entire Wadden Sea coastal area, those MERIS atmospheric corrected images which have not covered the entire area or polluted by clouds was removed. Then an IDL code was prepared by Salama (IN PLACE project) to

apply the bulk daily matching. Figure 4-2 shows the initial number of data as well as remained data frequency after matching temporally. Thereafter, 1-km MODIS SST and PAR images were converted to MERIS 300m resolution performing Nearest Neighbour method using available ENVI resampling code.
It should be reminded that MODIS L2 (SST & PAR) images were geo-referenced in Geographic Lat/Lon (WGS84) projection using the IDL code of ENVI Plugin for Ocean Colour (EPOC) after converted to batch mode with the help of Salama.

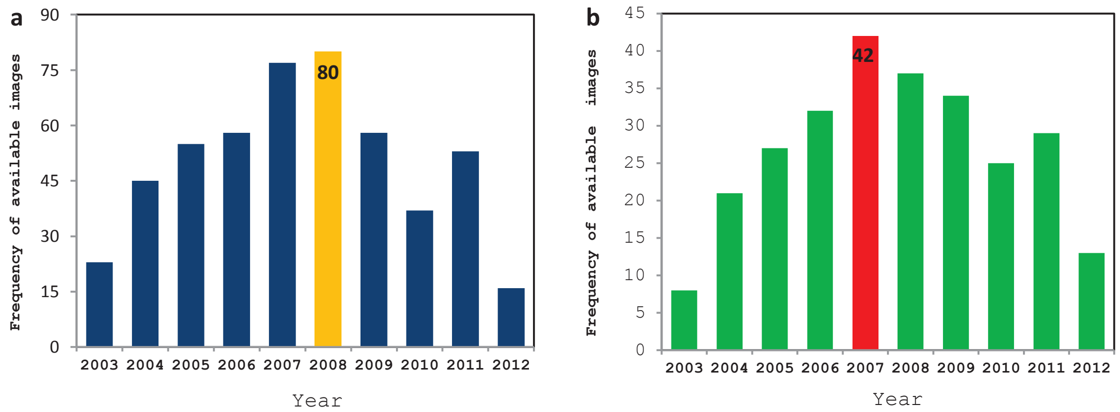

Figure 4-2- Frequency of MERIS L-1 images before (a) and after (b) temporal match-up (2003-2012).

4.4. Data validation and verification

Validation and verification are two distinctive indicators for level of accuracy and certainty of available data. In this way we endeavoured to assay the accuracy of satellite retrieved SST and PAR with the help of available relevant field data. For this aim, we performed validation for Chl_a and verification for SST and PAR usable data series. These procedures have been done for two important reasons: first to increase the certainty of VGP Model output for the WS coastal area and second to examine the accuracy of physical and biomass data since they are going to be compared to achieve the second aim of the study.

4.4.1. Chl_a validation

We used in-situ Chlorophyll_a data in 102 stations determined by Rijksoverheid (for 10 years). Afterwards field data which are matching MERIS pixels in time and location were extracted using Chl_a images. Regression analysis was applied to estimate the accuracy of C2R-based Chl_a with respect to field measurements.

4.4.2. SST & PAR verification

All related studies have confirmed the critical mutual interference between SST and air temperature [e.g., (Rueda et al., 2009; Silva et al., 2006; Galbraith & Larouche, 2011; Galbraith et al., 2012)]. Although ground-based measurement of air temperature cannot decisively indicate the sea temperature variations, it is the only representative that generates the dominant effect on sea-air temperature which will subsequently cause the SST fluctuations. Another type of the story can be defined to explain the correlation between global radiation and available sea surface radiation. Received radiation (at 0.4–0.7 µm) by underwater phytoplankton is a fraction of solar exposure reaching the sea surface. KNMI in-situ global radiation includes shortwave and longwave radiation whereas MODIS PAR products covers the wavelength in visible spectrum.
Here, SST and PAR were verified by comparing respectively to in-situ measured air temperature (TG) and global radiation (Q), easily accessed by KNMI climatological database, over West Frisian Islands (WFIs). The verification was solely done for the year 2007 since it carries the heaviest data load comparing to other 9 years.

4.5. Vertically Generalized Production Model (VGPM)

In this research VGPM, which is developed by Behrenfeld & Falkowski (1997), was applied to compute depth-integrated daily primary production (PP) for the duration of ten years from Jan-2003 till Mar-2012. The advantage of the VGPM is that it has minimal parameterization of input variables and incorporates remotely sensed satellite data to derive PP (Tripathy et al., 2012). The model disadvantage is that it`s actually developed for open ocean so it might result in output over- or under-estimation.
The parameters which are required to the model are: Chlorophyll-a concentration (Chl_a), euphotic depth (Z_{eu}), photoperiod (Dirr), PAR and Optimal Carbon fixation rate within a water column (P_b^{Opt}). Since there is still no direct method available to calculate the P_b^{Opt} parameter, it`s frequently been applied by scientists as a function of Sea Surface Temperature (SST) (e.g. Tripathy et al., 2012).
The main equation describing the relationship between surface chlorophyll-a and depth-integrated primary production is expressed as follows:

$$PP = 0.66125 \times P^B_{opt} \times PAR/(PAR+4.1) \times \text{Chl-a} \times Z_{eu} \times Dirr \qquad \text{(Eq.1)}$$

PP: Primary Production ($mgCm^{-2}d^{-1}$)
Chl-a: chlorophyll-a concentration ($mg\ m^{-3}$).
Dirr: Daily photoperiod (in decimal hours)
PAR: Sea surface daily Photosynthetically Active Radiation ($E.m^{-2}d^{-1}$)
Z_{eu}: Euphotic depth (m)
Which in turn can be defined applying Diffused Attenuation Coefficient (K_d) as:

$$Z_{eu} = (4.605)/K_d \qquad \text{(Eq.2)}$$

P_b^{Opt}: Optimal daily carbon fixation rate within a water column [mgC (mg Chl)$^{-1}$ h^{-1}]. Depending on temperature value, P_b^{Opt} can be modeled and equated as follows:

$$P_b^{Opt} = \begin{cases} 1.13 & \text{if } T < -1.0 \\ 4.00 & \text{if } T > 28.5 \\ P^B_{opt} & \text{other values of } T \end{cases}$$

$$P_b^{Opt} = 1.2956 + 2.749\times10^{-1}\,T + 6.17\times10^{-2}T^2 - 2.05\times10^{-2}T^3 + 2.462\times10^{-3}T^4 - 1.348\times10^{-4}T^5 + 3.4132\times10^{-6}T^6 - 3.27\times10^{-8}T^7 \qquad \text{(Eq.3)}$$

where T is sea surface temperature in ^{o}c.

4.6. Nominal Range Sensitivity Analysis (NRSA)

When dealing with a mathematical model, it`s also essential to highlight the sensitivity of input variables on obtained outputs using methods which can assign a distinctive rank to each critical parameter (Ostermann, 2005). Generally it is classified as local methods and global methods (Saltelli et al., 2000; Muleta and Nicklow, 2005) while some scientists categorize it into mathematical, statistical and graphical approaches (Frey and Patil, 2002). Among these methods, mathematical approaches are able to evaluate the sensitivity of a model output to its input variation domain (Frey et al., 2003). Two prominent and common mathematical methods are the Nominal Range (NRSA) and Differential Sensitivity Analysis (DSA)(Frey and Patil, 2002; Helton and Davis, 2003).
NRSA, also known as local or threshold sensitivity analysis (Cullen & Frey, 2001), is commonly being equated as shown in Eq4. In this way, each time one input variable varies athwart its overall range of possible values while keeping all other variables in their baseline (nominal) values. The calculated value was then brought up as the sensitivity of the corresponded parameter (Tang et al., 2007).

$$NRSA = \frac{Output_{\max input} - Output_{\min input}}{Output_{\text{nominal } input}} \quad \text{(Eq.4)}$$

NRSA is well-certified to apply for linear models whereas the analyst is ideally able to devote feasible ranges to specified input (Frey and Patil, 2002). Since the VGPM is considered as an one-dimensional linear model, we decided to operate the NRSA method for this study. Therefore, besides linear regression analysis and in order to investigate the sensitivity level of VGPM primary production to each single utilized parameter changes, including Chl_a, PAR, P_b^{Opt}, Dirr and Z_{eu}, Nominal Range Sensitivity Analysis was applied. The mean of each variable was considered as its nominal value.

5. RESULTS

In this section we show the outcomes of pre-processing and processing steps were described in previous sectors. To do this, we prepared the results in different forms of graphs, images or even comparing them using statistical approaches. The VGPM inputs and output were distinctively assessed either in disparate time scales (daily to a decade of 2003-2012) or different spatial scales (Frisian Islands to the entire Wadden Sea region). It should be mentioned that all the results which obtained in current research are based on the number of selected remote sensing data gathered over the study area after temporal match-up during aforesaid 10 years.

5.1. Atmospheric correction

In current research, we applied atmospheric effect correction on MERIS L1 images in order to retrieve the essential IOPs to run the VGPM. Atmospheric effect correction was done using C2R model. Figure 5-1 shows the same MERIS image before and after correction for the Wadden Sea. As seen, even after applying the C2R model, still the shadow of cloud can be observed which delivers the disability and weakness of the model. This will influence the IOPs quality which in turn will be appended to PP model. What we did here to decrease the uncertainty is to pick up those images in which almost no cloudiness sign could be seen at least over the entire study area. I should mention that the clear sky images were selected visually. Figure 5-2 illustrates one of the final chlorophyll images were retrieved from a clear sky image after C2R procedure.

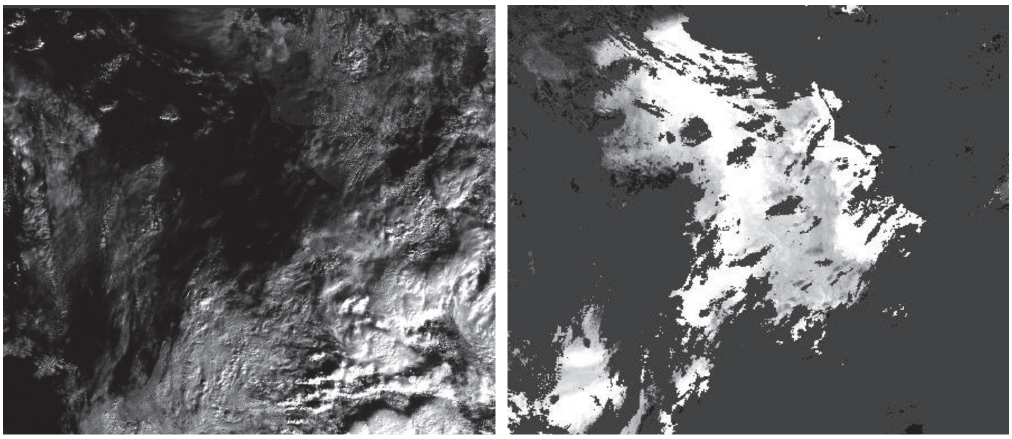

Figure 5-1- MERIS Full L1 Radiance image before (left) and after (right) adjacency and atmospheric effect correction (06-Feb-2008).The weakness of C2R model to remove cloud effect.

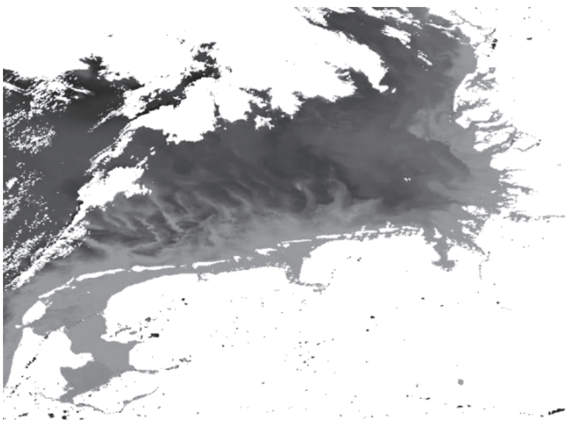

Figure 5-2- Typical MERIS 300m chlorophyll_a image retrieved by applying atmospheric effect correction on a clear sky image (09-Apr-2008).

5.2. Validation and verification

5.2.1. Chl_a validation

Since chlorophyll is one of the main variables to obtain the preliminary aims of this research, it`s been validated using 102 daily point stations data. For the first step, the bias between two sets of data was calculated about 3.52mg.m^{-3} which then was subtracted from Remote Sensing data since they are usually overestimated because of different way of measuring. Thereinafter linear regression analysis was done for the year 2009 which has the largest amount of Chl_a data after time matching (Figure 5-3). The results shows that there is a rather strong correlation between datasets with R^2=0.56 and MAE less than 4.5mg.m^{-3}.

The main reasons which might create the bias between in-situ and remote sensing Chlorophyll_a were summarized as:

1- The weakness of C2R model to derive the IOPs;
2- Inconsistency of sampling methods in space or time (point-based bottle versus 300m sample per pixel)
3- Different approximation processes (RS Chl_a is integrated through a great volume of water while in-situ samples include ~1 litre of water) (Morales et al., 2011)

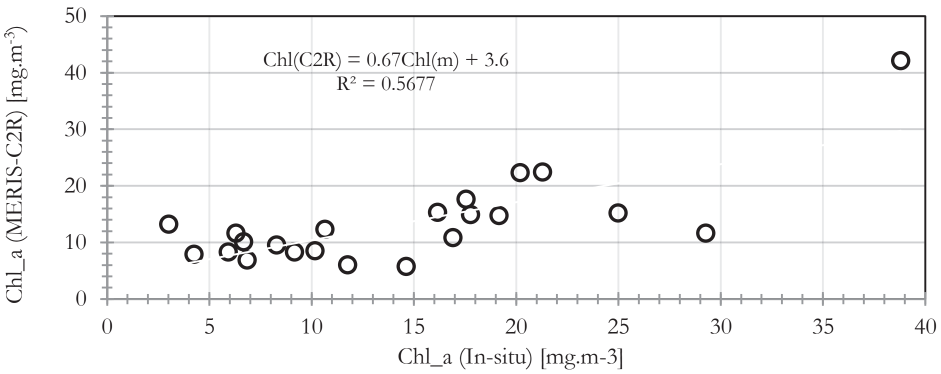

Figure 5-3- Linear regression trend result between Chl-a modelled by C2R and field measurement Chl_a concentration. The comparison was only done for the year 2009.

5.2.2. SST verification

The daily in-situ air temperature (AT) data are inscribed down at a measuring level of 1.5 meter and averaged for 24 observations for each 365 day. Figure 5-4 illustrates the temporal behaviour of MODIS daily SST and air temperature for the year 2007 with the correlation coefficient larger than 0.85 and maximum monthly value in August. SST daily values ranges between -1.97^{o}c and 20.25^{o}c while air temperature varies in the range of -3.5^{o}c and 22.9 ^{o}c. It seems evident that SST values have distributed in a wider range than air temperature.

Type 1 Linear regression between SST and AT was constructed for each selected Frisian Islands which suggests a reasonable linear relationship between two variables with the slope near 0.8 and correlation coefficient around 0.85 depending on the location (Figure 5-5). The alteration of determination coefficients in different islands is because of the impact of atmospheric dynamical instability (Silva et al., 2006). Although by looking at the R^2 and RMSE, the hypothesis that air temperature has outstanding effect on sea heat flux can be confirmed (Silva et al., 2006). Thus we are allowed to continue the research into further steps (Table 5-1).

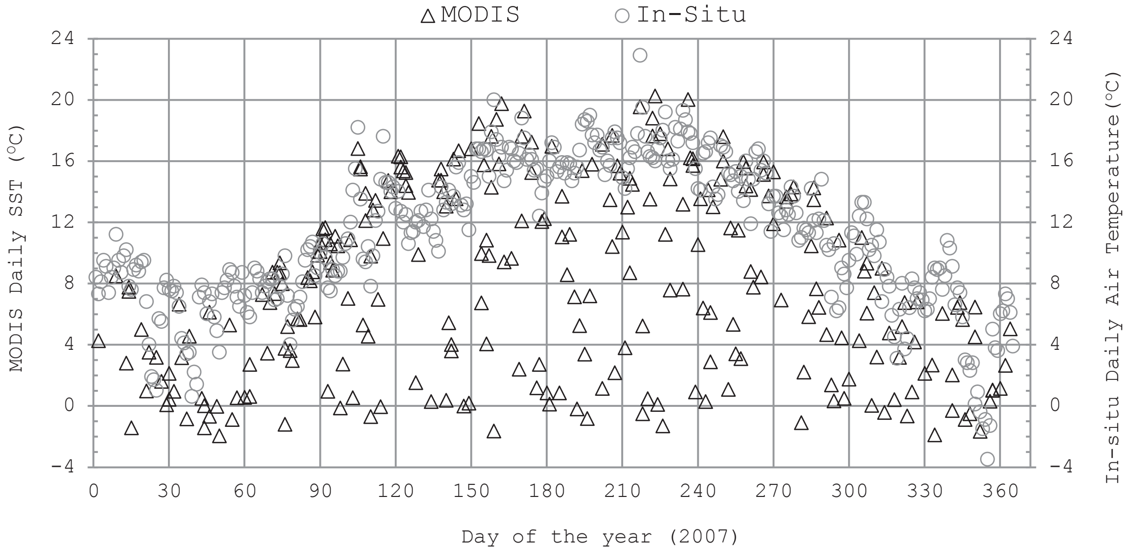

Figure 5-4- Comparison between daily MODIS sea surface temperature and the observed air temperature (R2=0.87). SST verification for Texel island.

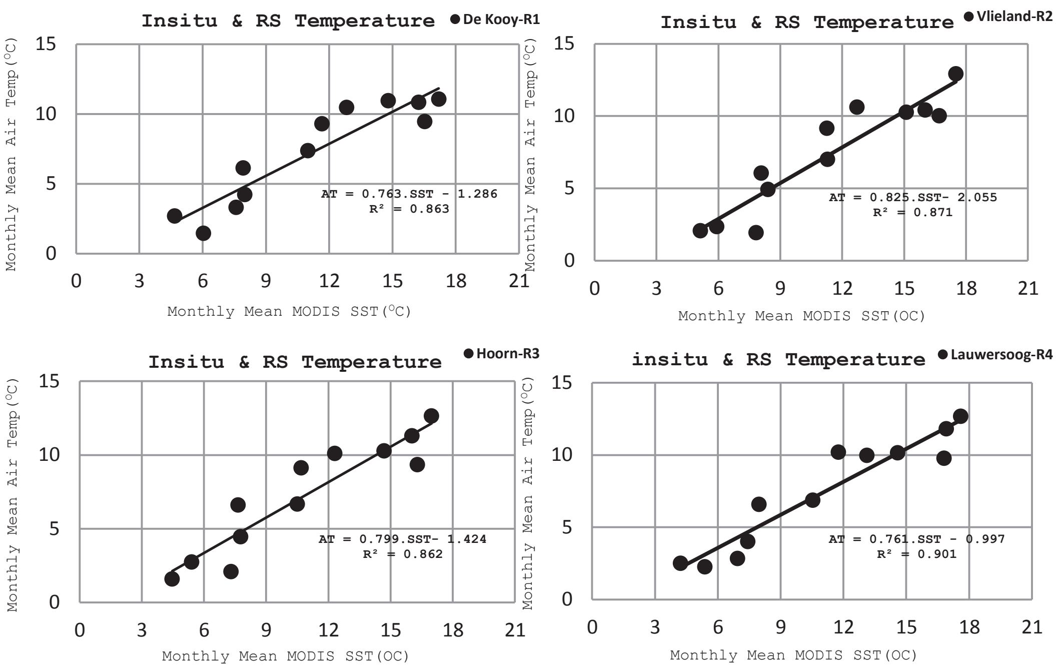

Figure 5-5- Average monthly SST versus monthly air temperature using linear trend in year 2007 for 4 West Frisian Islands: R1(Texel), R2(Vlieland), R3(Terschelling), R4(Ameland)

Table 5-1– Statistical result of linear regression of monthly SST versus air temperature calculated for West Frisian Islands (2007)

MODIS Sea Surface Temperature Verification				
SST vs AT(°c)	RMSE	R²	slope	intercept
Texel	4.26	0.86	0.76	-1.28
Vlieland	4.31	0.87	0.82	-2.05
Terschelling	3.94	0.86	0.79	-1.42
Ameland	3.98	0.90	0.76	-0.99

5.2.3. PAR versus global radiation

One year of MODIS daily PAR and global solar radiation were compared for Texel islands for the year 2007. To uniform the unit of parameters, PAR values were multiplied by 21 to convert from $E.m^{-2}d^{-1}$ into J/cm^2. As it is demonstrated in Figure 5-6, both parameters follow almost the same temporal behaviour with the coefficient of determination about 0.89. The lowest value of solar radiation (~25 J/cm^2) refers to winter season while in summer the earth receives the highest amount of solar radiation (~2900 J/cm2). Figure 5-7 shows the percentage ratio between PAR and total sun radiation calculated in monthly time scale for relevant stations to Texel (R1), Terschelling (R3) and Ameland (R4). No in-situ data were available for station close to Vlieland. The ratio varies basically between 35.5% in January and 55.7% in November. The PAR ratio is strongly influenced by atmospheric parameters such as air mass, water content and sky cloudiness as well as aerosol density (Gonzalez and calbo,2002), (Wang et al., 2007). The reason of achieving high September value is because of rising the amount of water vapour in the atmosphere in this period of time which in turn causes the decreasing of received sun radiation by the ground (Jacovides et al., 2003).

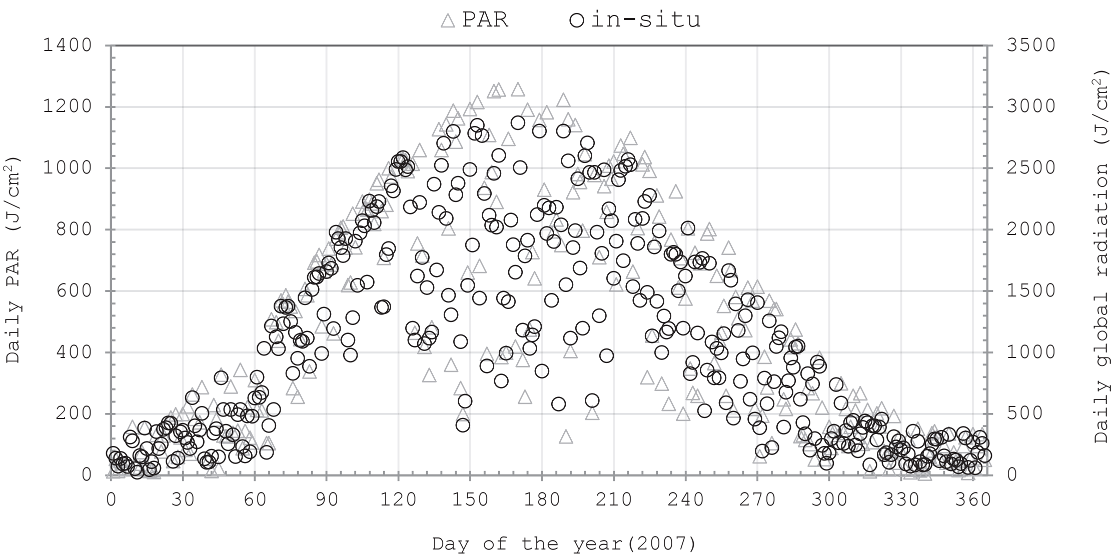

Figure 5-6- Daily variation of Texel MODIS PAR and De Kooy in-situ global radiation for the year 2007

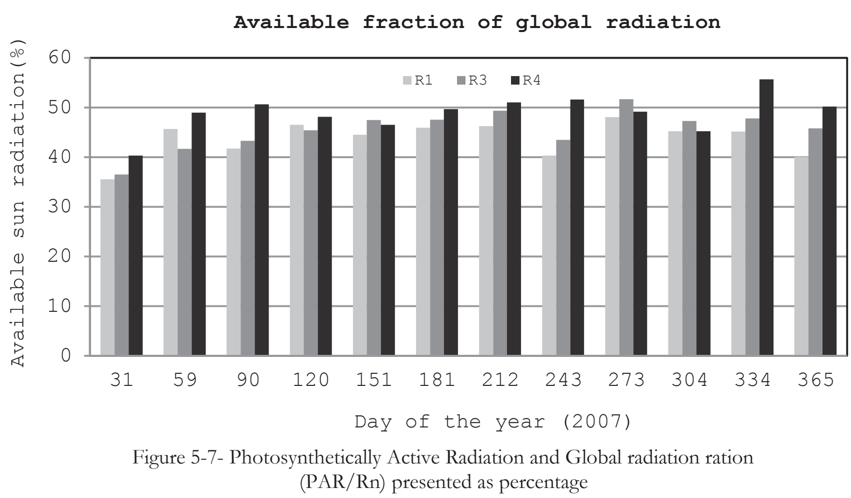

Figure 5-7- Photosynthetically Active Radiation and Global radiation ration (PAR/Rn) presented as percentage

Figure 5-8 shows the statistical results for each site concluded by applying linear regression procedure. As revealed, there is a strong agreement between two variables which confirms the accuracy of satellite-based PAR data. The coefficient of determination is around 0.98 for almost all areas which explains the high level of relevancy between two variables since one is a ratio of another but restricted wavelength.

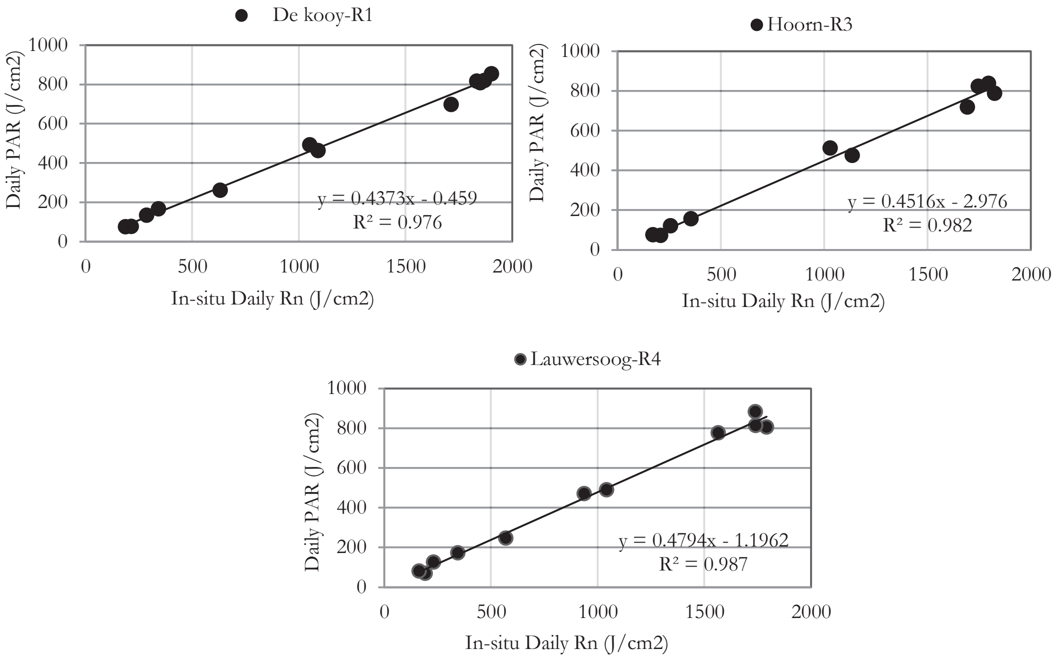

Figure 5-8- Average monthly PAR versus monthly global radiation using linear trend in year 2007 for 4 West Frisian Islands: R1(Texel), R2(Vlieland), R3(Terschelling), R4(Ameland)

5.3. Spatial and temporal time series of VGPM inputs

Long term spatial and temporal time series of PP were performed and demonstrated either as relevant maps or graphs as well as tables.

In order to separate the North Sea area and to focus the analysis only on WS, 5 different regions where located to represent the whole study area. This includes the Wadden Sea and 4 West Frisian Islands coastal areas (Figure 5-9). Time series analysis results which developed for the defined region of interests (ROIs) are discussed in following sections.

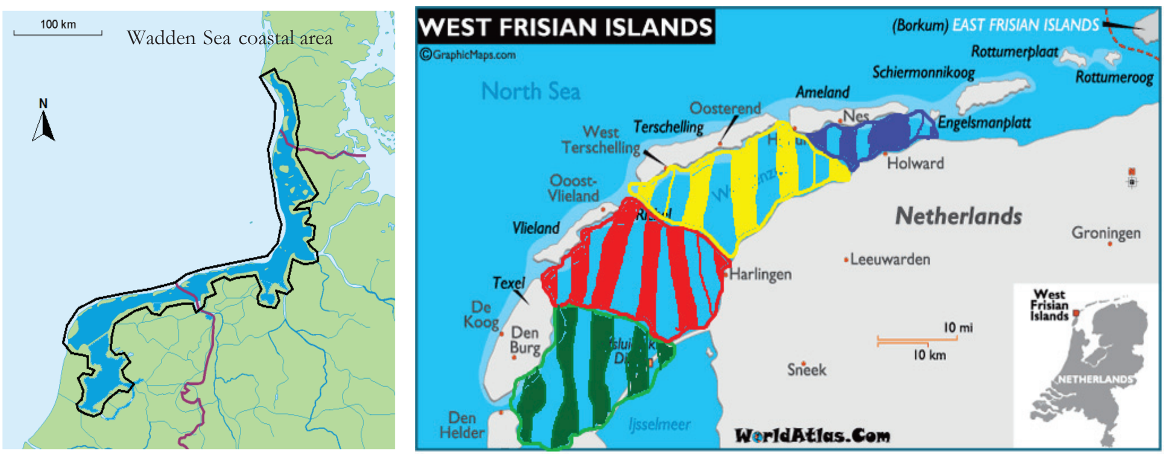

Figure 5-9- Schematic map of region of interests separated for the time series analysis. Wadden Sea coastal area (left) and West Frisian Islands (right) (Worldatlas, 2012)

5.3.1. VGPM input variables

In order to run the VGPM, we used two retrieved IOPs (Chl_a and Z_{eu}) from MERIS 300m L1 images and two MODIS 1-km L2 products (SST and PAR) plus Dirr. Spatial (resampling) and Temporal match-up stage were then done to prepare the inputs of the primary production model. The processed parameters were next forced to VGPM by which finally depth integrated PP was obtained as a daily output. This section is going to explain the results of pre-processing exerted on each single 5 variables accompanying with the statistical analysis done for them.

5.3.1.1. Chlorophyll_a concentration

After pre-processing the Chl_a images, the statistical analysis was performed for the remained potential data. As the main indicator of phytoplankton growth, Chlorophyll_a is calculated in $mg.m^{-3}$ and depicted as both temporal and spatial variation. Table 5-2 explains the monthly results for the selected ROIs as well as WS. The minimum and maximum values of WS daily Chl_a are computed about $3.4mg.m^{-3}$ and $28.4mg.m^{-3}$ which belong to 18th October of 2003 and 14th January of 2007 respectively. 10 years calculation shows that WS experiences the highest and lowest values of monthly mean Chl_a concentration of $26.9mg.m^{-3}$ in January 2007 and $10.9mg.m^{-3}$ in July 2005. The mean monthly amount of Chl_a rises up from Texel region to Ameland island. Texel with the coefficient variation up to 31% is classified as the most varied region among other coastal areas during the study period (2003-2012).

Table 5-2- Statistical analysis results calculated using monthly Chl_a data for defined ROIs from 2003 till 2012.

Chl_a ($mg.m^{-3}$)	WS	Texel	Vlieland	Terschelling	Ameland
MIN	10.9	3.6	12.0	13.1	2.5
MAX	26.9	29.1	31.2	27.1	32.2
MEAN	16.5	15.7	18.1	19.7	21.9
Std.	2.9	4.9	3.1	2.9	4.5
CV(=σ/μ)%	17.6	31.0	17.2	14.8	20.3

Seasonally variation of Chl_a concentration between West Frisian Islands (WFI) and the entire Wadden Sea coastal area has been represented in Figure 5-10. As seen in graph, all ROIs agree in decreasing quantities of seasonal Chl_a in summer except Ameland which happens in autumn. There is a seasonal exchange between marked areas for the maximum extent of concentration since it occurs in autumn for Vlieland and Ameland as well as WS (~21.4, 27.3 and $29.6mg.m^{-3}$ respectively), in spring for Texel (~$22.4mg.m^{-3}$) and in winter for Terschelling island (~$25.3mg.m^{-3}$).

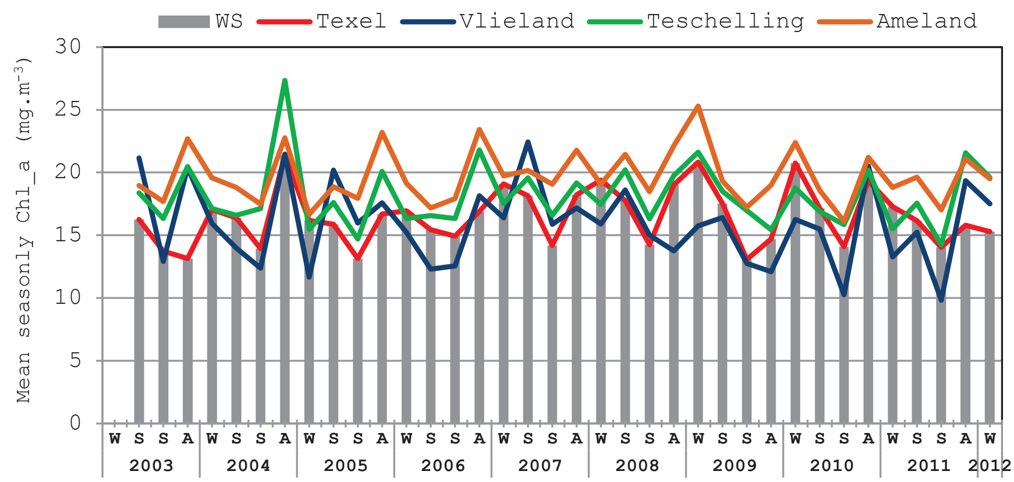

Figure 5-10- Seasonally mean variation of Chl_a concentration calculated for all regions of interests (2003 to 2012).

The highest Chl_a deviation of the mean among West Frisian Islands and the entire area of WS is calculated around 7.66mg.m^{-3} in year 2003 which is detected in Ameland area (Figure 5-11). Vlieland is the coastal area which has got the most similar decadal Chl_a oscillation to the whole WS with the lowest deviation of about 1.4mg.m^{-3}.

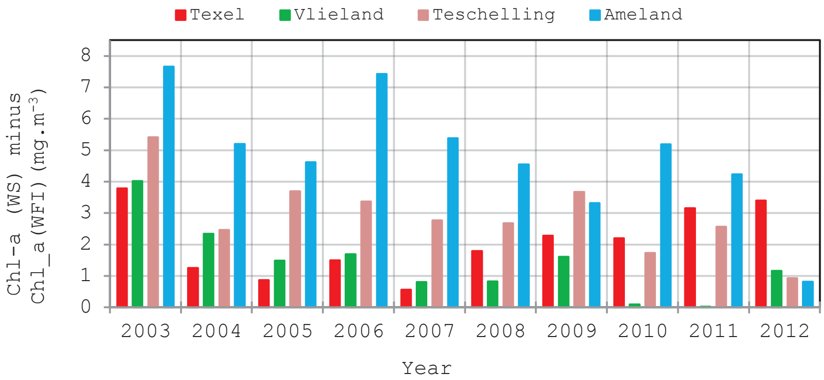

Figure 5-11- Regional mean Chl_a deviation of Chl_a (WS) for the period of 2003 to 2012.

An arbitrary day in the middle month of each season in year 2008 was chosen as a nominated day in order to illustrate the daily spatial variation of Chl_a for the coastal area of WS (Fig 5-12). The white colours portend the areas with none values covered whether by clouds or land. As seen in the images, in February as an indicator of winter, the coastal concentration enhances from WFI unto the Denmark WS. In May, in some parts of the area, e.g. German WS, the concentration values gradually decreases whereas in Dutch WS increases. This rising up continues in such a way that the whole area experiences the highest values of Chl_a in the end of August. The ascending trend happens again during the November and distributes toward the North Sea. Generally the amount of Chl_a concentration decreases from WS coastal areas toward the open North Sea which states the complex and quick variation of algae growth near coastal waters

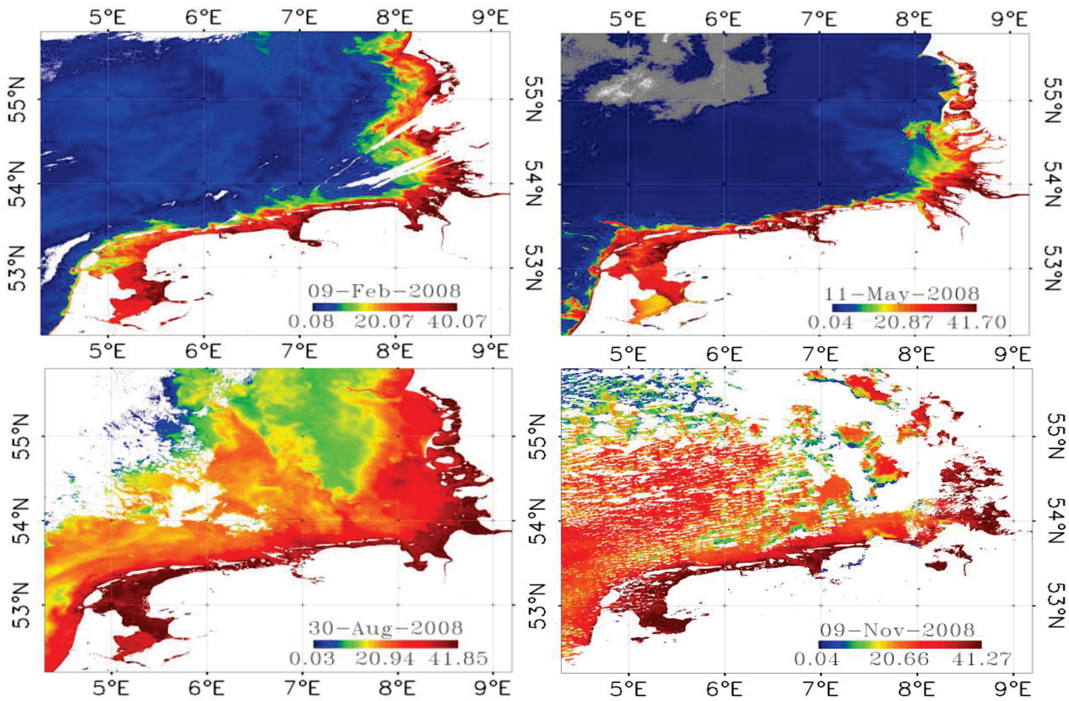

Figure 5-12- Spatial distribution of Chlorophyll_a concentration in seasonal nominated dates of the year 2008 including: 09-Feb, 11-May, 30-Aug and 09-Nov. The values are evaluated in mg.m^{-3} and it also included North Sea area.

5.3.1.2. Euphotic depth

Euphotic depth is usually considered as an indicator of water clarity and is an important parameter to evaluate model-based basin-scale primary production (Behrenfeld & Falkowski, 1997). It is also known as $Z_{1\%}$ that is practically defined as the water depth at which available radiation of photosynthesis (or PAR) reaches to 1% of its intensity just below the sea surface (Kirk, 1994).

In this way regardless of the study location, Z_{eu} and PAR usually have similar oscillation during a year (Figure 5-13). The positive relationship between two parameters can clearly be figured out.

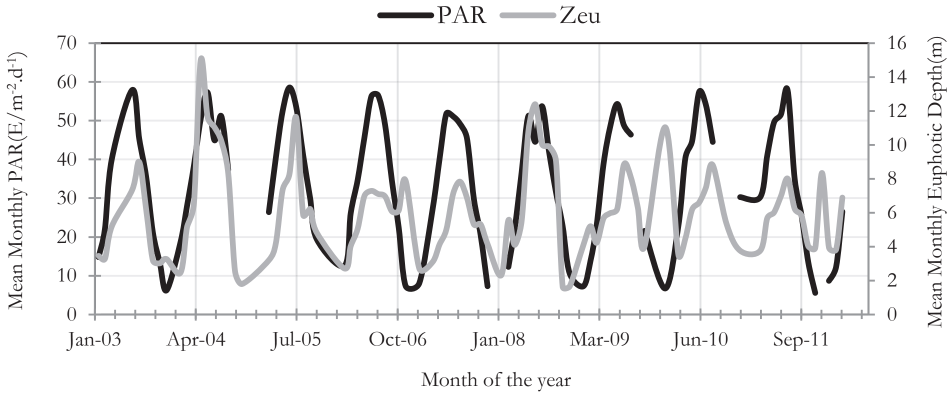

Figure 5-13- Monthly Euphotic depth and PAR relationship after temporal match-up

In 1989, Mueller and Lange were constructed a linear empirical relationship between Z_{eu} and diffused attenuation coefficient (K_d) at 490 nm based on Lambert-Beer law. In this study, the euphotic zone depth (Z_{eu}) data of Wadden Sea was assessed as a ratio (=4.605) of K_d. Similar to Chl_a, Z_{eu} data were then filtered in order to draw out appropriate clear sky images. Daily time series analysis of decadal euphotic depth is illustrated in Figure 5-14.

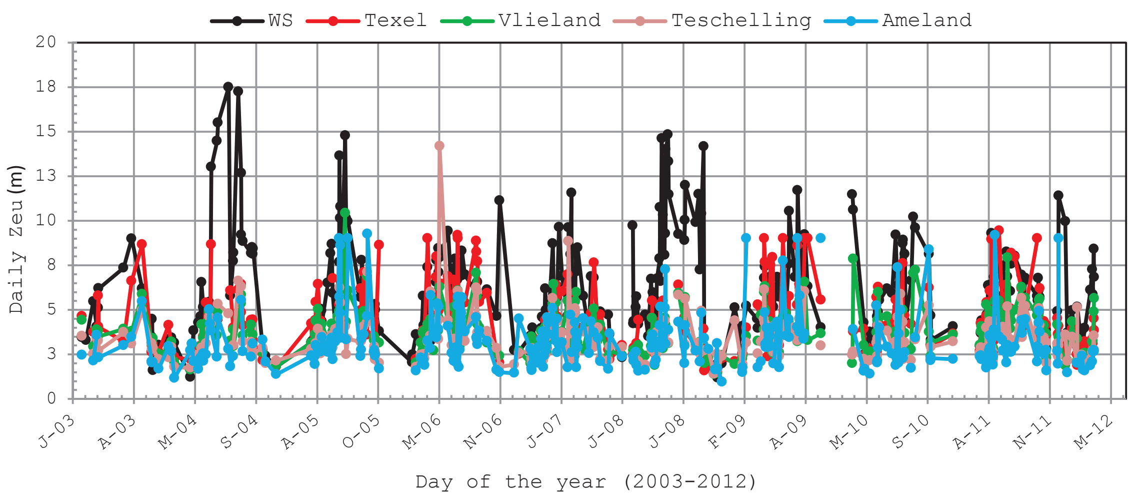

Figure 5-14- Daily time series of Euphotic Depth (Z_{eu}) over WS and WFIs during 2003 till 2012.

Euphotic depth for the entire coastal area, calculated as the mean of Dutch, German and Danish WS, varies from 1.18cm to 17.49m for the study period (2003-2012). The coastal area was experienced its own deepest and shallowest light penetration in Jun-2004 and Nov-2008 respectively. Among 4 WFIs, Texel has been recorded as the most variable region with respect to its wide range of euphotic depth from 1.49m in Oct-2008 to 16.05m in Sep-2009. In general, comparing all ROIs declares that the highest amounts of Z_{eu} appear in the middle of May till early in September while the shallowest values occur in October and November. In 2003 to 2012, summer showed desirable highlighted values since most peaks of euphotic depth happen in this season while lowest values were recorded for autumn and winter (Figure 5-15).

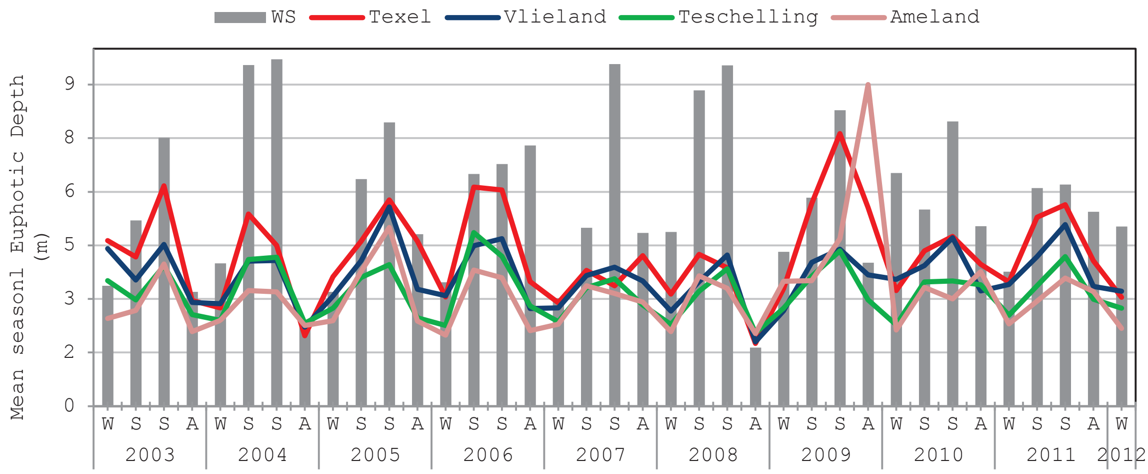

Figure 5-15- Seasonal variation of Euphotic Depth (Zeu) in WS and 4 WFIs.

Spatial distribution of Z_{eu} (Figure 5-16) manifests the point that in spite of seesaw pattern in entire period of 2003 till 2012, all regions of interest agree in highest values in summer and lowest in autumn and winter. Among all ROIs, the highest values of Z_{eu} belong to WS coastal area. Ameland, Terschelling, Vlieland and Texel were respectively labelled as the shallowest to deepest section comparing 10 years daily averaged data of 4 WFIs. Among all Frisian Islands, WS similar pattern was perceived for Texel which has the least deviation of the mean of the whole coastal span. One distinctive observation is that when slightly roaming from WS coastal areas toward the North Sea, it`s been revealed that the highest and lowest values of euphotic depth are virtually exchangeable between open and coastal water in spring and summer during each year.

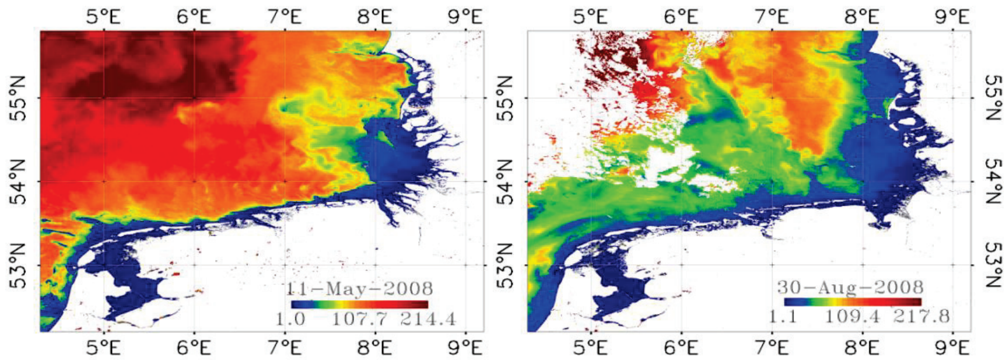

Figure 5-16- Spatial distribution of Euphotic Depth(Zeu) In nominated dates of spring and summer 2008 (11-May and 30-Aug). Values are presented in meter and it also included North Sea area.

5.3.1.3. Photosyntetically Active Radiation

Photosynthetically available radiation briefed as PAR is usually measured in visible spectral interval of 400 to 700nm since maximum Chl_a absorption happens in this range. PAR variation depends virtually on the amount of attenuation, absorption and scattering by water, algal pigments and total suspended materials respectively but in other hand it strongly follows the incoming solar radiation patterns.

Temporal and spatial matched-up MODIS monthly averaged PAR is illustrated in Figure 5-17. Looking at the monthly graph, we can see that PAR variation has an annual cycle in such a way that minimum occurs in winters whereas summer seasons cover the peaks. From the available data, the lowest and highest amount of PAR for entire coastal area of WS were recorded around 2.59 and 60.32 $E.m^{-2}d^{-1}$ which belong to Dec-2010 and Jun-2005 respectively. The decadal average of PAR was estimated by 36.5 $E.m^{-2}d^{-1}$ for the whole Wadden Sea.

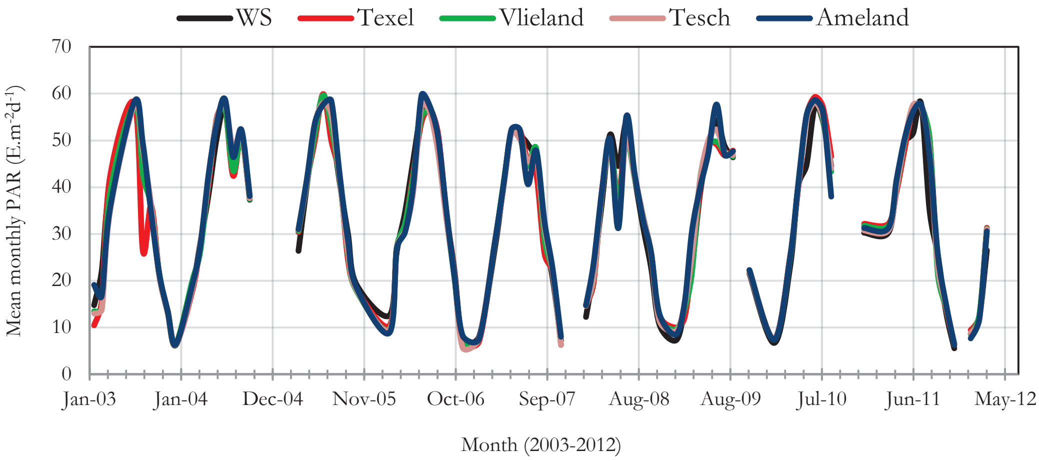

Figure 5-17- Monthly mean PAR variation over the ROIs. Missed values are as a result of temporal match-up.

Apart from North Sea, there is a considerable spatial distribution observed for the whole WS especially in Dutch coast (Fig 5-18). This variation usually rises up in spring and summer while decreasing in autumn and winter. In spring, as it`s shown in colored images, the most alteration in PAR values goes for WFIs, upper parts of German coastal areas and the entire district of Danish WS. With respect to North Sea, relatively all highest amount of PAR has been encompassed by coastal areas regardless of temporal scale. Comparing 4 WFIs, the one which follows the WS PAR pattern is Vlieland with the least deviation of mean equals to 7.58E.m^{-2}d^{-1} summed up for the whole 10 years. Among ROIs, Texel is marked as the most deviated region with coefficient of variation more than 45% (Fig 5-19).

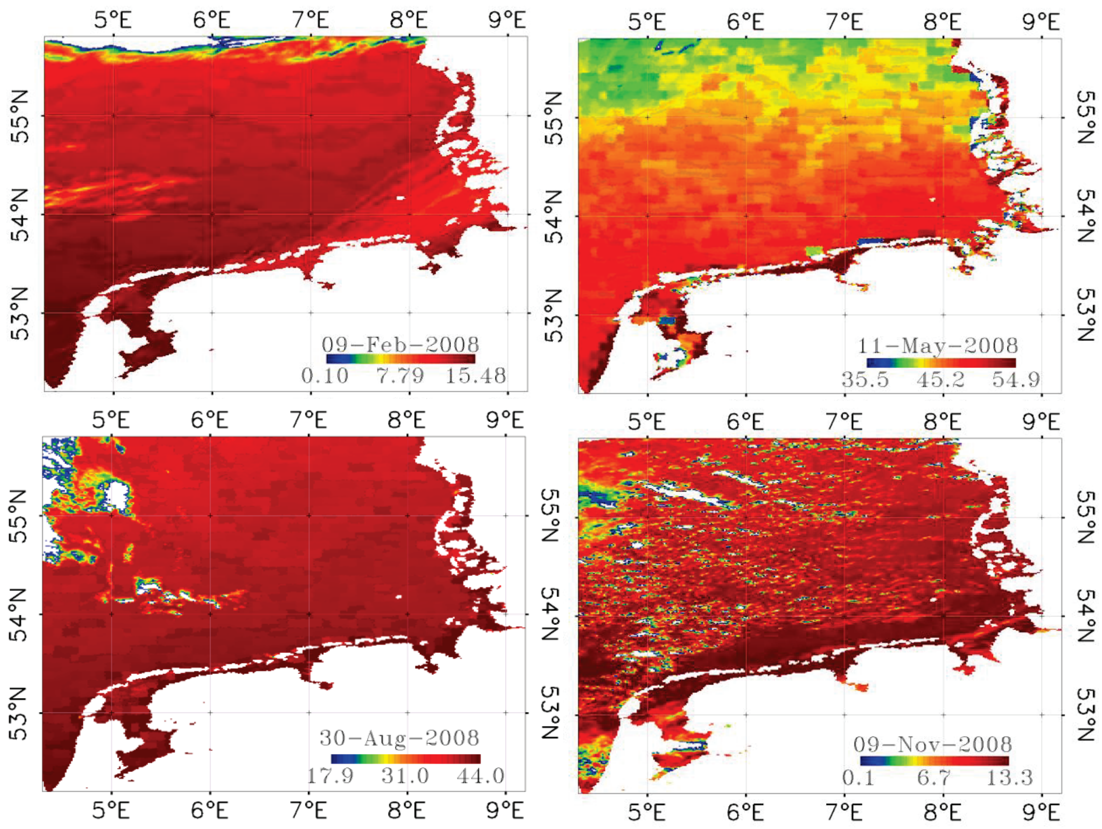

Figure 5-18- Mean PAR variation in seasonal nominated dates of the year 2008. (9-Feb, 11-May, 30-Aug and 9-Nov). All values are computed in E.m^{-2}d^{-1} and it also included North Sea area.

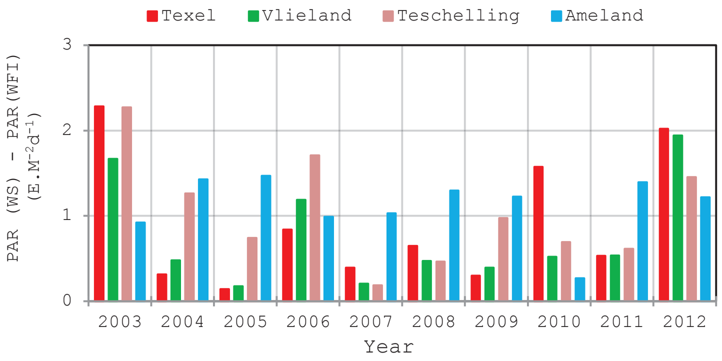

Figure 5-19- Regional mean PAR anomalies of WS mean PAR depicted in annual scale

5.3.1.4. Optimum carbon fixation rate

The dependency of magnitude and variability of P_b^{opt} on water surface temperature was proved by the strong correlation more than 0.84. 10 years temporal and spatial variability of computed P_b^{opt} was shown in Figure 5-20 and 5-21 respectively for different locations. As seen, the peaks of carbon fixation rate distinctively happen in summer while the undermost values refer to winter when surface water temperature is pretty low. It is quite obvious in graph that all WFIs are following the same temporal pattern in each year. Subsequently from 2003 to 2012, the highest and lowest values were estimated near to 1.108 mgC(mgChl^{-1})h^{-1} and 6.627 mgC(mgChl^{-1})h^{-1} which occurred in October-2011 and June-2005 respectively. The year 2007 was inscribed as the year with highest amount of P^{b}_{opt} equals to 4.77 mgC(mgChl^{-1})h^{-1}. The calculated coefficient of daily variation was recorded about 35% which was almost the same for all regions.

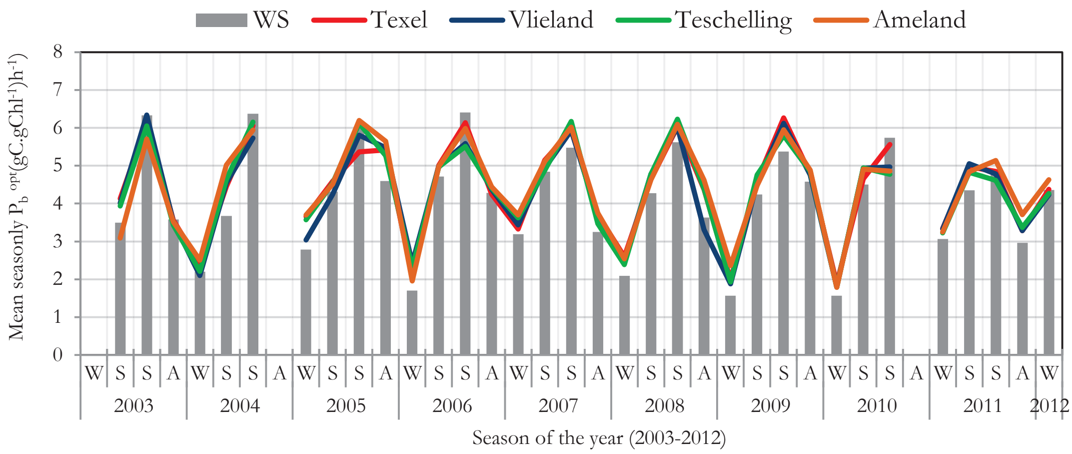

Figure 5-20- Seasonal changes in P_b^{opt} plotted over 10 years (2003-2012).

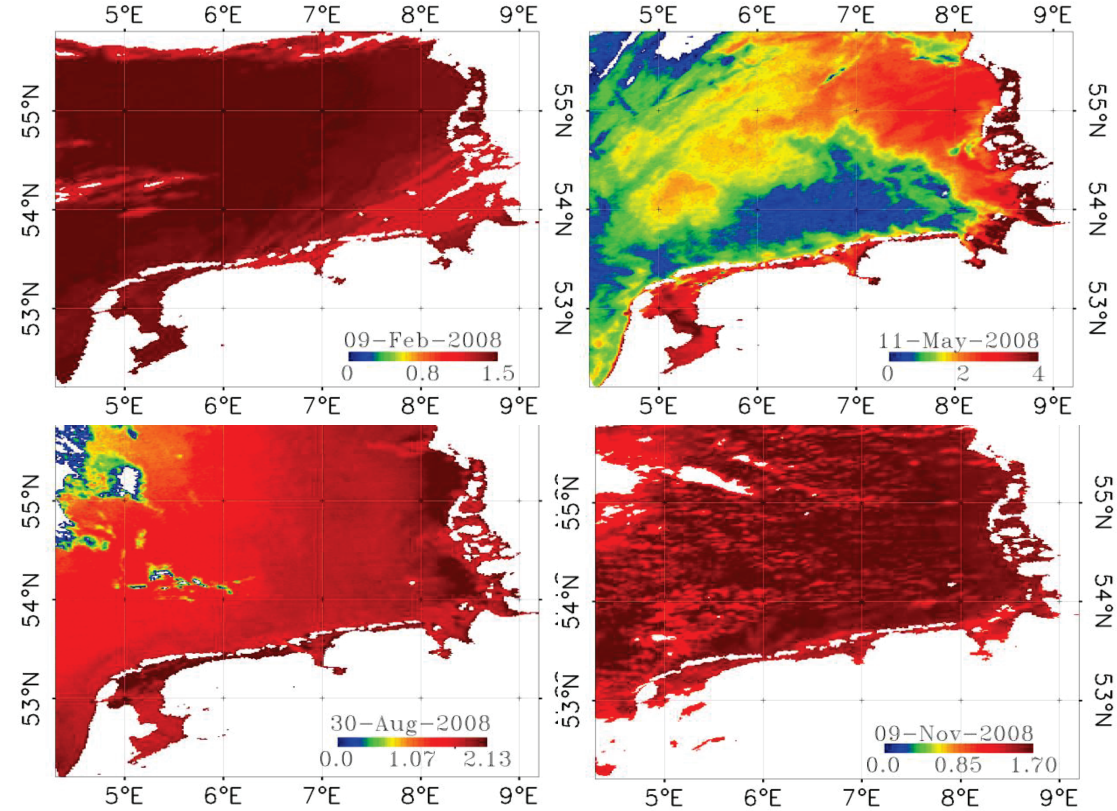

Figure 5-21- Spatial variation of optimum carbon fixation rate (Pbopt) in seasonal nominated dates of the year 2008 (09-Feb, 11-May, 30-Aug and 09-Nov). Values are in $mgC(mgChl^{-1})h^{-1}$ and it also included North Sea area.

5.3.1.5. Dirr

Photoperiod, also known as sunshine hour, specifically goes for the duration in which surface of the earth is irradiated by solar radiation directly or indirectly. Dirr is stated in decimal hours and computed as a function of latitude and longitude of the study area as well as sunshine hours (the interval between sunrise and sunset). The decadal variation of photoperiod was computed for the Wadden Sea. It was found that there is an ignorable change in duration year by year (2003 to 2012). All peaks correspond to summer months when the sun persists in its longest duration. The annual mean duration is estimated about 13.46dh (13' 27" 36) for the period of 2003 till 2012. The longest and shortest duration belong to the June- and December-2011 with the values of 17.07dh although the difference is very small year to year.

5.3.2. VGPM output (Depth-integrated Primary Productivity)

In current segment, we are going to describe the modelled daily primary productivity either in temporal scale as time series and in spatial scale comparing the obtained results for different IOPs.

5.3.2.1. Temporal variability of primary production

VGPM daily primary production was produced in 10 years for the study area. Regarding to frequency of available data in WS, the highest and lowest daily productivity value were ranged from 0.12 to 13.4 gC $m^{-2}d^{-1}$ which goes for Oct-2003 and May-2008 respectively (Figure 5-22). We evaluated the highest mean more than 5gC$m^{-2}d^{-1}$ which happens in year 2004 and 2008 and the least amount of mean production approximately equals to 2.2 and 2.4 gC $m^{-2}d^{-1}$ which in sequence belong to 2012 and 2003. From 2003 to 2012, daily average of 2.81, 2.68, 2.53 and 2.71 gC $m^{-2}d^{-1}$ occur in Texel, Vlieland, Teschelling and Ameland respectively. Table 5-3 shows the monthly mean values of PP. We can realize that the highest values of PP usually take place in July whereas in November and February the entire WS area faces the least amount of productivity.

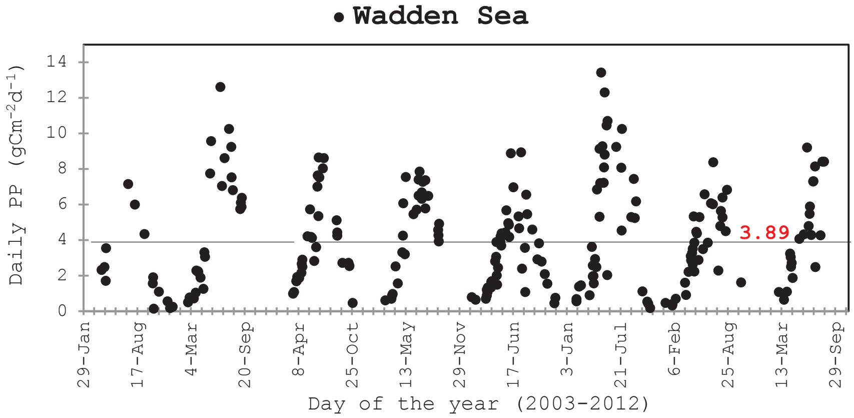

Figure 5-22- Daily distribution of VGPM primary production (scatter plot). Straight line represents the diurnal mean value over 10 years.

Table 5-3- Monthly average of primary productivity domain values (max &min) calculated from 2003 to 2012 for the whole WS area.

Mean monthly PP ($gC\ m^{-2}d^{-1}$)			
Month	**range**	**Month**	**range**
Jan	0.31-1.07	Jul	2.5-9.4
Feb	0.29-1.83	Aug	2.1-7.8
Mar	0.61-3.02	Sep	1.4-6.2
Apr	1.54-2.59	Oct	0.8-3.9
May	1.56-9.1	Nov	0.21-1.1
Jun	2.9-9.8	Dec	0.3-1.4

Seasonal variability of PP was computed by taking the average of each three months year by year regarding to data availability (Figure 5-23). During decadal period of 2003-2012, the lowest values of primary producing expectedly belong to winter and high amounts of depth-integrated PP refers to summer season. Comparing WFIs, the water-column PP slightly raises up to $5.19gCm^{-2}d^{-1}$ in summer 2009 which happened in Ameland region while the minimum value is recorded less than $0.5gC\ m^{-2}d^{-1}$ for winter 2008 in Terschelling coast. Unfortunately there were no matched dates between MERIS and MODIS found for the years 2004 and 2010 in autumn months.

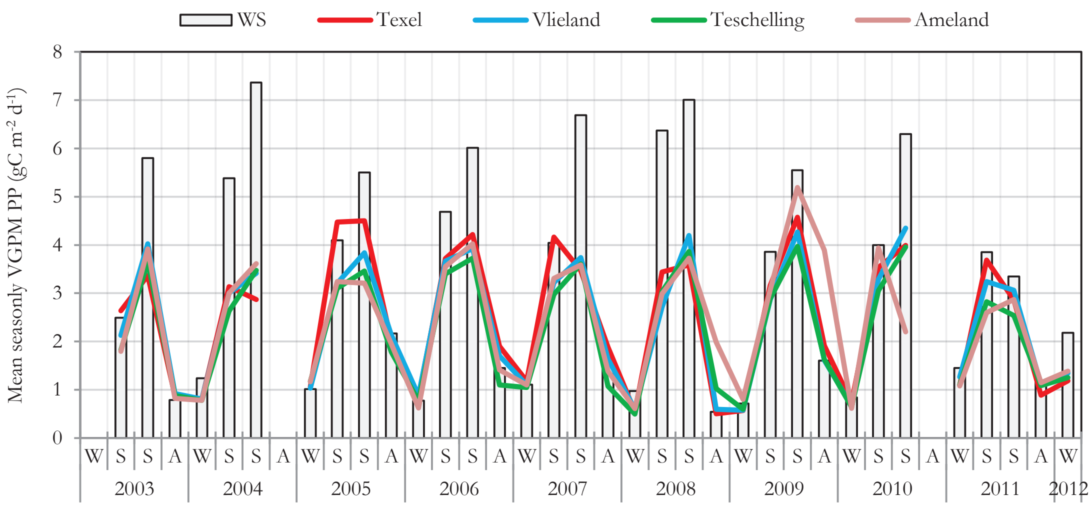

Figure 5-23- Seasonal alteration of depth integrated primary production over WS and WFIs.

Figure 5-24 demonstrates the decadal monthly mean water-column integrated primary production calculating the average of specific month data in whole period 2003 till 2012. It is obvious in almost all regions of interest that there are 2 main observable peaks of PP which are exchanging between months of summer as well as spring. In this way, in some locations like Texel and Ameland, it happened in June while in Terschelling, it goes for July. The maximum values vary between 3 and 5gC $m^{-2}d^{-1}$ considering all selected areas. The Wadden Sea has distinctively got the highest level of mean production more than 8.2gC $m^{-2}d^{-1}$ comparing to WFIs since it covers other coastal areas of German and Danish as well.

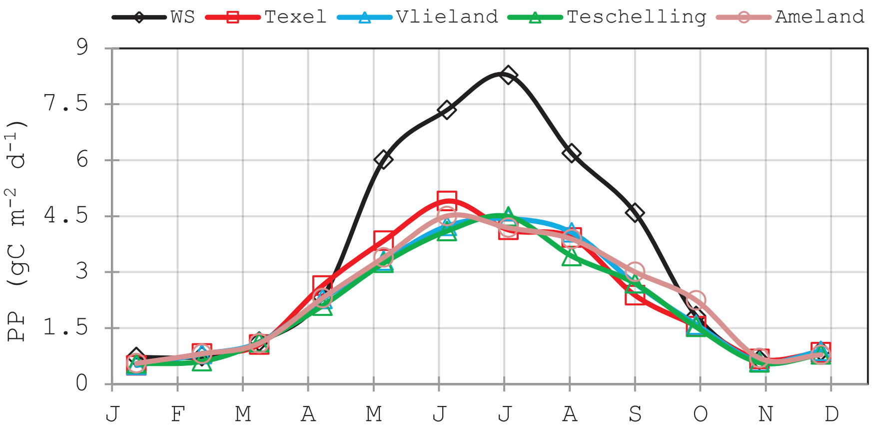

Figure 5-24- Monthly average of depth integrated primary production over 10 years (2003-2012).

5.3.2.2. Time- integrated primary productivity

The entire range of calculated daily PP was then annually summed up and weighted averaged (WA) based on the frequency of accessible data in each year during 10 years. In this way, yearly summed value was multiplied by number of data in that year in order to obtain one averaged value for a decade. Table below shows the statistical analysis of total amount of pelagic primary production contrasting the WFIs with WS. The WA of whole coastal area was then taken into account as an ideal value by which deviation of other regions was evaluated. Annual mean PP of the WS was subsequently plotted in conjunction with ±SD (Figure 5-25). The year 2005 is markedly contained the most deviation among other study years.

Table 5-4- The statistical analysis of total VGPM depth-integrated primary production obtained for different coastal areas. DF, WA, DM and CV respectively meant as data frequency, weighted average, deviation of mean and coefficient of variation.

Total Annual Primary Production (gC $m^{-2}y^{-1}$)							
Zone	Period	DF	Min	Max	WA	DM	%CV
WS	2003-2012	281	28.3	190.5	122.8	-	37.9
Texel	2003-2012	186	10.7	79.2	58.7	111.3	38.7
Vlieland	2003-2012	236	16.1	92.0	70.9	98.5	35.6
Teschelling	2003-2012	245	15.0	105.3	71.7	85.2	37.8
Ameland	2003-2012	236	12.5	106.0	74.9	84.5	39.0

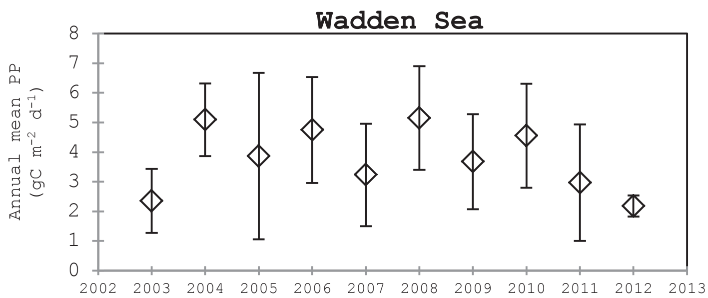

Figure 5-25- Annual mean PP in conjunction with calculated standard deviation.

5.3.2.3. Long-term spatial variability of PP

In order to better feature the seesaw of derived primary producing in each region of interest, we prepared the annual mean pp out of the entire calculated outputs in each year (Figure 5-26). Glimpsing at 12 provided images below, we are able to find out that the Dutch WS is the coastal area which has almost every year owned the highest amount of producing regardless of North Sea. German and Danish WS distinctively represent wider range of changes than other coastal areas. Peaks and falls are markedly alternating during a decade for the entire range of WS coordinate (from 52^{o} 12’ N to 55^{o} 42’ N). The maximum value of annual mean is attached to the years 2006 and 2008 with the value of 4.1gC.m^{-2}d^{-1} and the least (≈1.9gC.m^{-2}d^{-1}) goes for the year 2012 which has been evaluated till March. More pp oscillation can be appointed for the right coastal part of the Wadden Sea comparing with the left coasts. Generally no clear harmonic pattern can be observed for the study area during 10 years although producing rate is always changing in a single year.

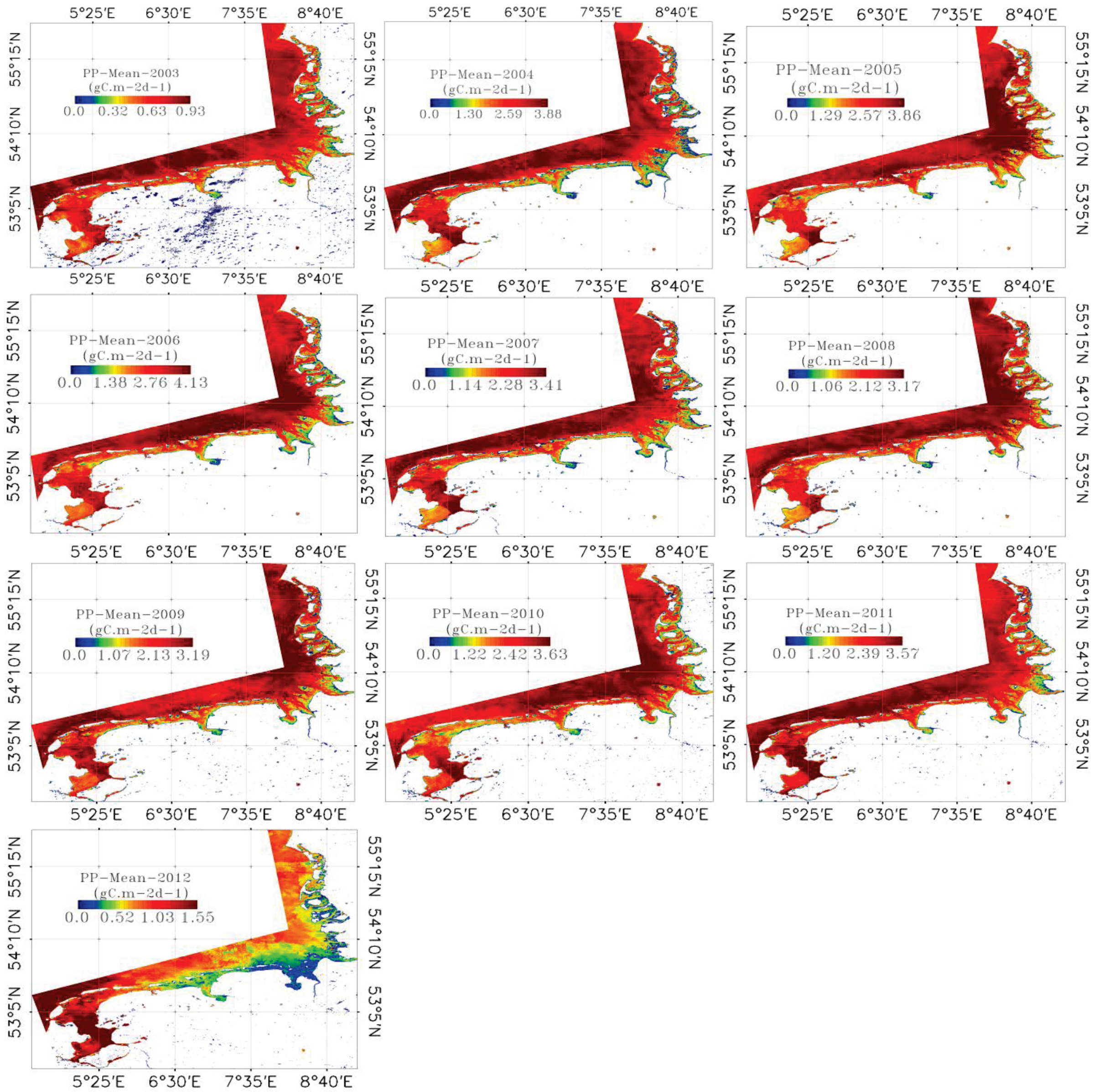

Figure 5-26 - Spatial variability of yearly mean PP over a decade of 2003 to 2012. Red and dark blue colors indicates maximum and minimum production respectively. The values are also included part of North Sea.

5.4. Sensitivity analysis

In this study, in order to represent the effect of each VGPM input parameter on model output (pp) in a numerical way, we decided to perform the Nominal Range Sensitivity Analysis. It`s often referred as the well-sensitivity-indicator for linear models. Here we have applied mentioned approach using daily WFIs data and compared the results gained based on alteration of each parameter out of its min and max range while other factors remains constant. NRSA is a user friendly number which illustrates the degree of sensitivity regard to specified parameter.

The results show that euphotic depth and Chl_a are among the most factors to which primary production is sensitive in almost all regions (Figure 5-27). The highest NRSA was computed by 2.59 and refers to Z_{eu}. Chl_a, P_b^{opt}, Dirr and PAR are respectively the rest of parameters which influences the VGPM pp.

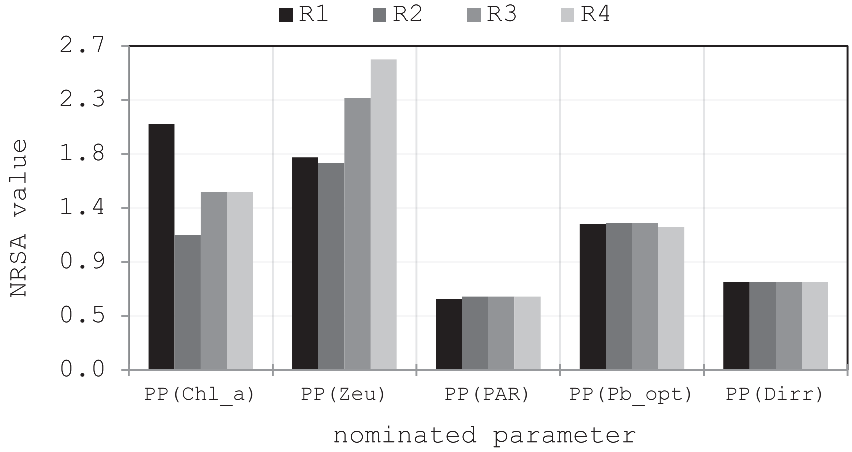

Figure 5-27- Regional scale Nominal Range Sensitivity Analysis results applied on daily parameters.

5.5. Ancillary climate variables and Chl_a

The second prominent aim of this research is to investigate any plausible relationship between biomass activity and physical parameters. In this way, MERIS 300m resolution Chl_a and MODIS 1-km SST and PAR were faced together for the Wadden Sea coastal area either spatially or as time series analysis in following sections.

We filtered the SST based on MODIS quality assessment which is usually attached to SST products as a separate layer. They attributed values between 1 and 4 to each SST pixel in a descending quality pattern based on cloud contamination quantity. In this way, the pixels with SST more than -2^{o}c were used in analysis as they all contained quality equal to 1 meaning the clear sky. To do this, an IDL code was prepared to remove the polluted pixels by cloud.

5.5.1. Temporal variation of SST and PAR versus Chl_a

In this study, selected climate indicators (SST and PAR) against the most dominant algae mass indicator (Chl_a) were plotted in order to illustrate the daily variability of parameters in a particular location close to the coast. Based on results shown on previous sections, Texel is recorded the most variable region. As such, one point in Texel region (52.9N, 4.8E) was marked as a constant control point to track the temporal variation of SST, PAR and Chl_a in a decadal scale (Figure 5-28). As seen, there is a daily incompatibility between climate factors and chlorophyll which is stronger during cold days. This idea will be disclosed taking a look at the monthly variation of parameters represented in Figure 5-29 (a&b) for the same location. During January and April there is a totally inverse relationship between Chl_a and PAR as well as SST. On the other hand in July and August the winter discrepancy is going to be weaker. While maximum values of SST and PAR usually occur in hot months of summer, Chl_a concentration rises up in cold season of winter. Spring and autumn afford the values in between.

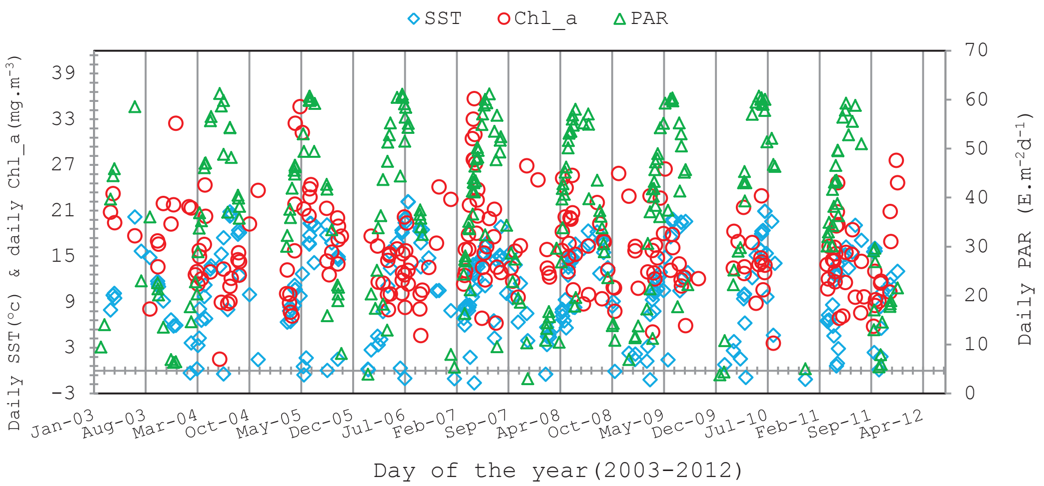

Figure 5-28- Daily variation of MODIS PAR, SST and MERIS Chl_a concentration. plotted for a location with coordinate of 52.99N and 4.85E in Texel island.

SST and PAR are agreed in almost all months in such a way that for example from winter 2007 to spring 2008 by more than 7.5°c increasing in SST, PAR also enriched more than 25.6E.m^{-2} per day. Whereas for the same period the amount of phytoplankton bloom reduced by seasonally average from 19.3 to 17.8 mg.m^{-3}. This situation has been slightly changed by entering to summer since SST and PAR are still rising up, Chl_a decreased near to 1.4mg.m^{-3}.

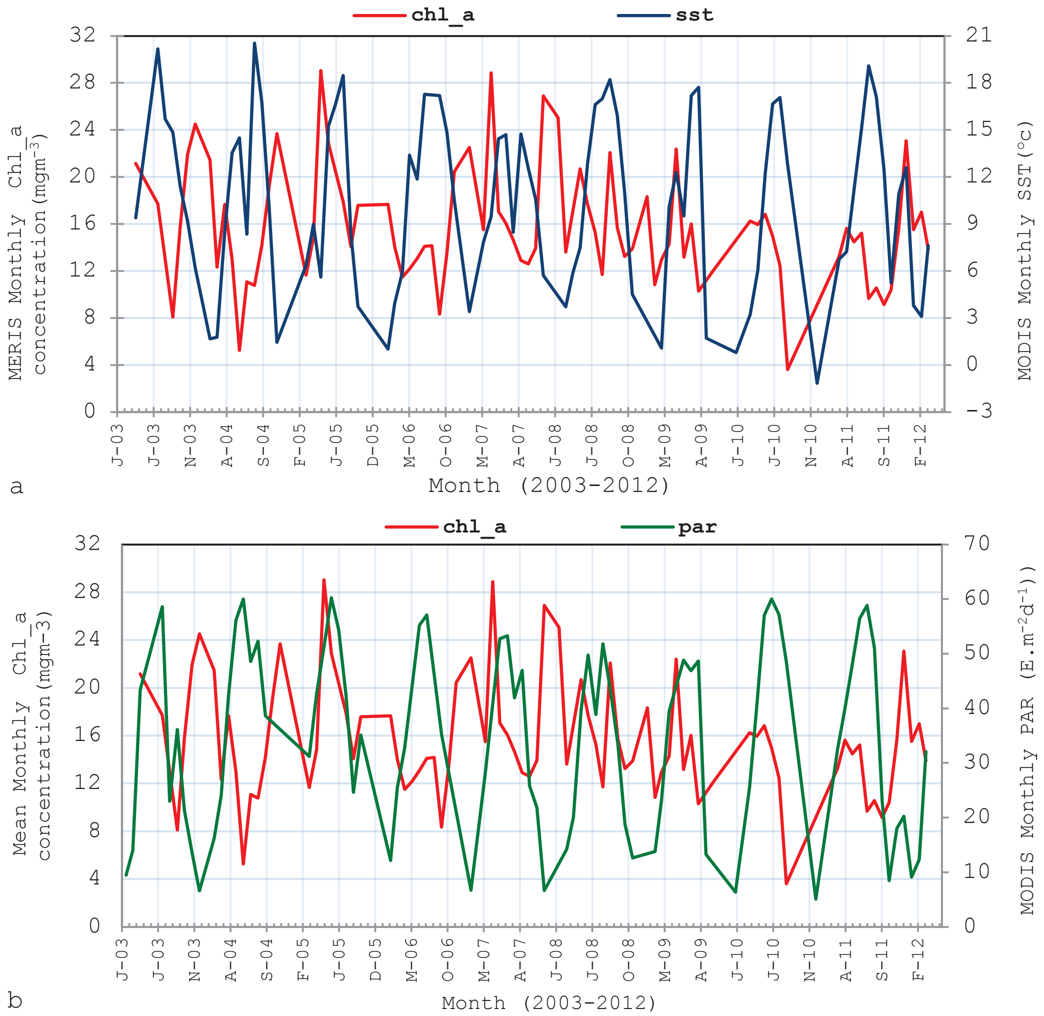

Figure 5-29- The mean monthly relationship of Chl_a with SST(a) and PAR(b) for a location with coordinate of 52.99N and 4.85E in Texel island.

5.5.2. Spatial variation of SST, PAR and Chl_a

In this section, owing to detect the spatial distribution of defined parameters, regardless of time variation, we signed 25 ground control points (GCP) considering the closest distance from the islands and well-distributed points in whole WS tracing from 52.2N to 55.8N. Figure 5-30 (a&b) indicates the lat/long of picked out GCPs located in the area.

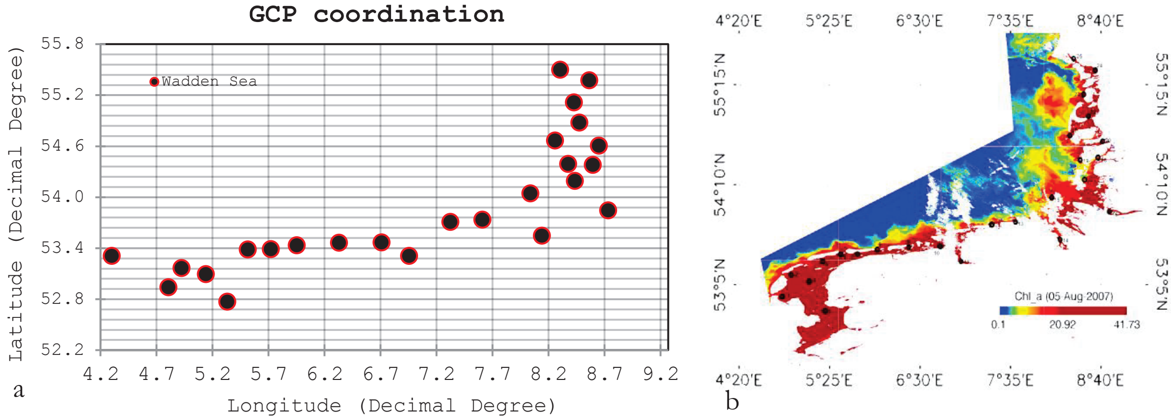

Figure 5-30- The exact location of selected ground control points over the Wadden Sea (a & b).

A day in the middle of summer season was chosen based on Chl_a summer bloom expectation. Graph below (Figure 5-31) illustrates the variation of climatic parameters and Chl_a going from Texel region (GCP1: 52.97N, 4.84E) into the entire border of Danish WS coasts (GCP25: 55.53N, 8.33E). There is a severe up and down trend seen in SST and PAR especially in German and Danish WS. WF islands comparing to rest of areas, contain similar and slight variation for all 3 parameters. Then SST and PAR inconsistency with Chlorophyll_a can be obviously seen in some locations particularly the ones marked in German and Danish WS. An instant fall happened in SST and PAR is related to point 16 (53.87N, 8.76E) and located in a stream enters to German WS.

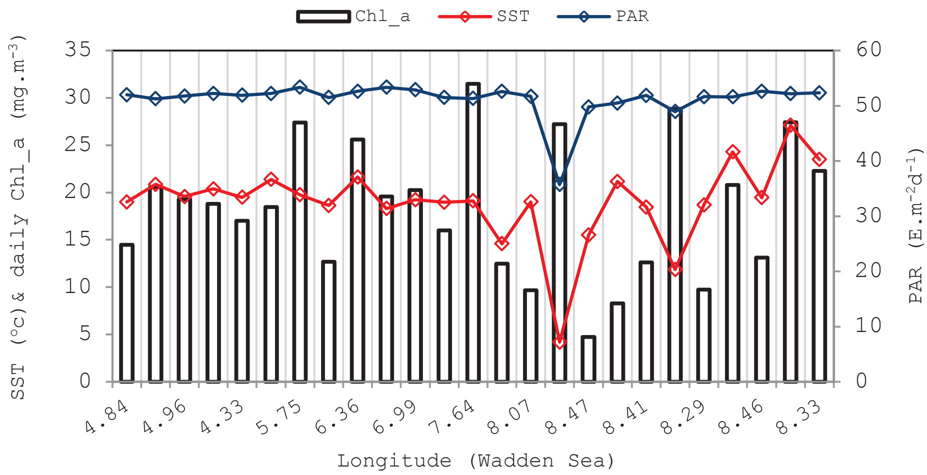

Figure 5-31- Spatial seesaw of SST and PAR accompanying Chl_a concentration delineated for 5th Aug-2007. 25 GCPs assigned covering the entire study area.

5.5.3. Long-term statistical analysis of climate indicators and Chl_a

Here we analysed the physical and aquatic biological activities statistically for a time series of 10 years. Statistical calculations were done based on Figure 5-32 which represented in table 5-5. A decade of WS` Chl_a, SST and PAR data were monthly averaged and plotted against each other. The peaks of PAR and SST happened between June and September while Chl_a reaches its minimum concentration value less than 22 mg.m-3. Weighted monthly average of each parameter was estimated based on available data in each month from 2003 till 2012. This time scale graph also can clearly mirror the incompatibility of chlorophyll concentration with available radiation and water temperature even for a long term try over Wadden Sea.

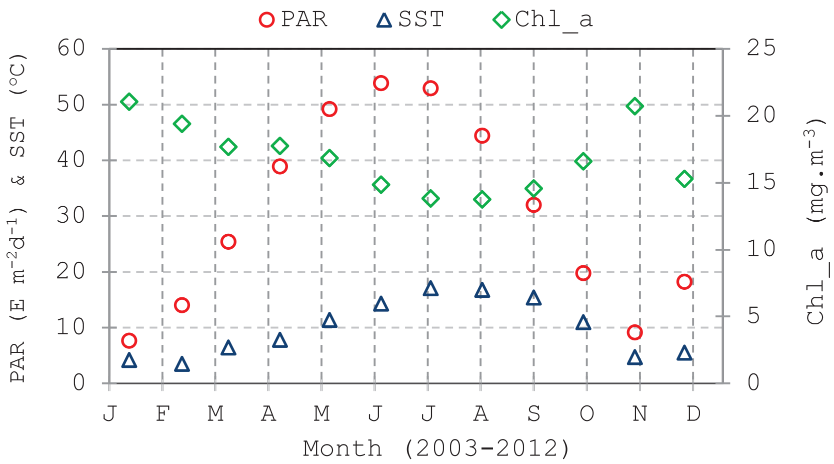

Figure 5-32- 2003-2012 monthly averaged PAR, SST and Chl_a concentration.

Table 5-5- Initial statistic results containing minimum, maximum, weighted average and coefficient of variation computed for three investigated parameters. The values reflect monthly variability results from 2003 to 2012

Wadden Sea					
parameter	period	min	max	WA	CV%
Chl_a ($mg.m^{-3}$)	2003-2012	13.7-Aug	21.1-Nov	16.6	14.7
PAR ($E.m^{-2}d^{-1}$)	2003-2012	7.7-Jan	53.9-Jun	34.6	47.2
SST (^{o}c)	2003-2012	3.5-Feb	17.1-Jul	10.9	45

To further test the result, linear type 1 regression line was passes through each pair of parameters (Chl_a-PAR, Chl_a-SST and even PAR-SST). The obtained results are shown either as a produced scatter plots (Figure 5-33) or table (5-6). A negative slope is gained for both SST and PAR against Chl_a which strongly confirms the inverse relationship between climatic indicators and phytoplankton growth in the area. PAR and SST have agreeably shown a positive correlation. The regression coefficient value resulted for Chl_a-SST is not only more than Chl_a-PAR but even more than PAR-SST comparison value. The logarithmic state of parameters was also tested but didn`t make any specific sense in results.

Table 5-6- Regression analysis results for a decade of 2003 to 2012 between Chl_a, SST and PAR.

Wadden Sea (2003-2012)			
parameter	R^2	Slope	Intercept
Chl_a PAR	0.56	-0.11	20.26
Chl_a SST	0.74	-0.42	21.08
PAR SST	0.67	2.72	3.57

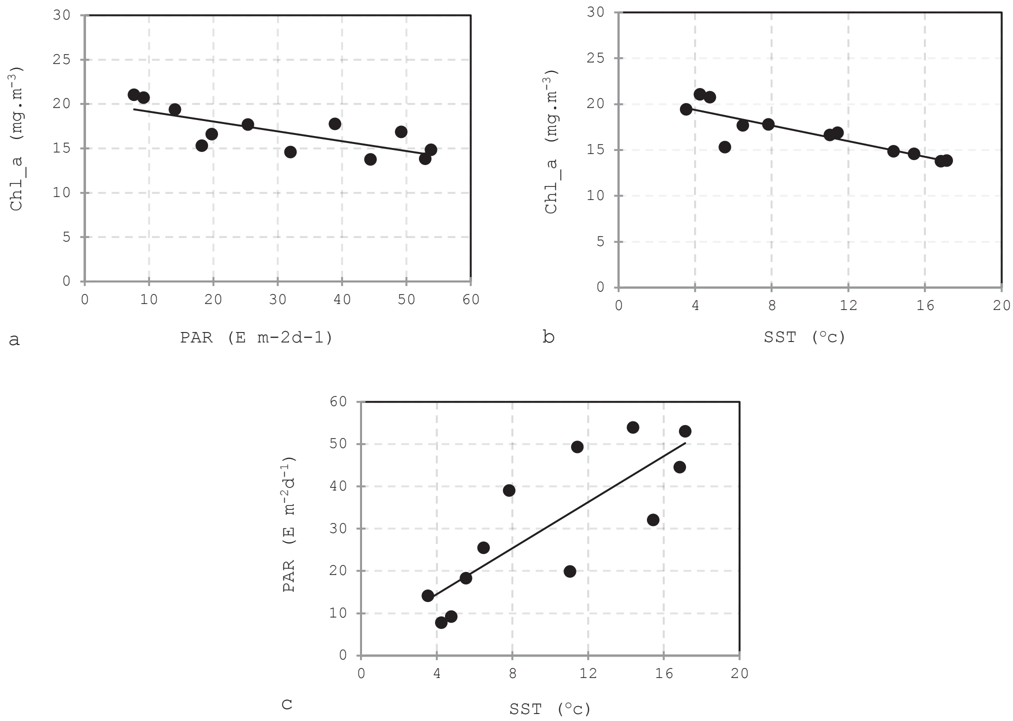

Figure 5-33- Linear regression analysis results performed for each single variable against another (a) Chl_a-PAR, (b) Chl_a-SST and (c) SST-PAR

6. DISCUSSION

In this section, we put the findings of this study in the context of relevant studies. The point is that since there is no recent study has been done considering the entire coastal area of Wadden Sea especially German and Danish territories, we attempt to evaluate our results either with outdated researches or the ones which been done only for Dutch WS.

6.1. VGPM input variables interaction with IPP

The seasonal and interannual variability of Chl_a concentration is evaluated in Wadden Sea as well as WFIs as shown in Figure 6-1. Two strong algal blooms occurred late in winter and fall when the maximum amount of rainfall and runoff will push the river flows toward the Wadden Sea. It can be described as late fall bloom in January and late summer bloom in November which recorded for all regions. Moreover, April and July are two months when the area faces quick and low peaks which might be as a result of increasing in diatoms (Cadee & Hegeman, 1979). Neither of these months is comparable with winter and autumn phytoplankton activities especially in Texel coast where a sharp drop-off up to ~12mg.m^{-3} happens between September and October. Comparing to other WFIs, Texel region shows a different Chl_a seesaw pattern during a year as it coincides with Marsdiep tidal inlet currents.
Phytoplankton bloom in winter is not an abnormal state since it sometimes occurs in coastal regions with high level of tidal currents [e.g. (Teira et al., 2005; Maybin et al., 2009; Schwartz et al. 2010)]. But since we couldn`t find any study which report the winter biomass bloom in WS so these peaks are most likely due to error in Chl_a retrieval by C2R model. It might also be explained by other reasons generated by upwelling happens in cold month in North Sea coastal areas which then leads to WS through inlets. In this way, the upwelling currents will direct the North Sea`s nutrient loads which lay deep in the water column into the surface layer and then toward the WS. Cadee & hegeman (1979) also claimed that this can be described by water mixed layer depth variations as a result of tidal currents which produced by winds. The effect of tidal advection and wind on reducing the biomass concentration is also presented by Tillmann et al. (2000) for the German WS coast. However, the wind speed in coastal regions of WS is not considered as much dominant as in North Sea.

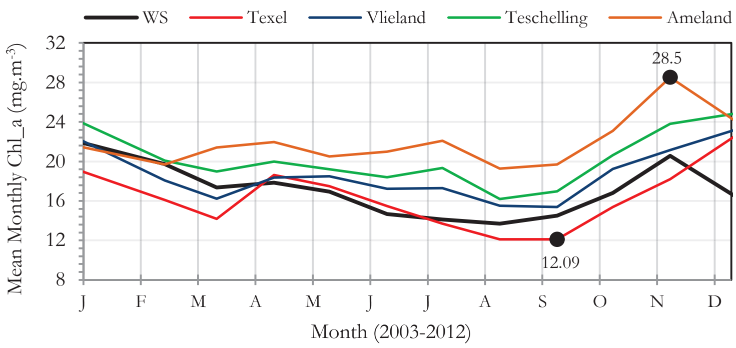

Figure 6-1- Decadal averaged Chl_a concentration in each month plotted for WFIs and WS. Maximum and minimumvaluesbelong to Ameland (~28.5mg.m-3) and Texel (~12.1mg.m-3) respectively.

Nevertheles, collation of Chl_a and pp mean monthly time series in Wadden Sea is apparently similar to other regions, like the NW Spanish coast (Bode et al., 2011). In contrast with Chlorophyll concentration which changes based on thermal and nutrient stratification, primary production is correlated with this phenomenon in a negative way. It seems that there are other dominants' factors rather than Chl_a concentration influenced the primary producing in Wadden Sea since Chl_a and pp variations show often different behaviour during a year. Primary producing is found to be forcefully dependent on level of euphotic zone in WS as photic depth variation and sensitivity analysis represent.

Euphotic zone determines the water depth up to which sun light can transpire. It is usually considered as the most prominent element affecting the pelagic productivity through water column. In this study, like other relevant studies (e.g. Tripathy et al. 2012), it is also measured as the most vital and sensitivity-generator factor to estimate primary productivity since it owns the highest values of correlation with PP by $R^2 \approx 0.66$. In comparison with North Sea, Wadden Sea, as a case II shallow water, represents realistic lower values of Z_{eu} for all regions in all seasons. For example, the peak value of Z_{eu} for North Sea recorded more than 200m but less than 18m in WS. Summers and winters are the seasons with maximum and minimum amount of light-penetrated depth similar to primary production pattern respectively. Besides the received solar radiation, the amount of Z_{eu} can be controlled by concentration of Colored Dissolved Organic Matters (CDOM) and Total Suspended Materials (TSM) which then limits the plagic productivity. In this way it can be a proper indicator of turbidity through the water column accompanying with Chl_a and PP variations.

Turbidity can be one of the main reasons which causes the primary production variability in Wadden Sea coastal area since it determines the amount of light entering into the water column. The variability of primary production over surface Chl_a concentration with Z_{eu} is provided in Figure 6-2. The deeper the light penetrates into the water, the higher values of this ratio obtain as a result of turbidity impression on primary productivity. This result is similar to what Cadee & Hegeman (1979) shown for the Dutch Wadden Sea. According to them, high standard deviations of PP in monthly mean (in this study SD $\approx \pm 58$ & CV$\geq$65%) can be explained with the changes in euphotic depth rather than the highest and lowest amount of turbidity in winter and summer produced by suspended materials variation.

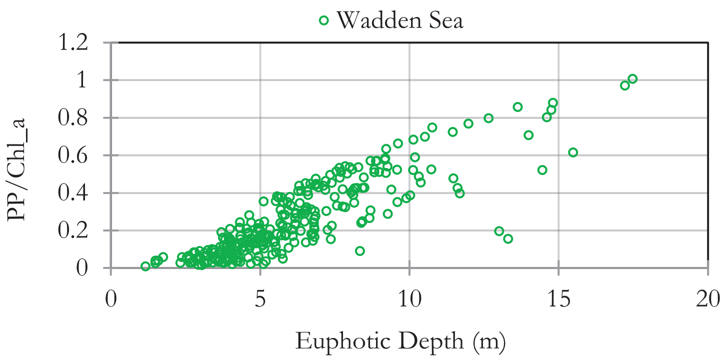

Figure 6-2- The ratio between daily PP and Chl_a concentration over the range of euphotic zone in Wadden Sea. At the same time, the graph shows the inter relationship between Chl_a, Zeu and PP.

Apart from euphotic zone, PAR and P_b^{opt} are comprised as dominant factors which have shown strong level of correlation on Wadden Sea PP temporal variation. As such, high summer growth rate of WS in July happens during a period when PAR and P_b^{opt} were swiftly enhancing as a result of warming up the surface water temperature. 6^{o}c increasing in monthly averaged Wadden Sea surface temperature from June to July made the productivity rate rising up more than $1.5 gC.m^{-2}.d^{-1}$. Time traveling between 2003 and 2012 reveals that a significant positive correlation more than 0.55 was computed for both PAR and P_b^{opt} against primary production variability which confirms the foresaid findings.

Although it`s usually ignored inadvertently to discuss about, sunshine duration is among those important parameters required to estimate primary productivity. In fact it is not remarkably changes year by year. Here in this study, it is expectedly well-correlated with temporal behaviour of phytoplankton growth rate.

Table 6-1 shows the weighted average of VGPM inputs and output monthly variation during 2003-2012 for the whole Wadden Sea. Although the number of available data in cold months (e.g. Jan & Dec) is lower than their counterpart in other months of the year, the modelled PP variations during a year compromise to those estimated by Cadee and Hegeman (1979) and Woldegiorgis (2011).

Table 6-1- Mean monthly values of VGPM inputs and output estimated as daily variation of Chl_a, Zeu, PAR and Pbopt for the Wadden Sea during 2003-2012

Month	Mean Chl_a($mg.m^{-3}$)	Mean Z_{eu} (m)	Mean PAR ($E.m^{-2}d^{-1}$)	Mean P_b^{opt} ($gC(gChl^{-1})h^{-1}$)	Mean PP ($gC.m^{-2}d^{-1}$)	Data Frequency
Jan	21.9±3.8	4.9±3.1	7.5±1.5	2.3±1.1	0.7±0.3	10
Feb	19.7±3.2	4.1±1.7	13.1±3.5	2.9±1.7	1.25±0.7	16
Mar	17.3±2.0	4.2±1.4	26.3±4.9	2.8±0.9	1.5±0.8	34
Apr	17.8±2.6	5.1±1.5	39.2±4.5	3.6±0.9	2.73±1.0	66
May	16.9±2.2	7.6±3.1	49.8±4.9	4.7±1.0	5.9±2.6	42
Jun	14.6±2.5	4.8±2.9	54.6±6.6	5.4±1.3	6.3±2.3	31
Jul	14.1±2.5	8.5±2.5	52.5±7.2	5.6±1.2	6.7±2.0	37
Aug	13.6±1.9	7.8±1.8	45.4±4.6	5.8±1.2	5.7±1.8	23
Sep	14.5±1.5	6.8±2.3	31.7±4.4	5.7±0.8	4.3±1.5	27
Oct	16.8±3.7	4.1±1.6	18.2±5.3	4.1±1.2	1.7±0.8	24
Nov	20.5±2.1	3.6±2.5	8.8±3.2	2.4±0.8	0.6±0.2	12
Dec	15.3±6.4	5.5±3.2	5.3±1.5	2.7±0.03	0.3±0.1	7

6.2. Short-term variation of primary production

A clear but large daily and monthly oscillation of primary production was recorded for the WS region. If the average daily about 3.8 $gCm^{-2}d^{-1}$ has been considered as a threshold of bloom rate, in 35% of days (between 2003-2012) the bloom were taken place more between May and August and less in April and September. Generally a cyclic pattern is observed for 10 years monthly WS pp variation in such a way that from Jan to May we observed a sharp increase in PP which continues slightly until July and quickly falls down reaching a minimum in December. The estimated pp has shown a high correlation with daily variation of solar insolation (Fee, 1973). Then, the high level of available radiation accompanying with high temperature in warm days of the year are highlighted as two predominant controlling factors on such variation in pelagic primary production. Cadee and Hegeman (2002) expressed that the penetrated light is a limiting factor for biomass bloom in turbid waters. In such cases, the dynamical characteristic of WS should also be noticed since it will cause a rapid change in algal composition as a result of advection (Poremba et. al, 1999). Cadee & Hegeman (1979) showed that nutrient supply variations (e.g. NO_3, PO_4, Si & so on) played no part in short-term oscillation of phytoplankton primary productivity in WS. On the other hand van Bennekom et al. (1974) and Fransz (1976) showed that short-term variation of algal biomass is controlled by grazing. To summarize all discussed, we conclude that euphotic depth and carbon fixation rate are supposed to be the most effective parameters for PP variations since they follow the similar temporal pattern to that of PP.

6.3. Seasonally and long-term variation of primary production

WS coastal area showed a significant seasonal variability of primary production during a study period. The year 2011 was the only year in which spring surpassed summer with a trivial difference near to 0.5$gC.m^{-2}d^{-1}$. In this subject our results are compatible with the outcomes of Woldegiorgis (2011) in which he claimed that most of the peaks of primary production in Dutch WS happened in July but some occurred in June. The largest seasonal variability in WS coastal region was estimated in 2008 to be about 6.47$gC.m^{-2}d^{-1}$ during summer and autumn. In general, spring and summer are carrying the maximum seasonal values of production almost in each year which is in accordance with previous studies in the area (Woldegiorgis (2011); Andebrhan, (2012); Tillmann et al. (2000)). Since the WS has shallow water, it can be affected by quick variation in surface temperature. In winter and fall, precipitation can cause sudden collapse in

temperature (Rasmussen et al., 1983) which then will reduce the amount of carbon fixation rate and PP. In contrast, during the warm seasons with higher temperature, lower tides and shallower mixed-layer the euphotic zone will increase and thus primary productivity. This situation will accelerate the photosynthesis process since it facilitates the accessibility of nutrients through the stable water column. But this depends much on the kind of nutrients in the water as well. Philipart and Cadee (2000) investigated that seasonal primary producing variation in western WS is not stimulated to the supply of Nitrogen in the area. Rather than fundamental physicochemical characteristics of algae in the Wadden Sea, increasing in the amount of orthophosphate in summer can be a reason of excess primary productivity in this season while other kinds of nutrients are detracting (Jonge and postma, 1974; Hesse et al., 1995).
Disparate number of data in each year makes the estimation of annual primary production even very complex and hard. Scientists usually apply different remedies to cope with this problem (e.g. Platt, 1975). In this study although we used the exact number of data in each year to calculate the total annual productivity, in order to obtain a reliable mean production in a decade, we summed up the daily values of each year and multiplied them by the number of available data in that year (Decadal weighted average). The mean value was calculated near to 122gCm^{-2}y^{-1} which is more than what van Bueskom (2005) computed for the area as a consequence of German and Danish productivity rate. Actually van Bueskom defined a nutrient linkage model between river flows, North Sea and WS (Figure 6-3). He believes that a part of WSs` supply of nutrients is provided by North Sea currents toward the coastal areas. Cadee (1978) attributed yearly size changes of spring bloom to North Sea organic materials rill into the inner sections of WS through Marsdiep inlet. Moreover, Eleveld et al. (2007) showed that algal photosynthesis decreases in the shallow Southern North Sea cause the suspended sediments limits penetration of sun light into the water layers. Cadee and Hegeman (2002) represented that total amount of primary productivity decreased from ~400gCm^{-2}y^{-1} in year 1994 to 200-250gCm^{-2}y^{-1} in 2000. Based on our study, this value continued decreasing to 148.5gCm^{-2}y^{-1} in 2007 which then increased in 2008 to 190.5gCm^{-2}y^{-1}.

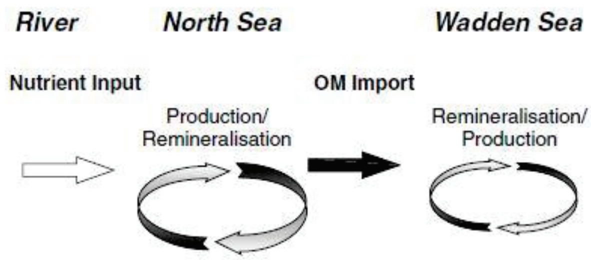

Figure 6-3- The organic matter feeding process of WS by North Sea and riverine nutrient inputs which then leads to productivity of WS constructed by van Bueskom (2005).

As a conclusion, although VGPM estimates productivity rate based on most effective factors, dependency of coastal pelagic phytoplankton biomass rate on CO_2 budget, the amount of terrestrial or riverine inorganic matters, water upwelling as well as nutrient recycling should be taken into account (Tripathy et al., 2012). Marine phytoplankton also can be changed by human activities which lead to rising nutrient loadings and fishing particularly in coastal areas (Feng & Zhu, 2012). Further studies in WS are better to focus on other important factors which play an indirect role on primary productivity such as wind, cloud cover, precipitation, salinity and sediment loads and so on.

6.4. Wadden Sea and West Frisian Islands temporal trend of primary productivity

Daily spatial variation of depth-integrated PP shows almost regular pattern between different study areas. From 2003 to 2012, the maximum daily productivity rate was calculated to be about 3 times more than what Woldegiorgis (2011) calculated for south part of Wadden Sea which happened in the same year

(2008). This large difference augments the positive effect of German and Danish coasts on total productivity more than before.

Texel demonstrated the quickest rate of daily production among other WFIs during the 10 years. The productivity in this region has been very much affected by the nutrient loads flow toward it from both Lake Ijsselmeer and Marsdiep tidal inlets. But in longer period of time like yearly analysis, the further from Texel coast to the north of WS the more amount of annual mean productivity is measured. This can be the cumulative influence of south islands on upper coasts where the coastal flowing water of two islands joins to each other which will then make an error as double-counting. Looking at the yearly mean phytoplankton biomass rate images, we understood that comparing to WFIs, Danish and German WS indicate diverse amount of productivity in each year. These regions dispute more with the cumulative effect of rivers (especially German coasts by river sediments) and North Sea. WS primary productivity is almost 2 times less than North Sea as a result of less Z_{eu} (Woldegiorgis, 2011) although it has been nutrient-fed by short streams or North Sea.

Not several studies done recently for the evaluation of primary production capacity of WS. Following lines reflect the comparison of our results with some related researches. In 1980, the western WS primary production was estimated by Cadee about 100gCm^{-2}y^{-1} in 1970s and Philipart & Cadee (2000) near to 40gCm^{-2}y^{-1} and 60 gCm^{-2}y^{-1} in mid-1970 and 1980s respectively. What we calculated for Texel and Vlieland (indicators of western WS) as weighted average of 10 years is around 65gCm^{-2}y^{-1} which is almost agreed with latter estimated value for 1980s. Cade and Hegeman (2002) represented that 30 years total amount of primary productivity in Dutch WS decreased from ~400gCm^{-2}y^{-1} in year 1994 to 200-250gCm^{-2}y^{-1} in 2000. Based on our study, this value continued decreasing to 148.5gCm^{-2}y^{-1} in 2007 which then increased in 2008 to 190.5gCm^{-2}y^{-1} for the entire coastal WS.

As seen in Figure 6-4, in spite of a similar decadal trend for WFIs, with respect to other years, WS showed a much higher values than other ROIs. As described before, this difference might be generated by the fact that it carries the loads of German and Danish as well which occupied a large part of the WS`s coastal area. This induces that the phytoplanktonic productivity of these two regions which is more highlighted in year 2008 and 2004 (132.5 & 72.3gCm^{-2}y^{-1} respectively) could dominance to Dutch WS. Texel accompanying with other WFIs show less decadal average of around 70gCm^{-2}y^{-1} than what previous studies estimated for the Marsdiep tidal inlet (~140gCm^{-2}y^{-1} by Cadee & Hegeman, 1974). This result is affirmed by Postma & Rommets (1970) and Colijn, (1978). They believe that the inlets include clearer waters than inner part of western WS so the Marsdiep region has to be more productive.

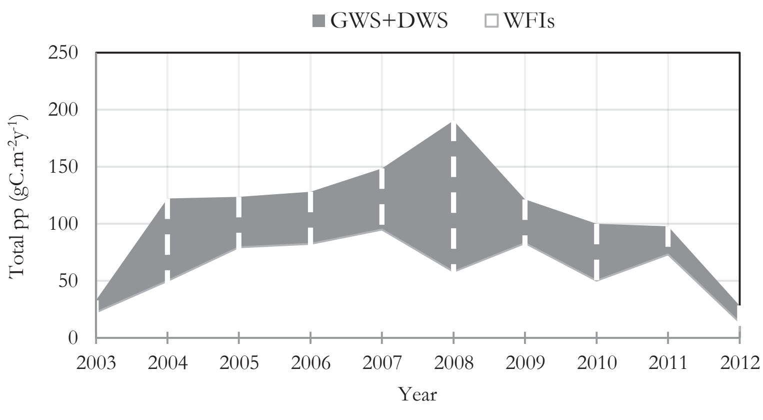

Figure 6-4- Total amount of annual pp variation year by year from 2003 till 2012.
The gray space represents the rest of WS area (German+Danish)

6.5. VGPM assessment

Comparing to former studies in which pp was estimated using in-situ measurements, the VGPM primary productivity was shown a realistic display of PP in WS. Similar to most of relevant researches, VGPM output of could subtly reflect the increasing and decreasing pattern of pelagic planktonic primary production in daily, seasonally and even yearly time scales in this study as well. Although this model is constructed to apply for oceanic productivity, it succeeded to represent a nearly realistic state of coastal phytoplankton generating rate with some overestimations (Tripathy et al., 2012). This could be illustrated by comparing modelled PP with field measurements which unfortunately was not done in this research due to no in-situ PP data for WS. Verification of VGPM using field data indicates that daily remote sensing inputs from sunny days overrate the primary productivity values (Ishizaka et al., 2007).

6.6. Chlorophyll_a interconnection with PAR and SST

Investigation of direct interaction between phytoplankton biomass and climatic indicators in Wadden Sea lagged for almost long time. We chose daily Chl_a concentration as an indicator of phytoplankton biomass and SST and PAR as two ancillary climate variables to peruse whether there is any considerable relationship between these parameters. Short-term and long-term time series showed that from 2003-2012, mean WS Chl_a concentration is increasing whenever SST and PAR are reducing (e.g. early in January). Even it was unchanged in some long intervals like from 2009 to 2011, average Chl_a concentration has remained steady in about 135mg.m^{-3}. In general, we discovered an inverse trend for biomass activities against temperature and radiation year by year. As such, the maximum growth of annual mean Chl_a concentration was recorded about 4.2mg.m^{-3} from 2005 to 2006, for SST around 3.3^{o}c in 2010 to 2011 and for PAR it was recorded near to 17.17E.m^{-2}d^{-1} from 2003 toward 2004. Actually there is no regular cyclic pattern found out to connect the 3 variables, although SST and PAR demonstrated nearly high positive correlation in most times of the year. This contradiction between physical and biological systems was shown in recent similar studies. Feng & Zhu (2012) found out only 1 stable year between SST and Chl_a for the study period of 2003 till 2009 in global scale. Another research has been done in coastal waters of North Carolina by Maybin et al. (2009) in which they contributed SST and Chl_a inverse behaviour to coastal upwelling currents as a result of wind. Wind speed and sun radiation were recognized as two important controlling parameters of phytoplankton growth in Bering Sea by Iida & Saitoh (2007). This opposite relationship was repeated in a research which has been done by Fox et al. (2005) on SST and PAR spatial and temporal variation effect on Chl_a oscillation in Gulf of Maine. They discovered a rising pattern of temperature and radiation in early spring when Chl_a showed a descending pattern. Looking at all these articles, what is common between them is that such kind of inverse variation often happens in coastal areas rather than open oceans.

Based on relatively high correlation coefficient computed between Chl_a and two selected ancillary variables, we can hardly accept any kind of interactions. Such relationships may be detailed by using longer period of datasets accompanying with applying other statistical methods. On the other hand, there might exist other stronger factors (climatic or non-climatic) which can nullify the impact of available radiation and surface temperature on phytoplankton biomass (e.g. Iida & Saitoh, 2007). Due to lack of recent researches about the current issue in Wadden Sea, we suffice to express some possible reasons that might intensify the opposite behaviour of chlorophyll_a in Wadden Sea:

- C2R disability to retrieve a realistic values of Chl_a;
- Unexpected variation of nutrient supply of WS coastal area as a result of North Sea tidal turbulence which then push the waters in through different inlets;
- The effect of temperature, rainfall and runoff especially in cold months;
- Collision of North Sea waters with upstream river flows in inner part of WS which might terminate to instability and deeper mixed layer;

- Resuspension of sediments as a result of quick tides in particular in German WS which leads to high level of turbidity (Poremba et al., 1998)

7. CONCLUSION AND RECOMMENDATION

7.1. Summary and conclusion

A decade of model-based daily primary production behaviour was evaluated for the entire coastal area of Wadden Sea as well as West Frisian Islands from Jan-2003 till Mar-2012 merging MERIS and MODIS products. The coastal line of Ameland was labelled as the most turbid region among WFIs since it is much under affection of turbid waters of German WS as well as Dutch WS nutrient loadings. During 10 years evaluation, Chl_a reached to its highest amount of concentration in year 2008. In spite of reasonable pp values driven by VGPM, the temporal variation of production rate is rather in contrast with chlorophyll changes since Chl_a showed a delay in spring and summer bloom. The Wadden Sea primary production depends much on light penetration depth and the amount of nutrients. As such, in warm months (e.g. July) the biomass producing level becomes higher than winter season as a result of more available light deep in the water. In between, euphotic depth was following temporal and spatial behaviour similar to that of primary production. The most spatial variable island of WF refers to Texel where the area has been affected by nutrients entries from 3 surrounded locations containing North Sea, Lake Ijssmijer and Marsdiep inlets. Moreover, decadal survey along the entire area of WS highlighted German WS as the largest range of primary production changes. We concluded that the primary productivity alteration in Wadden Sea is very complex and it`s really hard to label only one specific parameter. In conclusion, marine primary production has been changing by different bio-chemical, bio-physical and bio-optical properties of surrounded turbid waters and streams. Not only in WS, but similar issues in primary productivity derivation might be encountered in other coastal area (Cadee & Hegman, 1997).

In parallel, the interaction between two ancillary climate variables (SST & PAR) and Chl_a concentration was perused for the WS region. Our conclusion is based on a decadal remote sensing data which might not mirror the certain contribution of ancillary climatic variability with phytoplankton growth. In other words, there are limited numbers of remotely sensed physical and biological variables which cannot cover the whole range of factors affecting the phytoplankton biomass community (Schwarz et al., 2010). In current research, an opposite behaviour of Chl_a was sensed as a consequence of water surface temperature and available radiation either during short-term or long-term evaluation. We observed inconsistent pattern of Chl_a with SST and PAR which might be originated as a reason of C2R error in IOP retrieval, nutrient loads variation in WS, rapid flows of North Sea and margin rivers and other dominant physical phenomenon. Future studies should therefore concentrate first on other crucial climatological indices using applicable models and second on collecting field measurements to validate the algorithms.

7.2. Limitations

- No validation could be done for VGPM primary production due to complicated field measurements;
- Applying remote sensing data (which were available only for almost 10 years) limits clear understanding of the influence of selected climate variables on biomass activities in the area. Since the climatic studies are usually applied when at least 30 years data is available;
- Numbers of potential data were eliminated as a result of temporal match-up between MERIS and MODIS datasets.

7.3. Recommendation

- A developed C2R model should be constructed in order to decrease the IOPs` overestimation like Chl_a concentration;
- Customizing the VGP model for the coastal turbid water of Wadden Sea using the available in-situ data;
- Improving the VGPM calculating process by assigning a proper coefficient for the sensitivity-generating parameters such as Z_{eu}, P_b^{opt} and Chl_a;
- The estimation of P_b^{opt} can be improved by considering the TSM and CDOM rather than SST;
- Other dominant climatic factors could be studied in order to represent a clearer view of biological responses to atmospheric factors since WS is a coastal area affected by diverse form of parameters;
- Spatio-temporal changes of nutrient loadings supplied by rivers and North Sea is recommended.

LIST OF REFERENCES

Aas, E. (2010). Estimates of radiance reflected towards the zenith at the surface of the sea. *Ocean Science, 6*(4), 861-876. doi: 10.5194/os-6-861-2010

Anthony, K. R. N., Ridd, P. V., Orpin, A. R., Larcombe, P., & Lough, J. (2004). Temporal variation in light availability in coastal benthic habitats: Effects of clouds, turbidity, and tides. *Limnol. Oceanogr, 49*(6), 2201-2211. doi: 10.4319/lo.2004.49.6.2201

Antoine, D., André, J. M., & Morel, A. (1996). Oceanic primary production 2. Estimation at global scale from satellite (coastal zone color scanner) chlorophyll. *Global Biogeochemical Cycles, 10*(1), 57-69.

Antoine, D., & Morel, A. (1996). Oceanic primary production 1. Adaptation of a spectral light-photosynthesis model in view of application to satellite chlorophyll observations. *Global Biogeochemical Cycles, 10*(1), 43-55.

Archer, D. E., Eshel, G., Winguth, A., Broecker, W., Pierrehumbert, R., Tobis, M., & Jacob, R. (2000). Atmospheric pCO2 sensitivity to the biological pump in the ocean. *Global Biogeochem. Cycles, 14*(4), 1219-1230. doi: 10.1029/1999gb001216

Armstrong, R. A. (2006). Optimality-based modeling of nitrogen allocation and photoacclimation in photosynthesis. *Deep Sea Research Part II: Topical Studies in Oceanography, 53*(5–7), 513-531. doi: 10.1016/j.dsr2.2006.01.020

Arst, H., Nõges, T., Nõges, P., & Paavel, B. (2008). In situ measurements and model calculations of primary production in turbid waters. *Aquatic Biology, 3*, 19-30. doi: 10.3354/ab00059

Asanuma, I. (2007). Depth and Time Resolved Primary Productivity Model Examined for Optical Properties of Water-Chapter 4. In H. Kawahata & Y. Awaya (Eds.), *Elsevier Oceanography Series* (Vol. Volume 73, pp. 89-106): Elsevier.

Asmus, R., Jensen, M. H., Murphy, D., & Doerffer, R. (1998). Primary production of the microphytobenthos, phytoplankton and the annual yield of macrophytic biomass in the Sylt-Romo Wadden Sea *In: C. Gatje and K. Reise (eds.)*, 367–391.

Behrenfeld, & Falkowski. (1997). A consumer's guide to phytoplankton primary productivity models. *Limonology and Oceanography, 42*(7), 1479-1491.

Behrenfeld, M. J., Marañón, E., Siegel, D. A., & Hooker, S. B. (2002). Photoacclimation and nutrient-based model of light-saturated photosynthesis for quantifying oceanic primary production. *Marine Ecology Progress Series, 228*, 103-117.

Bode, A., Anadón, R., Morán, X. A. G., Nogueira, E., Teira, E., & Varela, M. (2011). Decadal variability in chlorophyll and primary -production off NW Spain. *Climate Research, 48*(2), 293-305. doi: 10.3354/cr00935

Bot, P. V. M., & Colijn, F. (1996). A method for estimating primary production from chlorophyll concentrations with results showing trends in the Irish Sea and the Dutch coastal zone. *Journal of Marine Science, 53*, 945–950. doi: 1054–3139/96/060945

Britannica. (2012). Frisian Islands, from http://www.britannica.com/EBchecked/topic/220483/Frisian-Islands

C., B. (2011, Dec 13, 2011). Bulk Processing with GPT, from http://www.brockmann-consult.de/beam-wiki/display/BEAM/Bulk+Processing+with+GPT

C.W.S.S. (2008). Nomination of the Dutch-German Wadden Sea as World Heritage Site. *Wadden Sea Ecosystem, 24*, 200.

Cadée, G. C. (1978). On the origin of organic matter accumulating on tidal flats of Balgzand, Dutch Wadden Sea. *Hydrobiological Bulletin, 12*(2), 145-150. doi: 10.1007/bf02260717

Cadée, G. C. (1986). Increased phytoplankton primary production in the Marsdiep area (Western Dutch Wadden Sea). *Netherlands Journal of Sea Research, 20*(2–3), 285-290. doi: 10.1016/0077-7579(86)90050-5

Cadée, G. C., & Hegeman, J. (1974). Primary production of the benthic microflora living on tidal flats in the dutch wadden sea. *Netherlands Journal of Sea Research, 8*(2–3), 260-291. doi: http://dx.doi.org/10.1016/0077-7579(74)90020-9

Cadée, G. C., & Hegeman, J. (1979). Phytoplankton primary production, chlorophyll and composition in an inlet of the Western Wadden Sea (Marsdiep). *Netherlands Journal of Sea Research, 13*(2), 224-241. doi: http://dx.doi.org/10.1016/0077-7579(79)90004-8

Cadée, G. C., & Hegeman, J. (1993). Persisting high levels of primary production at declining phosphate concentrations in the Dutch coastal area (Marsdiep). *Netherlands Journal of Sea Research, 31*(2), 147-152. doi: 10.1016/0077-7579(93)90004-c

Cadée, G. C., & Hegeman, J. (2002). Phytoplankton in the Marsdiep at the end of the 20th century; 30 years monitoring biomass, primary production, and Phaeocystis blooms. *Journal of Sea Research, 48*(2), 97-110. doi: http://dx.doi.org/10.1016/S1385-1101(02)00161-2

Campbell, J., Antoine, D., Armstrong, R. A., Arrigo, K. R., Balch, W., Barber, R., . . . Yoder, J. A. (2002). Comparison of algorithms for estimating ocean primary production from surface chlorophyll, temperature, and irradiance. *Global Biogeochem. Cycles, 16*(3), 1035. doi: 10.1029/2001gb001444

Cannizzaro, J. P., & Carder, K. L. (2006). Estimating chlorophyll a concentrations from remote-sensing reflectance in optically shallow waters. *Remote Sensing of Environment, 101*(1), 13-24. doi: 10.1016/j.rse.2005.12.002

Carr, M. E. (2002). Estimation of potential productivity in Eastern Boundary Currents using remote sensing. *Deep-Sea Research Part II: Topical Studies in Oceanography, 49*(1-3), 59-80.

Carr, M. E., Friedrichs, M. A. M., Schmeltz, M., Noguchi Aita, M., Antoine, D., Arrigo, K. R., . . . Yamanaka, Y. (2006). A comparison of global estimates of marine primary production from Ocean Color. *Deep-Sea Research Part II: Topical Studies in Oceanography, 53*(5-7), 741-770.

Chawira, M. (2012). *Monitoring blue green algae in the IJsselmeer using remote sensing and in situ measurements.* (MSc.), University of Twente Enschede. Retrieved from http://www.itc.nl/library/papers_2012/msc/wrem/chawira.pdf

Colijn, F. (1978). *Primary Production measurements in the Ems-Dollard estuary during 1975 and 1976.* Paper presented at the Intern Verslag Biologisch Onderzoek Eems Dollard Estuarium.

Cullen, A. C., & Frey, H. C. (2001). Probabilistic Techniques in Exposure Assessment. A Handbook for Dealing With Variability and Uncertainty in Models and Inputs. *Statist. Med, 20*, 2209-2217.

de Jonge, V., de Jong, D., & van den Bergs, J. (1996). Reintroduction of eelgrass (Zostera marina) in the Dutch Wadden Sea; Review of research and suggestions for management measures. *Journal of Coastal Conservation, 2*(1), 149-158. doi: 10.1007/bf02743048

de Jonge, V. N. (1990). Response of the Dutch Wadden Sea ecosystem to phosphorus discharges from the River Rhine. *Hydrobiologia, 195*(1), 49-62. doi: 10.1007/bf00026813

de Jonge, V. N., & Postma, H. (1974). Phosphorus compounds in the Dutch wadden sea. *Netherlands Journal of Sea Research, 8*(2–3), 139-153. doi: http://dx.doi.org/10.1016/0077-7579(74)90014-3

Doerffer, R., Schiller, H., & Peters, M. (2006). BEAM 3.7 Plug-ins, BEAM Help Manual.

Dube, T. (2012). *Primary Productivity of Intertidal mudflats in the Wadden Sea: A Remote Sensing Method.* (MSc. Thesis), Twente University.

Ebbesmeyer, C. C., & Helseth, J. M. (1977). An analysis of primary production observed during 1966-1975 in central Puget Sound, Washington (pp. 68). Inc. Seattle, Washington.

Eck, T. F., & Dye, D. G. (1991). Satellite Estimation of Incident Photosynthetically Active Radiation Using Ultraviolet Reflectance. *Remote Sensing Environment, 38*, 135-146.

Eleveld, M. A., van der Woerd, H. J., & Beck, H. (2007). *Improving the Estimation of North Ses Primary Production: MERIS Chl & Kd in VGPM*. Paper presented at the Proc. 'Envisat Symposium 2007', Switzerland.

Eppley, R. W., Stewart, E., Abbott, M. R., & Heyman, U. (1985). Estimating ocean primary production from satellite chlorophyll. Introduction to regional differences and statistics for the Southern California Bight. *Journal of Plankton Research, 7*(1), 57-70. doi: 10.1093/plankt/7.1.57

Fee, E. J. (1973). A Numerical Model for Determining Integral Primary Production and its Application to Lake Michigan. *Journal of the Fisheries Research Board of Canada, 30*(10), 1447-1468. doi: 10.1139/f73-235

Feng, J. F., & Zhu, L. (2012). Changing trends and relationship between global ocean chlorophyll and sea surface temperature. *Procedia Environmental Sciences, 13*, 626-631. doi: 10.1016/j.proenv.2012.01.054

Fox, M. F., Kester, D. R., & Yoder, J. A. (2005). Spatial and temporal distributions of surface temperature and chlorophyll in the Gulf of Maine during 1998 using SeaWiFS and AVHRR imagery. *Marine Chemistry, 97*(1-2), 104-123. doi: 10.1016/j.marchem.2005.04.004

Fransz, H. (1976). *The spring development of calanoid copepod populations in the Dutch coastal waters as related to primary production.* Paper presented at the 10th European Mrine Biology Symposium, Belgium.

Freitas, F. H. (2009). *Spectral merging of MODIS / MERIS Ocean Colour Data to improve monitoring of coastal water processes.* (MSc.), Twente University, ITC. (2007-15)

Frey, H. C., Mokhtari, A., & Danish, T. (2003). Evaluation of Selected Sensitivity Analysis Methods Based Upon Applications to Two Food Safety Process Risk Models (C. Department of Civil, and Environmental Engineering, Trans.): Computational Laboratory for Energy, Air, and Risk.

Frey, H. C., & Patil, S. R. (2002). Identification and Review of Sensitivity Analysis Methods. *Risk Analysis, 22*(3), 553-578. doi: 10.1111/0272-4332.00039

Galbraith, P. S., & Larouche, P. (2011). Sea-surface temperature in Hudson Bay and Hudson Strait in relation to air temperature and ice cover breakup, 1985–2009. *Journal of Marine Systems, 87*(1), 66-78. doi: 10.1016/j.jmarsys.2011.03.002

Galbraith, P. S., Larouche, P., Chassé, J., & Petrie, B. (2012). Sea-surface temperature in relation to air temperature in the Gulf of St. Lawrence: Interdecadal variability and long term trends. *Deep Sea Research Part II: Topical Studies in Oceanography, 77-80*, 10-20. doi: 10.1016/j.dsr2.2012.04.001

Gilmore, B. M. (2006). *Primary Production around the Galapagos Islands and the effects of cloud cover and differing light regimes.* (Senior Thesis), The University of Washington, School of Oceanography.

González, J. A., & Calbó, J. (2002). Modelled and measured ratio of PAR to global radiation under cloudless skies. *Agricultural and Forest Meteorology, 110*(4), 319-325. doi: http://dx.doi.org/10.1016/S0168-1923(01)00291-X

Harris, G. P., & Lott, J. N. A. (1973). Light intensity and photosynthetic rates in phytoplankton. *Journal of the Fisheries Research Board of Canada, 30*(12), 1771-1778. doi: 10.1139/f73-286

Hays, G. C., Richardson, A. J., & Robinson, C. (2005). Climate change and marine plankton. *Trends Ecol Evol, 20*(6), 337-344. doi: 10.1016/j.tree.2005.03.004

Helton, J. C., & Davis, F. J. (2003). Latin hypercube sampling and the propagation of uncertainty in analyses of complex systems. *Reliability Engineering & System Safety, 81*(1), 23-69. doi: http://dx.doi.org/10.1016/S0951-8320(03)00058-9

Henson, S. A., Sarmiento, J. L., Dunn, J. P., Bopp, L., Lima, I., Doney, S. C., . . . Beaulieu, C. (2010). Detection of anthropogenic climate change in satellite records of ocean chlorophyll and productivity. *Biogeosciences, 7*, 621–640.

Heritage, W. S. W. (2012). Wadden Sea, from http://www.waddensea-worldheritage.org/wadden-sea-world-heritage

Hesse, K. J., Tillmann, U., & Brockmann, U. (1995). *Factors controlling phytoplankton distribution in coastal waters of the German Bight (North Sea).* Paper presented at the 28th European Marine Biology Symposium, Greece.

Hommersom, A., Peters, S., Wernand, M. R., & de Boer, J. (2009). Spatial and temporal variability in bio-optical properties of the Wadden Sea. *Estuarine, Coastal and Shelf Science, 83*(3), 360-370. doi: 10.1016/j.ecss.2009.03.042

Honda, M. C., Sasaoka, K., Kawakami, H., Matsumoto, K., Watanabe, S., & Dickey, T. (2009). Application of underwater optical data to estimation of primary productivity. *Deep Sea Research Part I: Oceanographic Research Papers, 56*(12), 2281-2292. doi: 10.1016/j.dsr.2009.08.009

Howard, K. L., & Yoder, J. A. (1997). *Contribution of the sub-tropical oceans to global primary production.* Paper presented at the COSPAR Colloquium on Space Remote Sensing of Subtropical Oceans, Pergamon, New York.

Iida, T., & Saitoh, S. (2007). Temporal and spatial variability of chlorophyll concentrations in the Bering Sea using empirical orthogonal function (EOF) analysis of remote sensing data. *Deep Sea Research Part II: Topical Studies in Oceanography, 54*(23-26), 2657-2671. doi: 10.1016/j.dsr2.2007.07.031

Isada, T., Hattori-Saito, A., Saito, H., Ikeda, T., & Suzuki, K. (2010). Primary productivity and its bio-optical modeling in the Oyashio region, NW Pacific during the spring bloom 2007. *Deep Sea Research Part II: Topical Studies in Oceanography, 57*(17-18), 1653-1664. doi: 10.1016/j.dsr2.2010.03.009

Ishizaka, J. (1998). Spatial distribution of primary production off Sanriku, northwestern Pacific, during spring estimated by Ocean Color and Temperature Scanner (OCTS). *Journal of Oceanography, 54*(5), 553-564. doi: 10.1007/bf02742457

Ishizaka, J., Siswanto, E., Itoh, T., Murakami, H., & Yamaguchi, Y. (2007). Verification of Vertically Generalized Production Model and Estimation of Primary Production in Sagami Bay, Japan. *Journal of Oceanography, 63*, 517-524.

Jacovides, C. P., Tymvios, F. S., Asimakopoulos, D. N., Theofilou, K. M., & Pashiardes, S. (2003). Global photosynthetically active radiation and its relationship with global solar radiation in the Eastern Mediterranean basin. *Theoretical and Applied Climatology, 74*(3-4), 227-233. doi: 10.1007/s00704-002-0685-5

Joint, I. R., & Pomroy, A. J. (1981). Primary production in a turbid estuary. *Estuarine, Coastal and Shelf Science, 13*(3), 303-316. doi: 10.1016/s0302-3524(81)80028-x

Kameda, T. (2003). Studies on oceanic primary production using ocean color remote sensing data. *Bull. Fish. Res. Agen, 9*, 118-148.

Kameda, T., & Ishizaka, J. (2005). Size-Fractionated Primary Production Estimated by a Two-Phytoplankton Community Model Applicable to Ocean Color Remote Sensing. *Journal of Oceanography, 61*(4), 663-672. doi: 10.1007/s10872-005-0074-7

Kaplan, A., Cane, M. A., Kushnir, Y., Clement, A. C., Blumenthal, M. B., & Rajagopalan, B. (1998). Analyses of global sea surface temperature 1856-1991. *Journal of Geophysical Research, 103*(C9), 18567-18589.

Klemas, V. (2010). Remote Sensing Techniques for Studying Coastal Ecosystems: An Overview. *Journal of Coastal Research*, 2-17. doi: 10.2112/jcoastres-d-10-00103.1

Kratzer, S., & Vinterhav, C. (2010). Improvement of MERIS level 2 products in Baltic Sea coastal areas by applying the Improved Contrast between Ocean and Land processor (ICOL) – data analysis and validation. *Oceanologia, 52*(2), 211-236.

Loebl, M., Dolch, T., & van Beusekom, J. E. E. (2007). Annual dynamics of pelagic primary production and respiration in a shallow coastal basin. *Journal of Sea Research, 58*(4), 269-282. doi: 10.1016/j.seares.2007.06.003

Longhurst, A., Sathyendranath, S., Platt, T., & Caverhill, C. (1995). An estimate of global primary production in the ocean from satellite radiometer data. *Journal of Plankton Research, 17*(6), 1245-1271.

M´elin, F., & Hoepffner, N. (2011). Monitoring Phytoplankton Productivity from Satellite – An Aid to Marine Resources Management, in: Handbook of Satellite Remote Sensing Image Interpretation: Applications for Marine Living Resources Conservation and Management. In J. Morales, V. Stuart, T. Platt & S. Sathyendranath (Eds.), (pp. 79-93): EU PRESPO and IOCCG.

MacKenzie, B. R., & Schiedek, D. (2007). Long-term sea surface temperature baselines—time series, spatial covariation and implications for biological processes. *Journal of Marine Systems, 68*(3-4), 405-420. doi: 10.1016/j.jmarsys.2007.01.003

Marra, J., Ho, C., & Trees, C. (2003). An alternative algorithm for the calculation of primary productivity from remote sensing data. In L. T. Report (Ed.).

Maybin , B., Messan, Y., Moore, P., & Goins, C. (2009). *Temporal and Spatial Variations of Sea Surface Temperature and Chlorophyll a in Coastal Waters of North Carolina*. Elizabeth City State University.

McClain, C. R. (2009). A Decade of Satellite Ocean Color Observations*. *Annual Review of Marine Science, 1*(1), 19-42. doi: 10.1146/annurev.marine.010908.163650

Messié, M., & Radenac, M. (2006). Seasonal variability of the surface chlorophyll in the western tropical Pacific from SeaWiFS data. *Deep Sea Research Part I: Oceanographic Research Papers, 53*(10), 1581-1600. doi: 10.1016/j.dsr.2006.06.007

Migné, A., Spilmont, N., & Davoult, D. (2004). In situ measurements of benthic primary production during emersion: seasonal variations and annual production in the Bay of Somme (Eastern English Channel, France). *Continental Shelf Research, 24*(13-14), 1437-1449. doi: 10.1016/j.csr.2004.06.002

Miller, C. B. (2004). Biological Oceanography, Charles B. Miller (Nov. 2003). Blackwell, Malden MA, 402 pp. Price £29.99. ISBN 0632055367. *Journal of Plankton Research, 26*(9), 1133-1134.

Milutinović, S., & Bertino, L. (2011). Assessment and propagation of uncertainties in input terms through an ocean-color-based model of primary productivity. *Remote Sensing of Environment, 115*(8), 1906-1917. doi: 10.1016/j.rse.2011.03.013

Morales, J., Stuart, V., Platt, T., & Sathyendranath, S. (2011). Handbook of Satellite Remote Sensing Image Interpretation: Applications for Marine Living Resources Conservation and Management. *EU PRESPO and IOCCG*.

Morel, A., & Maritorena, S. (2001). Bio-optical properties of oceanic waters: A reappraisal. *J. Geophys. Res., 106*(C4), 7163-7180. doi: 10.1029/2000jc000319

Moses, W. J., Gitelson, A. A., Berdnikov, S., & Povazhnyy, V. (2009). Estimation of chlorophyll-aconcentration in case II waters using MODIS and MERIS data—successes and challenges. *Environmental Research Letters, 4*(4), 045005. doi: 10.1088/1748-9326/4/4/045005

Mueller, J. L., & Lange, R. E. (1989). Bio-optical provinces of the northeast Pacific Ocean: a provisional analysis. *LIMNOLOGY AND OCEANOGRAPHY*, 1572-1586.

Muleta, M. K., & Nicklow, J. W. (2005). Sensitivity and uncertainty analysis coupled with automatic calibration for a distributed watershed model. *Journal of Hydrology, 306*(1–4), 127-145. doi: http://dx.doi.org/10.1016/j.jhydrol.2004.09.005

Nair, A., Sathyendranath, S., Platt, T., Morales, J., Stuart, V., Forget, M., . . . Bouman, H. (2008). Remote sensing of phytoplankton functional types. *Remote Sensing of Environment, 112*(8), 3366-3375. doi: 10.1016/j.rse.2008.01.021

O'Reilly, J. E., Maritorena, S., Mitchell, B. G., Siegel, D. A., Carder, K. L., Garver, S. A., . . . McClain, C. R. (1998). Ocean color chlorophyll algorithms for SeaWiFS. *J. Geophys. Res., 103*(C11), 24937-24953. doi: 10.1029/98jc02160

O'Reilly, J. E., Maritorena, S., O'Brien, M. C., Siegel, D. A., Toole, D., Menzies, D., . . . Culver, M. (2000). SeaWiFS Postlaunch Calibration and Validation Analyses, Part 3. In B. H. Stanford & R. F. Elaine (Eds.), *SeaWiFS Postlaunch Technical Report Series* (Vol. 11). Greenbelt, Maryland: NASA/TM.

Odum, H. T. (1955). *Primary Production in Flowing Waters*. Paper presented at the Symposium, Primary Production in Waters, American Society of Limnology and Oceanography meeting.

Ondrusek, M. E., Bidigare, R. R., Waters, K., & Karl, D. M. (2001). A predictive model for estimating rates of primary production in the subtropical North Pacific Ocean. *Deep Sea Research Part II: Topical Studies in Oceanography, 48*(8–9), 1837-1863. doi: 10.1016/s0967-0645(00)00163-6

Ostermann, A. (2004). *Sensitivity analysis*. Analyzing Uncertainty in Civil Engineering.

Philippart, C. J. M., & Cadée, G. C. (2000). Was total primary production in the western Wadden Sea stimulated by nitrogen loading? *Helgoland Marine Research, 54*(2-3), 55-62. doi: 10.1007/s101520050002

Platt, T., Caverhill, C., & Sathyendranath, S. (1991). Basin-Scale Estimates of Oceanic Primary Production by Remote Sensing: The North Atlantic. *J. Geophys. Res., 96*(C8), 15147-15159. doi: 10.1029/91jc01118

Platt, T., & Sathyendranath, S. (1988). Oceanic Primary Production: Estimation by Remote Sensing at Local and Regional Scales. *Science, 241*(4873), 1613-1620.

Poremba, K., Tillmann, U., & Hesse, K. J. (1999). Tidal impact on planktonic primary and bacterial production in the German Wadden Sea. *Helgoland Marine Research, 53*(1), 19-27. doi: 10.1007/pl00012133

Postma, H. (1954). *Hydrography of the Dutch Wadden Sea ; a study of the relations between water movement, the transport of suspended materials, and the production of organic matter*. N.p.

Postma, H., & Rommets, J. W. (1970). Primary production in the Wadden Sea. *Netherlands Journal of Sea Research, 4*(4), 470-493. doi: http://dx.doi.org/10.1016/0077-7579(70)90009-8

R., A. (2012). *Quantification of Primary Production Using Remote Sensing in Dutch Wadden Sea.* (PGD), Twente University.

Rasmussen, M. B., Henriksen, K., & Jensen, A. (1983). Possible causes of temporal fluctuations in primary production of the microphytobenthos in the Danish Wadden Sea. *Marine Biology, 73*(2), 109-114. doi: 10.1007/bf00406878

Richardson, A. J., & Schoeman, D. S. (2004). Climate Impact on Plankton Ecosystems in the Northeast Atlantic. *Science, 305*(5690), 1609-1612.

Rueda, G., Rosell-Melé, A., Escala, M., Gyllencreutz, R., & Backman, J. (2009). Comparison of instrumental and GDGT-based estimates of sea surface and air temperatures from the Skagerrak. *Organic Geochemistry, 40*(2), 287-291. doi: http://dx.doi.org/10.1016/j.orggeochem.2008.10.012

Saba, V. S., Friedrichs, M. A. M., Antoine, D., Armstrong, R. A., Asanuma, I., Behrenfeld, M. J., . . . Westberry, T. K. (2011). An evaluation of ocean color model estimates of marine primary productivity in coastal and pelagic regions across the globe. *Biogeosciences, 8*(2), 489-503. doi: 10.5194/bg-8-489-2011

Saltelli, A., Tarantola, S., & Chan, K. P. S. (1999). A quantitative model-independent method for global sensitivity analysis of model output. *Technometrics, 41*(1), 39-56.

Santer, R., & Zagolski, F. (2009). ICOL. Improve contrast between ocean and land. ATBD–MERIS level-1C. *Univ. Littoral, France., D6*(1).

Santer, R., Zagolski, F., & Gilson, M. (2007). ICOL ATBD. *Univ. Littoral, France, 0.1*.

Sarmiento, J. L., Slater, R., Barber, R., Bopp, L., Doney, S. C., Hirst, A. C., . . . Stouffer, R. (2004). Response of ocean ecosystems to climate warming. *Global Biogeochem. Cycles, 18*(3), GB3003. doi: 10.1029/2003gb002134

Scardi, M. (2001). Advances in neural network modeling of phytoplankton primary production. *Ecological Modelling, 146*(1–3), 33-45. doi: 10.1016/s0304-3800(01)00294-0

Schwarz, J. N., Raymond, B., Williams, G. D., Pasquer, B., Marsland, S. J., & Gorton, R. J. (2010). Biophysical coupling in remotely-sensed wind stress, sea surface temperature, sea ice and chlorophyll concentrations in the South Indian Ocean. *Deep Sea Research Part II: Topical Studies in Oceanography, 57*(9-10), 701-722. doi: 10.1016/j.dsr2.2009.06.014

Siegel, D. A., Westberry, T. K., O'Brien, M. C., Nelson, N. B., Michaels, A. F., Morrison, J. R., . . . Hammer, M. A. (2001). Bio-optical modeling of primary production on regional scales: the Bermuda BioOptics project. *Deep Sea Research Part II: Topical Studies in Oceanography, 48*(8–9), 1865-1896. doi: 10.1016/s0967-0645(00)00167-3

Silva, V. d. P. R., Sousa, F. d. A. S., Cavalcanti, E. P., Souza, E. P., & da Silva, B. B. (2006). Teleconnections between sea-surface temperature anomalies and air temperature in northeast Brazil. *Journal of Atmospheric and Solar-Terrestrial Physics, 68*(7), 781-792. doi: http://dx.doi.org/10.1016/j.jastp.2005.12.002

Smyth, T. J., Tilstone, G. H., & Groom, S. B. (2005). Integration of radiative transfer into satellite models of ocean primary production. *J. Geophys. Res., 110*(C10), C10014. doi: 10.1029/2004jc002784

Tang, S., Chen, C., Zhan, H., & Zhang, T. (2008). Determination of ocean primary productivity using support vector machines. *International Journal of Remote Sensing, 29*(21), 6227-6236. doi: 10.1080/01431160802175355

Tang, Y., Reed, P., Van Werkhoven, K., & Wagener, T. (2007). Advancing the identification and evaluation of distributed rainfall-runoff models using global sensitivity analysis. *Water Resources Research, 43*(6), W06415.

Tang, Y., Reed, P., Wagener, T., & van Werkhoven, K. (2007). Comparing sensitivity analysis methods to advance lumped watershed model identification and evaluation. *Hydrol. Earth Syst. Sci, 11*, 793-817.

Teira, E., Mouriño, B., Marañón, E., Pérez, V., Pazó, M. J., Serret, P., . . . Fernández, E. (2005). Variability of chlorophyll and primary production in the Eastern North Atlantic Subtropical Gyre: potential factors affecting phytoplankton activity. *Deep Sea Research Part I: Oceanographic Research Papers, 52*(4), 569-588. doi: 10.1016/j.dsr.2004.11.007

Tentij, M., Beusekom, R. v., Gemerden, B. v., Grell, M. B., Stampe, T., Hötker, H., . . . Eijk, A. v. (2009). The Wadden Sea :A vision for the conservation of a Natural Heritage. *Vogelbescherming Nederland, Dansk Ornitologisk Forening & NABU 2009*.

Tillmann, U., Hesse, K. J., & Colijn, F. (2000). Planktonic primary production in the German Wadden Sea. *Journal of Plankton Research, 22*(7), 1253-1276.

Tripathy, S. C., Ishizaka, J., Siswanto, E., Shibata, T., & Mino, Y. (2012). Modification of the vertically generalized production model for the turbid waters of Ariake Bay, southwestern Japan. *Estuarine, Coastal and Shelf Science, 97*(0), 66-77. doi: 10.1016/j.ecss.2011.11.025

Tunnell Jr, J. (2002). Geography, climate and hydrography. *The Laguna Madre of Texas and Tamaulipas*, 7-27.

Uitz, J., Yannick, H., Bruyant, F., Babin, M., & Caustre, H. (2008). Relating phytoplankton photophysiological properties to community structure on large scales. *Limnol. Oceanogr, 53*(2), 614–630.

van Aken, H. M. (2010). Meteorological forcing of long-term temperature variations of the Dutch coastal waters. *Journal of Sea Research, 63*(2), 143-151. doi: 10.1016/j.seares.2009.11.005

van Bennekom, A. J., Krijgsman-Van Hartingsveld, E., Veer, G. C. M. V. D., & Voorst, H. F. J. V. (1974). The seasonal cycles of reactive silicate and suspended diatoms in the Dutch Wadden Sea. *Netherlands Journal of Sea Research, 8*(2–3), 174-207. doi: http://dx.doi.org/10.1016/0077-7579(74)90016-7

van Beusekom, J. E. E. (2005). A historic perspective on Wadden Sea eutrophication. *Helgoland Marine Research, 59*(1), 45-54. doi: 10.1007/s10152-004-0206-2

Vantrepotte, V., Brunet, C., Mériaux, X., Lécuyer, E., Vellucci, V., & Santer, R. (2006). Bio-optical properties of coastal waters in the Eastern English Channel. *Estuarine, Coastal and Shelf Science, 72*(1), 201-212.

Wang, Q., Kakubari, Y., Kubota, M., & Tenhunen, J. (2007). Variation on PAR to global solar radiation ratio along altitude gradient in Naeba Mountain. *Theoretical and Applied Climatology, 87*(1-4), 239-253. doi: 10.1007/s00704-005-0220-6

Woldegiorgis, M. G. (2012). *Quantification of primary production in Wadden sea using remote sensing and field measurements.* University of Twente Faculty of Geo-Information and Earth Observation (ITC), Enschede. Retrieved from http://www.itc.nl/library/papers_2012/msc/wrem/micael.pdf

Worldatlas. (2012). West Frisian Ilands, from http://www.worldatlas.com/aatlas/infopage/frisians.htm.

Yamada, K., Ishizaka, J., & Nagata, H. (2005). Spatial and Temporal Variability of Satellite Primary Production in the Japan Sea from 1998 to 2002. *Journal of Oceanography, 61*, 857-869.

Yokoyama, R., & Konda, M. (1996). Sea surface effects on the sea surface temperature estimation by remote sensing—Part 2. *International Journal of Remote Sensing, 17*(7), 1293-1302. doi: 10.1080/01431169608948704

Yokoyama, R., Tanba, S., & Souma, T. (1995). Sea surface effects on the sea surface temperature estimation by remote sensing. *International Journal of Remote Sensing, 16*(2), 227-238. doi: 10.1080/01431169508954392

Appendix A

The exact coordinate of 102 MWTL stations used for Chl_a validation.

station.id	station.name	x	y	Longitude	Latitude
1	220008	4223511	3550990	8.475	55.055
2	220057	4210337	3513254	8.283	54.713
3	220051	4246114	3446132	8.855	54.117
4	220055	4224263	3475284	8.512	54.375
5	220052	4220360	3445126	8.462	54.103
6	220004	4226868	3480796	8.550	54.425
7	220010	4246252	3447985	8.857	54.133
8	220054	4222870	3460657	8.495	54.243
9	220005	4203535	3499505	8.183	54.588
10	220006	4217012	3499557	8.392	54.592
11	220065	4233667	3433546	8.668	54.002
12	220066	4212049	3444197	8.335	54.093
13	220087	4220947	3431756	8.475	53.983
14	220064	4246345	3480632	8.850	54.427
15	220058	4210320	3534590	8.275	54.905
16	220003	4215536	3458403	8.383	54.222
17	220002	4232929	3458047	8.650	54.222
18	220067	4200485	3546896	8.117	55.013
19	220061	4220726	3521367	8.442	54.788
20	220015	4224923	3552259	8.497	55.067
21	220007	4211129	3554608	8.280	55.085
22	220062	4229146	3508022	8.577	54.670
23	220063	4238259	3488373	8.723	54.495
110	HUIBGOT	4099860	3388716	6.662	53.560
28	ZEEHVKNMDG	4121587	3360968	7.007	53.320
310	HUISDNBSD	3967312	3330063	4.731	52.964
41	DELFZBTHVN	4118791	3361352	6.965	53.322
55	ZOUTKPLG	4064097	3376036	6.133	53.431
61	OOSTFSGJE	4120635	3365724	6.990	53.362
71	ZOUTKPLZGT	4060829	3381306	6.080	53.476
810	OOSTFSGJMDN	4120844	3369047	6.991	53.392
910	INST	3999255	3350097	5.186	53.163
103	OOSTFSGJND	4116177	3374065	6.917	53.435
111	OOSTHD	4122138	3360722	7.015	53.318
121	ZUIDOLWNOT	4085605	3380928	6.453	53.484
131	ZUIDOLWOT	4089486	3376948	6.514	53.450
141	OOSTMP	4015358	3365711	5.411	53.312
151	EILDBG	4077804	3380373	6.336	53.476
161	EMDVWTR	4128467	3362050	7.109	53.332
171	BLAUWSOT	4005887	3356641	5.278	53.226

181	OUDWTES	4105655	3381381	6.754	53.497
191	KOOGBSD	3970124	3345240	4.757	53.101
201	BOCHTVWTM	4117516	3362957	6.945	53.336
211	GAATJBND	4122743	3361961	7.024	53.329
221	BOCHTVWTMDOT	4115415	3364644	6.912	53.350
231	GAATJBNWT	4122186	3361403	7.016	53.324
24	BOCHTVWTMDWT	4115045	3367373	6.905	53.375
25	GAATJBWT	4122207	3361024	7.016	53.320
26	BOCHTVWTND	4114546	3370842	6.895	53.406
27	BOCHTVWTZD	4118453	3362408	6.959	53.331
29	BORNDP	4028926	3379130	5.602	53.440
31	BOSCHGWT	4022183	3375551	5.504	53.404
32	RA	4099612	3379813	6.664	53.480
33	LAUWOHVMD	4068456	3373704	6.201	53.412
34	LAUWS	4085154	3384815	6.443	53.519
35	VLIESM	3998690	3367023	5.160	53.314
36	VLIESZD	3999112	3361283	5.172	53.263
37	MALZN	3978948	3332642	4.901	52.994
38	GROOTGND	4131542	3358973	7.157	53.305
39	GROOTGZD	4131890	3356006	7.164	53.279
40	MARSDND	3968750	3332188	4.750	52.984
43	HARLGHVMWT	4013480	3350845	5.397	53.178
44	MONDVDDLD	4126572	3360019	7.082	53.313
45	DANTZGND	4036599	3374582	5.721	53.404
46	DANTZGT	4036989	3374407	5.727	53.402
47	HELSDR	3968606	3329941	4.751	52.963
49	WESTMP	4003100	3363936	5.229	53.289
50	NOORDMOT	4010428	3368832	5.334	53.338
51	DOOVBOT	4005486	3341029	5.288	53.085
52	DOOVBWT	3988202	3338670	5.033	53.054
53	NOORDPDZL	4095092	3377316	6.598	53.456
54	HOLWDBG	4052734	3378515	5.960	53.447
99	HARLGVHVN	4014060	3350508	5.406	53.175
511	TERSLG4	3998799	3378263	5.151	53.415
521	BOOMKDP	3999725	3374232	5.169	53.380
531	ROTTMPT5	4092899	3391562	6.555	53.583
541	ROTTMPT3	4093427	3389666	6.564	53.566
78	1	4223400	3550807	8.473	55.053
79	3	4230209	3555491	8.578	55.097
80	1510001	4201983	3602888	8.117	55.517
81	1510003	4189018	3592113	7.917	55.417
82	1510007	4216255	3582502	8.350	55.337
83	1510009	4202404	3575047	8.135	55.267
84	1510022	4215742	3596613	8.337	55.463
85	1610001	4218439	3599148	8.378	55.487

86	1610002	4216291	3601980	8.343	55.512
87	1610003	4212494	3606150	8.282	55.548
88	1610006	4221052	3598163	8.420	55.478
89	1610008	4221015	3596494	8.420	55.463
90	1610009	4220458	3595207	8.412	55.452
91	1610010	4223505	3594585	8.460	55.447
92	1610011	4225697	3593425	8.495	55.437
93	1620012	4229977	3585918	8.565	55.370
94	1620013	4224107	3583442	8.473	55.347
95	1620014	4228844	3582231	8.548	55.337
96	1630016	4230053	3574044	8.570	55.263
97	1052	4191863	3580899	7.967	55.317
98	1059	4210045	3545172	8.267	55.000
991	1086	4213028	3580350	8.300	55.317
100	JaBu_W_1	4198056	3380026	8.147	53.514
101	Nney_W_2	4133836	3402684	7.166	53.699
102	Nney_W_3	4133902	3402681	7.167	53.699